



**HAL**  
open science

# Tailoring the nuclear Overhauser effect for the study of small and medium-sized molecules by solvent viscosity manipulation

Pedro Lameiras, Jean-Marc Nuzillard

► **To cite this version:**

Pedro Lameiras, Jean-Marc Nuzillard. Tailoring the nuclear Overhauser effect for the study of small and medium-sized molecules by solvent viscosity manipulation. *Progress in Nuclear Magnetic Resonance Spectroscopy*, 2021, 123, pp.1-50. 10.1016/j.pnmrs.2020.12.001 . hal-03191060

**HAL Id: hal-03191060**

**<https://hal.univ-reims.fr/hal-03191060v1>**

Submitted on 28 Jun 2021

**HAL** is a multi-disciplinary open access archive for the deposit and dissemination of scientific research documents, whether they are published or not. The documents may come from teaching and research institutions in France or abroad, or from public or private research centers.

L'archive ouverte pluridisciplinaire **HAL**, est destinée au dépôt et à la diffusion de documents scientifiques de niveau recherche, publiés ou non, émanant des établissements d'enseignement et de recherche français ou étrangers, des laboratoires publics ou privés.

# Tailoring the nuclear Overhauser effect for the study of small and medium-sized molecules by solvent viscosity manipulation

Pedro Lameiras<sup>a,\*</sup>, Jean-Marc Nuzillard<sup>a,\*</sup>

<sup>a</sup> Université de Reims Champagne-Ardenne, CNRS, ICMR UMR 7312, 51097 Reims, France

## ABSTRACT

The nuclear Overhauser effect (NOE) is a consequence of cross-relaxation between nuclear spins mediated by dipolar coupling. Its sensitivity to internuclear distances has made it an increasingly important tool for the determination of through-space atom proximity relationships within molecules of sizes ranging from the smallest systems to large biopolymers. With the support of sophisticated FT-NMR techniques, the NOE plays an essential role in structure elucidation, conformational and dynamic investigations in liquid-state NMR. The efficiency of magnetization transfer by the NOE depends on the molecular rotational correlation time, whose value depends on solution viscosity. The magnitude of the NOE between <sup>1</sup>H nuclei varies from +50 % when molecular tumbling is fast to -100% when it is slow, the latter case corresponding to the spin diffusion limit. In an intermediate tumbling regime, the NOE may be vanishingly small. Increasing the viscosity of the solution increases the motional correlation time, and as a result, otherwise unobservable NOEs may be revealed and brought close to the spin diffusion limit. The goal of this review is to report the resolution of structural problems that benefited from the manipulation of the negative NOE by means of viscous solvents, including examples of molecular structure determination, conformation elucidation and mixture analysis (the *ViscY* method).

## Contents

1. Introduction	2
2. Structure and conformation elucidation	4
2.1. Acetic acid- <i>d</i> <sub>4</sub>	4
2.2. Chlorotrifluoroethylene polymer (CTFEP)	5
2.3. Dimethylformamide- <i>d</i> <sub>7</sub> (DMF- <i>d</i> <sub>7</sub> )/water blend	8
2.4. Dimethylsulfoxide- <i>d</i> <sub>6</sub> (DMSO- <i>d</i> <sub>6</sub> )	9
2.4.1. Structural and conformational study of Ristocetin A and B	9
2.4.2. Structural and conformational study of Vancomycin	11
2.4.3. Structural and conformational study of Valinomycin	13
2.5. Dimethylsulfoxide- <i>d</i> <sub>6</sub> (DMSO- <i>d</i> <sub>6</sub> )/water blend	14
2.6. Ethylene glycol (EG)	17

2.7. Ethylene glycol (EG)/water blend	22
2.8. Phosphoric acid- $d_3$	25
2.9. Sulfolane- $d_8$	26
2.10. Supercooled water	28
2.10.1. Micro-emulsions	28
2.10.2. Glass capillaries	28
2.10.3. Polymer gels	29
2.11. Viscous solvents under high pressure	32
2.11.1. Model membrane systems in $D_2O$	32
2.11.2. Ethylhexylbenzoate- $d_{22}$ under high pressure	34
2.12. Enkephalins: a case study of the application of different viscous cryoprotective media to determine bioactive conformations	35
2.12.1. DMSO- $d_6$ /water blend	37
2.12.2. EG- $d_6$ /water and DMF- $d_7$ /water blends	40
2.12.3. Polyacrylamide gel in DMSO- $d_6$ /water blend	40
3. Small molecule mixture analysis in Viscous solvents by NMR spin diffusion spectroscopy: ViscY	42
3.1. Chlorotrifluoroethylene Polymer (CTFEP)	43
3.2. Glycerol (GL) and Glycerol Carbonate (GC)	46
3.3. Supercooled water	49
3.4. Dimethylsulfoxide- $d_6$ (DMSO- $d_6$ ) blends	51
3.4.1. Dimethylsulfoxide- $d_6$ (DMSO- $d_6$ )/Glycerol (GL) and DMSO- $d_6$ /Glycerol- $d_8$ (GL- $d_8$ ) blends	51
3.4.1.1. Study of a low polarity mixture of $\beta$ -Ionone, ( $\pm$ )-Citronellal, (+)-Limonene, and Flavone in DMSO- $d_6$ /GL- $d_8$ (5:5 v/v)	53
3.4.1.2. Through-bond chemical shift correlations of $\beta$ -Ionone, ( $\pm$ )-Citronellal, (+)-Limonene, and Flavone mixed in DMSO- $d_6$ /GL- $d_8$ (5:5 v/v)	54
3.4.2. Dimethylsulfoxide- $d_6$ (DMSO- $d_6$ )/ethylene glycol (EG) blend	55
3.4.3. Dimethylsulfoxide- $d_6$ (DMSO- $d_6$ )/water blend	57
3.4.3.1. Study of the Leu-Val, Leu-Tyr, Gly-Tyr, and Ala-Tyr mixture in DMSO- $d_6$ /H $_2$ O (7:3 v/v)	59
3.4.3.2. $2^{\alpha}FTp3^{\alpha}FT$ in DMSO- $d_6$ /H $_2$ O (8:2 v/v) blend	59
3.5. Carbohydrate-based solutions	61
3.5.1. Sucrose solution	61
3.5.2. Agarose gel	63
3.6. Sulfolane blends	65
3.6.1. Sulfolane/dimethylsulfoxide- $d_6$ (DMSO- $d_6$ ) blend	65
3.6.2. Sulfolane/water blend	67

3.7. Overview of advantages/disadvantages of viscous solvents in molecule mixture analysis	68
4. Conclusion	71
Acknowledgements	71
References	71
Glossary	82

## 1. Introduction

There is no doubt that the nuclear Overhauser effect (NOE) is one of the most important tools for the evaluation of distances between atomic nuclei within molecules, since the NOE magnitude is related to dipolar coupling strength, which is itself related to these distances. The effect was first described in 1953 by A. W. Overhauser, as a large polarization of nuclear spins in metals, and was observed by saturation of electronic spin magnetization. [1-3] Two years later a description of the nuclear analogue, the NOE, was published by Solomon and still remains the fundamental basis of NOE theory. [4] Two events subsequently contributed to the practical uptake of the NOE. The first was the publication of the book by Noggle and Schirmer [5] that summarized the state of the art of the NOE in the early 1970s when only continuous-wave 1D NMR was available and was employed to characterize small molecules. The second event occurred in the '80s with the determination of the 3D structures of small proteins and DNA fragments based on NOE measurements using 2D FT-NMR spectra. [6] NOE studies then became an integral part of structural, conformational and dynamic analysis in liquid-state NMR.

The theoretical maximum value of the NOE, whether resulting from the steady-state or the transient effect, depends on  $\omega\tau_C$ , where  $\omega$  is the Larmor angular frequency and  $\tau_C$  is the molecular rotational correlation time, whose value depends strongly on solution viscosity. The

microviscosity description by Gierer and Wirtz gives a theoretical framework to the relationship between viscosity, temperature and rotational correlation time [7] In the absence of external relaxation, the maximum positive steady-state NOE of 50% is reached (for a two-spin system) when  $\omega\tau_C \ll 1$ , in the so-called extreme narrowing limit, while the most negative NOE of -100 % occurs when  $\omega\tau_C \gg 1$ , corresponding to the spin diffusion limit. However, when  $\omega\tau_C \sim 1$  the NOE may become vanishingly small for medium-sized molecules of masses in the 500 - 2000 g mol<sup>-1</sup> range when dissolved in a low-viscosity medium. A simple way of addressing this issue is to resort to a lower operating frequency in order to decrease  $\omega\tau_C$  and therefore to observe positive NOEs, at the price of a reduction of sensitivity and resolution. Another way of reducing  $\omega\tau_C$  is to increase the sample temperature, within the limits of solute chemical stability and solvent boiling point. Keeping the NOE positive is possible without altering the sample, by using rotating frame NOESY experiments (formerly known as CAMELSPIN [8] and renamed ROESY [9]). Because of the different dependence of the rotating frame NOE on motional frequencies, positive NOEs are observed for all values of  $\omega$  and  $\tau_C$ . The maximum theoretical ROE intensity varies between 38.5 % and 67.5 % and does not reach the 100%

limit (in absolute value) of the NOE. Moreover, complications due to Hartmann-Hahn transfers between scalar coupled protons and the practical difficulties in setting up this experiment limit its practical use, and consequently the following discussion will be limited to the NOE. One way to enhance the NOE in small molecules by moving them towards the spin diffusion limit is to anchor them to larger molecules such as cyclodextrins or crown ethers, so that the tumbling rate of the anchored compounds is slowed down. [10] Considering the limitations of having a single NMR spectrometer field available, of avoiding the addition of a tumbling speed reduction agent to the sample, and of preferring low temperatures to high ones, the easiest way to favour the observation of the NOE is to operate in conditions of spin diffusion by increasing the solvent viscosity, and to modulate it by the choice of the sample temperature. Molecules reach then the negative NOE regime and the maximum negative value of 100 % is accessible. Moreover, full intramolecular magnetization exchange can occur through spin diffusion for long saturation (steady-state NOE) or mixing times (transient NOE). However, in the case of very active spin diffusion, the determination of interproton distances and thus of molecular structure and conformational may be complicated.

In this review, we report the reasons for which it is particularly useful to manipulate the sign and size of the NOE by means of viscous solvents, first in structure and conformation elucidation (section 2), and then in mixture analysis taking advantage of spin diffusion (section 3). Section 2 is organized into sub-sections according to the alphabetic order of the solvent (or solvent blend) names, whereas sub-sections in section 3 are chronologically ordered.

The reader is encouraged to read selected publications, reviews and books in order to access a comprehensive

theoretical and practical description of the nuclear Overhauser effect (NOE). [5, 11-15] The reader should keep in mind that the basic steady-state NOE experiment associated with NOE difference spectroscopy that is mentioned several times in the following section is no longer employed for the study of small and medium-sized molecules in structural organic chemistry. These days, the steady-state difference NOE experiment has been replaced by more efficient 1D or 2D gradient-enhanced transient NOESY experiments.

## 2. Structure and conformation elucidation

### 2.1. Acetic acid- $d_4$

Acetic acid- $d_4$ , as a polar protic solvent, has the advantages of dissolving polar compounds such as inorganic salts (dielectric constant  $\epsilon$  is 6.2 at 25°C) and being sufficiently viscous (viscosity  $\eta$  of 1.06 cP at 25°C) [16] to lower the tumbling rate of mid-sized compounds in solution in order to give rise to relevant negative NOE enhancements.

In 1981, Neuhaus *et al.* took advantage of the viscosity of acetic acid- $d_4$  [17] to enhance negative NOEs in order to resolve an issue of positional isomerism in dihydrodaphnine diacetate, a bisbenzylisoquinoline derivative isolated from the Queensland plant *Daphnandra repandula*, by means of 1D steady-state NOE difference spectroscopy, at 250 MHz ( $^1\text{H}$ ), at room temperature (Fig. 1).

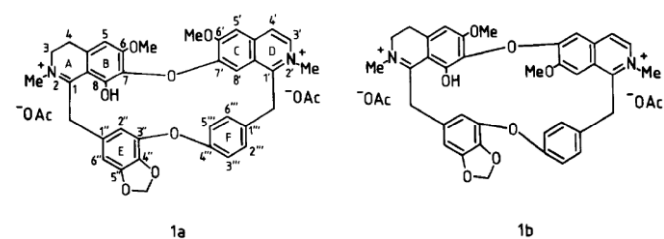
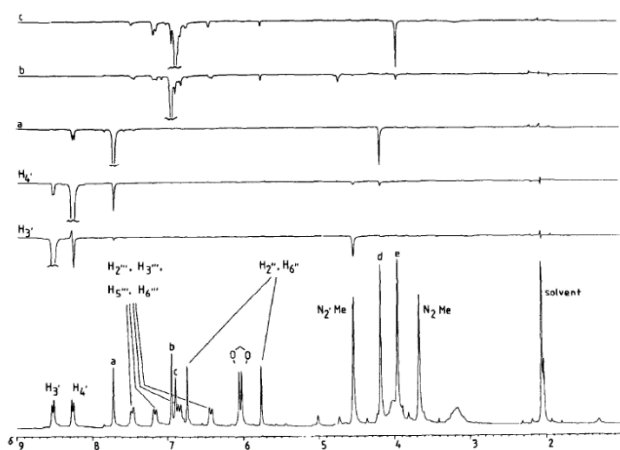


Fig. 1. Positional isomers of dihydrodaphnine diacetate. Reproduced from [17].

Each NOE difference spectrum in Fig. 2 was calculated by subtracting the conventional proton spectrum from the spectrum in which the marked resonance peak (shown truncated in Fig. 2) had been partially saturated by a very low power saturation field of high selectivity. The authors assessed the magnitude of the resulting steady-state NOEs at about -5%.



**Fig. 2.** Normal and nOe difference spectra of 1 at 250 MHz in  $\text{CD}_3\text{CO}_2\text{D}$ . Each NOE difference spectrum (upper five traces) is identified using the normal spectral peak which was pre-irradiated in the corresponding experiment. Vertical amplitude is only approximately constant within the difference spectra, being roughly four times that of the normal spectrum. Reproduced from [17].

Clear negative NOEs appeared between  $\text{H}_3'$  and the methyl group  $\text{N}_2'$ , between  $\text{H}_3'$  and  $\text{H}_4'$ , between  $\text{H}_4'$  and the peak *a*, and between peaks *a* and *d*. The latter established a chain of proximity relationships at the periphery of rings C and D which led to the assignment of the peak *a* to  $\text{H}_5$ , and suggested that  $\text{H}_5$  was adjacent to a methoxy group. This deduction was validated by the presence of a similarly intense negative NOE between peak *c* (assigned to  $\text{H}_5$ ) and peak *e* (assigned to the  $\text{C}_6$  methoxy group), and by the absence of strong effects involving peak *b* (assigned to  $\text{H}_8$ ). As a result, the correct dihydrodaphnine diacetate structure was assigned as *1a*.

## 2.2. Chlorotrifluoroethylene polymer (CTFEP)

CTFEP is a hydrogen-free extremely viscous solvent. [18] It is aprotic, chemically inert, and much more viscous ( $\eta = 1550$  cP at  $25^\circ\text{C}$ ) than any of the other viscous solvents described in this review such as dimethylsulfoxide ( $\eta = 2.003$  cP at  $25^\circ\text{C}$ ), [19] sulfolane ( $\eta = 10.295$  cP at  $30^\circ\text{C}$ ), [20] ethylene glycol ( $\eta = 17$  cP at  $25^\circ\text{C}$ ), [21] phosphoric acid ( $\eta = 63$  cP at  $25^\circ\text{C}$ ), [22] glycerol carbonate ( $\eta = 85.4$  cP at  $25^\circ\text{C}$ ) [23] or glycerol ( $\eta = 934$  cP at  $25^\circ\text{C}$ ). [23] It is readily miscible with all usual organic solvents such as chloroform or dichloromethane, and easily dissolves non-polar compounds. The resulting solvent blend constitutes a medium in which organic synthesis may be carried out, and which increases the molecular correlation time  $\tau_C$ . The manipulation of the NOE enhancement therefore makes possible the structure and conformational elucidation of non-polar compounds in solution. However, its low dielectric constant value of 2.6 at  $25^\circ\text{C}$  does not favour the dissolution of polar compounds. [24]

Williamson *et al.* illustrated for the first time in 1981 the use of CTFEP (also known as Voltalef 10S) in mixture with  $\text{CDCl}_3$  (1:1 v/v,  $\eta_{\text{CTFEP}/\text{CDCl}_3} \sim 10 \cdot \eta_{\text{CDCl}_3} \sim 5.4$  cP at  $25^\circ\text{C}$ ) for the determination of the conformation of the antibiotic Echinomycin (MW =  $1101.26$  g mol $^{-1}$ , Fig. 3) by manipulating the NOE in solution, by means of 1D steady-state NOE difference spectroscopy, at 400 MHz ( $^1\text{H}$ ) and at room temperature. [25]

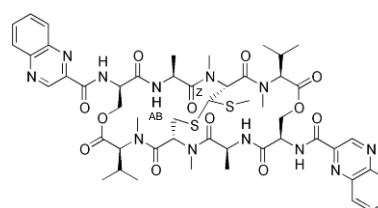


**Fig. 3.** Chemical structure of Echinomycin

Echinomycin is a cyclic octapeptide antibiotic, which acts by intercalation of both quinoxaline rings between the base pairs of DNA. The goal of this study was to determine its interactions with different DNA bases. [26] Cheung *et al.* first studied its conformation by means of NMR spectroscopy, model building, and potential energy calculations, to deduce a set of closely related conformations. [27] However, the configuration at the thioacetal CH<sup>2</sup> position remained to be elucidated. Williamson *et al.* solved this problem with the observation of large negative (up to -25%) and characteristic NOEs by means of viscous CTFEP/CDCl<sub>3</sub> (1:1 v/v) blend due to the slowdown of the molecular tumbling. As a result, they deduced the relative chirality (*S*) at the carbon bearing H<sup>Z</sup> (negative NOE between Cys-NMe → H<sup>Z</sup>) and, combined with the <sup>3</sup>*J* coupling constant value, the conformation of the cross-bridge (Fig. 4). Nonetheless, the conformation of the methylene (AB) cross-bridge remained unsolved because of the lack of relevant NOE enhancements.

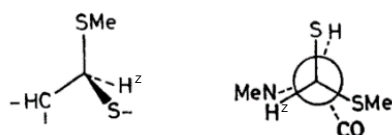


**Fig. 4.** Cram projection of the carbon bearing H<sup>Z</sup> and Newman projection of the cross-bridge including H<sup>Z</sup>. Reproduced from [25].

In 1992, Luck *et al.* also considered the use of CTFEP mixed with an organic solvent for extending solution structure determinations to small, non-polar reactive organometallic complexes and organic compounds by taking advantage of large and negative NOE enhancements using 1D steady-state NOE difference and 2D transient NOE spectroscopy, at 500 MHz (<sup>1</sup>H) and 10°C. [28]

The authors illustrated the utility of CTFEP/benzene-*d*<sub>6</sub> binary solvent systems in the study of three non-polar compounds: bis(benzyl)bis(tertbutylcyclopentadienyl)zirconium(IV) (1), (*S,S*)-1,2-ethanediylbis[(*o*-methoxyphenyl)-

phenylphosphine oxide] (Dipampo, 2), and a dipeptide, *N*-acetyl-*L*-prolyl-*D*-alanine methylamide (3) (Fig. 5). The use of the CTFEP/benzene-*d*<sub>6</sub> (8:2 w/w) solvent blend clearly gave rise to full magnetization exchange over compounds 1 and 2 due to spin diffusion after respectively selective saturation of the benzylic protons (largest negative NOE = -42%) and aromatic proton 4 (largest negative NOE = -29%), in 1D steady-state NOE difference experiments (Figs. 6 and 7). In contrast, compounds 1 and 2 did not present any relevant negative NOE enhancement in pure benzene-*d*<sub>6</sub> due to its low viscosity.

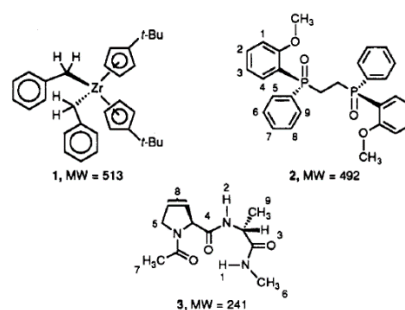


**Fig. 5.** Chemical structures of bis(benzyl)bis(tertbutylcyclopentadienyl)zirconium(IV) (1), (*S,S*)-1,2-ethanediylbis[(*o*-methoxyphenyl)phenylphosphine oxide] (Dipampo, 2), and a dipeptide, *N*-acetyl-*L*-prolyl-*D*-alanine methylamide (3). Reproduced from [28].

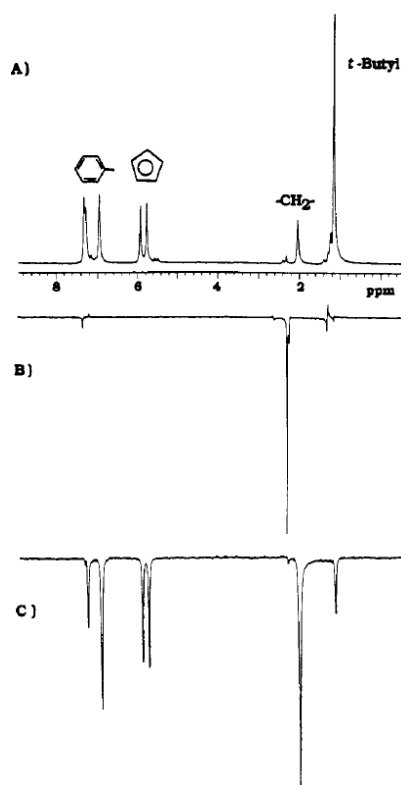


**Fig. 6.** (A) 500 MHz  $^1\text{H}$  NMR spectrum of 1 in 80% halocarbon wax and 20% benzene- $d_6$  at  $10^\circ\text{C}$ . (B) Difference NOE spectrum of 1 in benzene- $d_6$  after irradiation of the benzylic protons. (C) Difference spectrum of 1 dissolved in 80% halocarbon wax and 20% benzene- $d_6$  after irradiation of benzylic protons. Reproduced from [28].

The authors also demonstrated the applicability of the CTFEP/ $\text{CDCl}_3$  (7.5:2.5 w/w) solvent blend to the 2D NOESY experiment in a study of compound 3. Despite its low molecular mass ( $\text{MW} = 241 \text{ g mol}^{-1}$ ), the NOESY spectrum of dipeptide 3 reveals distinct large and negative NOE enhancements all over the molecule due to a considerably lowered overall correlation time (Fig. 8).

Luck and co-workers proved the significance of the use of viscous and aprotic CTFEP/benzene- $d_6$  binary solvent in the determination of solution structure of non-polar compounds with molecular mass as low as  $241 \text{ g mol}^{-1}$  by means of 1D and 2D NOE spectroscopy.

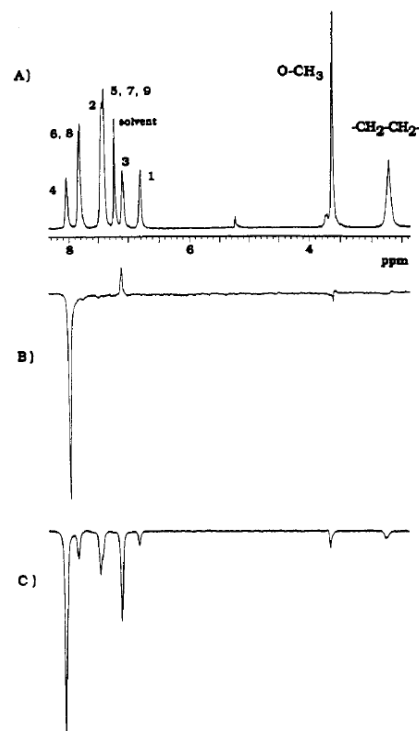


**Fig. 7.** (A) 500-MHz  $^1\text{H}$  NMR spectrum of 2 in 80% halocarbon wax and 20% benzene- $d_6$  at  $10^\circ\text{C}$ . (B) Difference NOE spectrum of 2 in benzene- $d_6$  after irradiation of position 4. (C) Difference spectrum of 2 dissolved in 80% halocarbon wax and 20% benzene- $d_6$  after irradiation of position 4. Reproduced from [28].

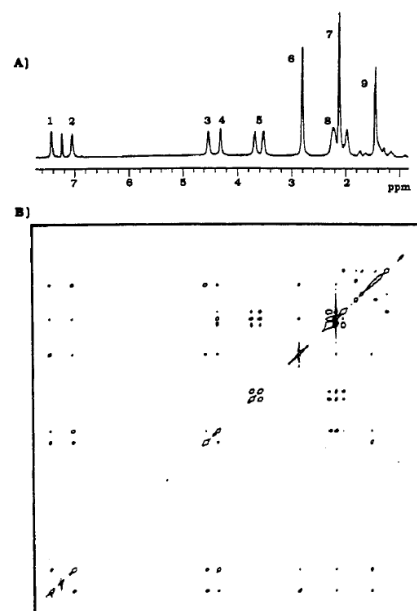


**Fig. 8.** (A) 500-MHz  $^1\text{H}$  NMR spectrum of 3 in 75% halocarbon wax and 25% chloroform- $d$  at  $10^\circ\text{C}$ . (B) Pure absorption phase  $1\text{k} \times 1\text{k}$  2D NOE contour map for 2 taken with a 500 ms mixing time. Reproduced from [28].

In 1995, Landis and co-workers considered CTFEP in mixture with  $\text{CDCl}_3$  (7.5:2.5 w/w) for conformational analysis

of the dipeptide Ac-(L)Proline-(D)Alanine-NHMe using negative NOE data from 2D transient NOESY experiments, at 500 MHz ( $^1\text{H}$ ) and  $10^\circ\text{C}$ . [29]

This dipeptide is known to adopt at least three conformations in non-hydrogen bond-donating solvents giving environments similar to those inside proteins (Fig. 9). [30, 31] Examination of such compounds in organic solvents was considered worthy of interest for providing insights into the factors responsible for the secondary and tertiary structures of proteins. [31-34]

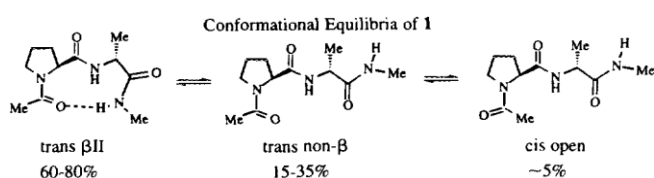


**Fig. 9.** Conformational equilibria of the Ac-(L)Proline-(D)Alanine-NHMe dipeptide. Reproduced from [29].

Under high viscosity conditions, the dipeptide exhibits large and negative NOE enhancements due to very slow molecular tumbling ( $\tau_c = 1$  ns), allowing multi-conformational analysis of the quantified 2D NOESY data by means of the conformer population analysis (CPA) tool. [35, 36] An example of a 2D NOESY spectrum of the dipeptide (published in 1992) is shown in Fig. 8. [28]

After recording 2D NOESY spectra in the viscous solvent blend, the CPA procedure consisted of 1) building trial solution structures employing conformational searching methods combined with molecular mechanics energy minimizations, 2) optimizing rotational correlation times and external rate parameters involved in the back-calculation of NOE spectra for trial solution structures, and 3) analysing the observed NOE data so as to find out the set of populations of discrete structures that best fitted with the observed NOE data.

The authors focused on the validity of structure characterization of dipeptide conformations yielded by CPA software, bringing attention to generic concerns about the interpretation of NOE data. Indeed, the experimental NOE data were investigated to discover the factors influencing the structural characterization of flexible dipeptide conformations. Both quantitative and qualitative interpretations of solution NOE data were demonstrated to depend critically on the contribution of empirical force-field energetics to the determination of viable structures, and on the protocols involved for proposing trial structures. The relative influence weighting of large vs small NOEs has to be considered as well as that of inclusion vs exclusion of null data on the fitting-error function (involvement or not of the absence of NOE cross peaks in the fitting procedure). Factors assumed not to have significant influence on the interpretation of NOE data were assessed: 1) conformational interconversion was assumed to be either slow or fast in comparison with  $T_1$ , 2) diagonal cross peak inclusion in the fitting procedure, and 3) which structures were considered in deducing the rotational correlation time from the experimental NOE data.

At the end of the study, the authors pointed out significant doubts about the realistic information content of NOESY spectra for flexible molecules, in particular for the Ac-(L)Proline-(D)Alanine-NHMe dipeptide. However, multi-conformer models such as CPA, Nikiforovich Monte Carlo [37-40], and MEDUSA procedures [41] seemed to lead to a more accurate evaluation of molecular solution structures of flexible molecules than those based on a single-conformer model [42].

The use of CTFEP was also described in 1998 by Lienin *et al.* for investigating its viscosity-dependent retarding effect on the rotational motion of 1,3-dibromoadamantane ( $\text{MW} = 294.03 \text{ g mol}^{-1}$ ) by means of  $^{13}\text{C}$  NMR relaxation studies and (steady-state) NOE measurements, at 400 and 600 MHz ( $^1\text{H}$ ).

[18] They focused on the relaxation properties of the methine  $^{13}\text{C}$  in the hope of deriving an appropriate motional model in the accessible temperature-dependent viscosity range between  $10^2$  and  $10^5$  cP. They concluded that the relaxation data of 1,3-dibromoadamantane in highly viscous CTFEP could not be explained by isotropic, or by realistically anisotropic, tumbling in a single environment, but only by considering rapid exchange between at least two different environments. Lienin and co-workers pointed out that the tumbling behaviour of small solute molecules in highly viscous solvents such as CTFEP was not as simple as expected when intramolecular motion was taken into account.

### 2.3. Dimethylformamide- $d_7$ (DMF- $d_7$ )/water blend

Pure dimethylformamide (DMF) and water respectively have viscosity values of 0.808 [43] and 0.898 cP [19] at  $25^\circ\text{C}$ , and freezing points of  $-60.5^\circ\text{C}$ , and  $0^\circ\text{C}$ . [44] Their mixture produces a viscous solvent blend whose viscosity and freezing point depend on composition. The melting point can reach temperatures down to  $-100^\circ\text{C}$ . [44] Change of the sign and intensity of NOEs over a wide temperature range is possible due to the ability of the solvent blend to become highly viscous at sub-zero temperatures. In addition, the values of the dielectric constants, respectively to 38.45 and 80.4 for DMF [45] and water [44] at  $20^\circ\text{C}$ , allows a wide range of polar or moderately apolar compounds to be dissolved, provided that the compound of interest is initially dissolved either in DMF- $d_7$  or water alone. Furthermore, similarly to DMSO/water and ethylene glycol/water, the DMF- $d_7$ /water blend is cryoprotective, owing to its very low freezing point and the capability to mimic water behaviour even at sub-zero temperatures, a property that makes it suitable for the study of biomolecules. [44, 46-49] At equal amounts of DMF and water (by volume), the dielectric constant value is similar at  $-20^\circ\text{C}$  to that of pure water at  $+20^\circ\text{C}$ . [44] Even though DMF- $d_7$  is expensive, it is commercially available at a

relatively high enrichment level (99.5%), so that residual proton solvent resonances are weak in the spectra.

An example of the use of DMF- $d_7$ /water blend as cryoprotective solution in the conformational study of enkephalins is described in section 2.12.2.

### 2.4. Dimethylsulfoxide- $d_6$ (DMSO- $d_6$ )

DMSO has a relatively low viscosity (2.20 cP at  $20^\circ\text{C}$ ), [50] but sufficient to enhance the NOE of medium-sized molecules in structure elucidation investigations by 1D and 2D NOE spectroscopy. The observation of relevant negative NOE enhancements in DMSO- $d_6$  should be of general applicability for rigid molecules of molecular weight  $> \sim 700$  g  $\text{mol}^{-1}$  that tumble isotropically in solution, at Larmor frequencies above 300 MHz and at room temperature. In addition, the high dissolution power of DMSO- $d_6$  ( $\epsilon = 46.02$  at  $20^\circ\text{C}$ ) [50] opens the way to NMR investigation of a very wide range of polar and moderately apolar organic compounds.

From the late '70s to date, neat DMSO- $d_6$  has been used in many NMR studies, carried out at various temperatures, for the observation of negative NOE enhancements. [51-93]

The following examples focus on the investigation of several well-known antibiotics such as Vancomycin, Valinomycin, and Ristocetin, all dissolved and analysed in pure DMSO- $d_6$ . This solvent also has the ability to minimize labile proton exchange by comparison to aqueous solutions.

#### 2.4.1. Structural and conformational study of Ristocetin A and B

Ristocetin is a glycopeptide antibiotic produced by the micro-organism *Nocardia lurida*, in two forms A and B which differ in their sugar content. [94] Both forms are known to act by binding to bacterial cell-wall mucopeptides of acyl-*D*-Ala-*D*-Ala structure. [95-97] Cross-linking of the cell wall constituent is then prevented during biosynthesis, inhibiting the growth and consequently leading to cell destruction by

lysis. [98, 99] Both forms were used in the past to treat staphylococcal infections. Ristocetin is no longer used clinically because it gave rise to thrombocytopenia and platelet agglutination. [100] Currently, it is employed in the diagnosis of von Willebrand disease (VWD) and of Bernard-Soulier syndrome.

Williams and co-workers published several studies involving the use of DMSO-*d*<sub>6</sub> [58, 101, 102] for NMR structural and conformational studies of Ristocetin A (MW = 2067.94 g mol<sup>-1</sup>) and for understanding its interaction with a cell wall peptide analogue by means of negative NOEs. [60, 61, 67] The combination of the molecular weight of at least 2050 g mol<sup>-1</sup> and the involvement of spectrometers operating between 270 and 360 MHz (<sup>1</sup>H), under conditions of moderate sample viscosity at room temperature (and above), led to negative NOE enhancements observed by steady-state NOE difference spectroscopy.

In 1979, Williams and co-workers confirmed the structure of the Ristocetin A aglycone by means of <sup>1</sup>H steady-state negative NOEs and analogies between a part of the structure of the antibiotic and that of Vancomycin. [61] They succeeded in proposing the absolute stereochemistry of eight of the nine asymmetric centres. The NMR analysis was carried out from 24 to 70°C on 270 and 360 MHz spectrometers.

The observed negative NOEs allowed the molecular geometry of Ristocetin A to be deduced. Furthermore, in order to reduce the impact of any <sup>1</sup>H spectrum misassignment on the interpretation of NOEs and consequently on the molecular geometry, the authors also combined the NMR results with part of the X-ray structure of Vancomycin. [103] The remaining details of the structure of Ristocetin A were successfully established in the same year (Fig. 10) by the same team during the investigation of the

interaction between the Ristocetin A and bacterial cell wall peptide analogue. They reported the occurrence of slow exchange of the complex of Ristocetin A with peptide Ac-*D*-Ala-*D*-Ala in DMSO-*d*<sub>6</sub> at 30°C and 270 MHz (<sup>1</sup>H), making it possible to map the binding site and thus to establish the molecular basis of the antibiotic action. [60] To achieve this goal, they considered four NOEs between the bacterial analogue peptide and Ristocetin A. As a result, they highlighted the bonding of the carboxyl terminus of Ac-*D*-Ala-*D*-Ala to several amide protons of Ristocetin A (Fig. 11). In 1983, this binding site was validated by the measurement of intermolecular distances in antibiotic/peptide complexes by means of negative time-dependent NOEs extracted from NOE difference spectra in neat DMSO-*d*<sub>6</sub> at 400 MHz (<sup>1</sup>H) (Fig. 12 and Table 1). [67]

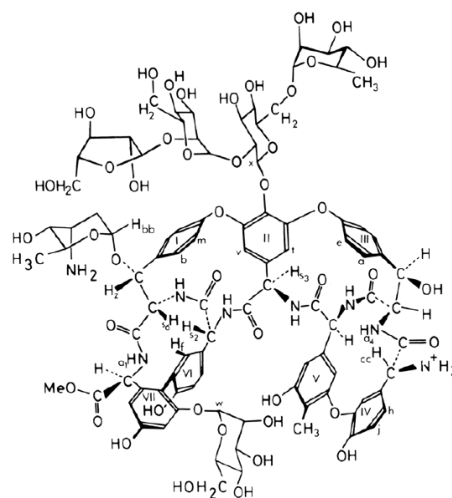
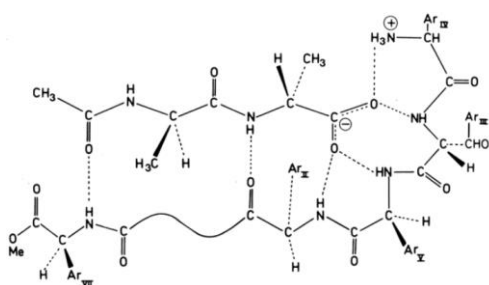
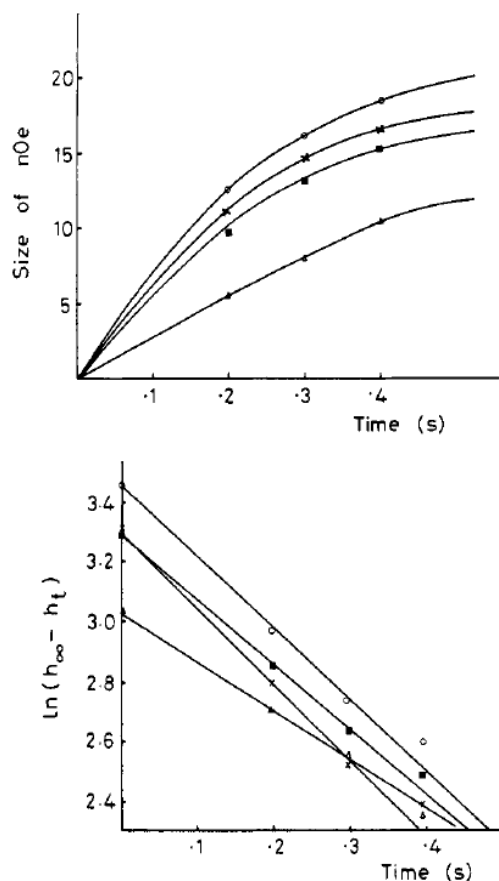


Fig. 10. Chemical structure of Ristocetin A. Reproduced from [67].



**Fig. 11.** A view of the binding of Ac-*D*-Ala-*D*-Ala to Ristocetin A. A portion of the peptide backbone of Ristocetin A which is not involved in binding Ac-*D*-Ala-*D*-Ala by hydrogen bonding is indicated by a curved line, to simplify the diagram. Reproduced from [60].



**Fig. 12.** (a, Upper) Examples of the rate of buildup of the NOE after irradiation of bound alanine methyl protons in the Ristocetin A (Fig. 10)/tripeptide complex:  $\circ$  {Ala<sub>1</sub>β} → e;  $\blacksquare$  {Ala<sub>2</sub>β} → x;  $\times$  {Ala<sub>1</sub>β} → j;  $\blacktriangle$  {Ala<sub>1</sub>β} → w. The irradiation power was sufficient to saturate the irradiated peak essentially instantaneously. The size of the NOE is measured in arbitrary units. (b, Lower) Plot of the data in (a) as  $\ln(h_\infty - h_t)$  against time;  $h_t$  is the size of the NOE shown above at time  $t$ . The gradient of the straight line gives the rate at which the NOE is building up, which is proportional to  $\gamma^{-t}$ . Points at later times are given a lower weighting. Reproduced from [67].

**Table 1.** NOE-Derived Intermolecular Distances for the Ristocetin A. Tripeptide Complex<sup>a</sup>. Adapted from [67].

Proton pair	Distance, Å	Proton pair	Distance, Å
Ala <sub>1</sub> β-e	2.3	Ala <sub>2</sub> β-j	2.4
Ala <sub>1</sub> β-a	> 2.5	Ala <sub>2</sub> β-w	2.2
Ala <sub>1</sub> β-x	2.3	Ala <sub>2</sub> β-f	2.1
Ala <sub>1</sub> β-m	2.3	Ala <sub>2</sub> α-s <sub>2</sub>	2.5
Ala <sub>1</sub> α-j	2.8	Lys ε-CH <sub>3</sub> CO-bb <sub>1</sub>	> 2.6

<sup>a</sup>Distances are  $\pm 0.1$  Å. In each case the first named proton of the pair was irradiated and the NOE buildup to the second observed. In most cases the reverse NOE could not be measured; this is not surprising as NOEs to methyl groups would be expected to be small.

#### 2.4.2. Structural and conformational study of Vancomycin

Vancomycin is the most prominent representative of the family of glycopeptide antibiotics. It is still widely used to treat bacterial infections such as complicated skin infections, bloodstream infections, endocarditis, bone and joint infections, and especially meningitis caused by methicillin-resistant *Staphylococcus aureus*. [104] It was first isolated from a culture of the gram-positive bacterial strain *Amycolatopsis orientalis* in 1956 in a screening program of Eli Lilly and Company. [105] Since then, many structurally related glycopeptides have been isolated from bacterial strains. The activity of Vancomycin relies on its ability to bind selectively to peptides of *D*-Ala-*D*-Ala C-terminal sequence, [95] since mucopeptides terminating in the sequence *D*-Ala-*D*-Ala are precursors involved in cell wall biosynthesis. As for Ristocetin, the binding of Vancomycin to mucopeptides inhibits the cross-linking of the cell wall. [67, 96, 98, 99]

The first attempt to determine the structure of Vancomycin, reported in 1965, deduced the presence of *N*-methylleucine, glucose, and chlorophenol units. [106, 107] However, solving such a complex structure by NMR would have required different experiments and operating frequencies higher than those available at that time.

Williams and co-workers deployed important efforts to solve the structure and the conformation of Vancomycin in the 1970-80s in neat DMSO-*d*<sub>6</sub> [108, 109] by means of steady-state NOE difference spectroscopy. [53, 64, 67]. In 1977, they investigated the structures and mode of action of Vancomycin (MW = 1449.25 g mol<sup>-1</sup>) and Aglucovancomycin (MW = 1143.94 g mol<sup>-1</sup>) in DMSO-*d*<sub>6</sub>, at 270 MHz (<sup>1</sup>H) and

30°C. [53] All detected NOEs were negative (-15 to -50% in intensity), and sufficiently relevant to determine approximate interproton distances. However, the NMR data were not accurate enough to deliver a unique structure for Vancomycin, or a detailed depiction of its binding to Ac-*D*-Ala-*D*-Ala. Despite missing NMR data, they established the connexion between units (1) and (4) through six secondary amide bonds. The structure was completed by a free carboxyl group bounded to the alpha-carbon of ring D and a primary amide group. They also deduced that the sugar Vancosamine and glucose are linked in  $\alpha$  and  $\beta$  anomeric forms, respectively. The site of attachment of the nitrogen atom of aspartic acid was determined, and a carboxyl group was revealed to be part of a biphenyl-2,3'-diyl diglycinate unit. They asserted that Vancomycin was tricyclic, and Ac-*D*-Ala-*D*-Ala binds by inserting into the cavity of this tricyclic structure such that the carboxylate group can be attached to the *N*-methyl groups of leucine.

In 1978, a further advance was then offered by the resolution of the crystal structure of CDP-1, a degradation product of Vancomycin. [103] However, the resulting structure proposal for Vancomycin was incorrect, in particular the conformation of the chlorinated aromatic ring and the incorporation of an isoasparagine residue (rather than of an asparagine residue) was misinterpreted. The former error was corrected in 1981 by Williamson and co-workers, [64] and latter by Harris and Harris, [110] to give the presently accepted structure (Fig. 13).

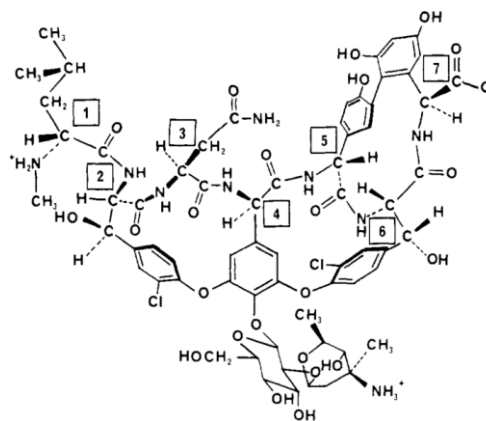


Fig. 13. Structure of Vancomycin. Reproduced from [110].

In 1981, Williamson and co-workers also established the extent to which reaching the negative NOE regime could be useful in structure elucidation. It is still correct to write that the initial rate of buildup of the NOE is proportional to  $\sqrt{\gamma}^{-\epsilon}$  even though spin diffusion may take over at longer irradiation times. As a result, rates of NOE buildup that are derived from data gathered over longer irradiation times will lead to inaccurate (too small) values of  $\sqrt{\gamma}$ . These authors undertook a study of the buildup rates of negative NOEs in the antibiotic Vancomycin [64] to complement the theoretical and experimental studies already published. [111-113] They were able to benefit from appreciable negative NOEs in Vancomycin, for which  $\sqrt{\omega\tau_C} > 1$ , at 270 MHz ( $^1\text{H}$ ) and 35°C. Furthermore, this molecule contains a relatively rigid, approximately globular peptide portion that is favourable for negative NOE detection. Vancomycin turned out to be an ideal model molecule to test the advantages and pitfalls associated with using negative  $^1\text{H}$  NOEs and spin diffusion.

Williamson and co-workers defined a saturation time equal to 6.4 seconds as giving steady-state NOE values  $n_\infty$ . The time  $t_{1/2}$  (s), taken to reach half the steady-state NOE, was used as a measure of the buildup rate of the NOE. They predominately met two issues: steady-state NOEs to isolated protons were often misleading, largely due to exchangeable

protons (-OH and -NH), and even a low-power saturation RF field affected more than one nucleus. With the help of the Bothner-By and Noggle tables, [111] they deduced where NOEs arose directly and not through spin diffusion ( $t_{1/2} = 0.14$  s represented a distance of 2.0 Å). Hence, they defined a map of interproton distances to give detailed structural information on the antibiotic Vancomycin. The main conclusions were in agreement with a previous X-ray structure of CDP-I (a degradation product of Vancomycin). [103] They demonstrated that if spin diffusion was well-recognized, and minimized where necessary with deuterium exchange, 1D NOE difference spectroscopy method was at that time an extremely powerful approach for structure and conformation elucidation of unknown molecules.

In 1983, to understand the mode of action of Vancomycin on bacteria, its binding site with Ac-D-Ala-D-Ala was investigated by means of time-dependent NOE measurements, at 5°C, at 400 MHz ( $^1\text{H}$ ) in a DMSO- $d_6$ /CCl $_4$  (10:3 v/v) binary mixture. [67] The molecular tumbling of Vancomycin alone and of the Vancomycin/Ac-D-Ala-Ala complex were sufficiently slow for relevant negative NOEs to be observable and for intermolecular distances to be deduced (Fig. 14 and Table 2). As a result, the authors managed to define the formation of a "carboxylate anion binding pocket" upon complexation with Ac-D-Ala-D-Ala. This pocket has hydrophobic walls on two sides, composed of aromatic and aliphatic hydrocarbon groups, so consolidating the hydrogen bonds that happen within it. The occurrence of a similar pocket was established in the complex between Ristocetin A and Ac $_2$ -L-Lys-D-Ala-D-Ala. However, in this case, the two walls of the pocket were composed of aromatic hydrocarbon groups.

**Table 2.** Selected NOEs observed for the Vancomycin/Ac-D-Ala-D-Ala Complex<sup>a</sup>. Adapted from [67].

Resonance irradiated	Resonance(s) reduced in intensity, %
a $_4$	i(25), a $_5$ (20), cc(20)
a $_5$	a $_4$ (19), a $_3$ (30), i(17), o(15)
Ala $_1\beta$ bound	d(7)
Ala $_2\beta$ bound	f(7), ii/jj(30)
Ala $_2$ CH $_3$ CO	Ala $_2$ NH bound (15)
Ala $_2$ NH bound	Ala $_2$ CH $_3$ CO (20)
ii/jj	Ala $_2\beta$ bound (25)

<sup>a</sup>Vancomycin/Ac-D-Ala-D-Ala (1:2) in DMSO- $d_6$ /CCl $_4$  (10:3); data recorded at 400 MHz and 5°C.

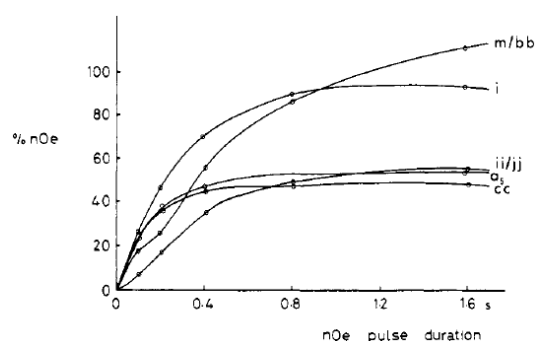


**Fig. 14.** Time dependence of NOEs seen after irradiation of proton a $_4$  in the Vancomycin/Ac-D-Ala-D-Ala complex (~ 10 mM) in DMSO- $d_6$ /CCl $_4$  solution at 5°C. Irradiation duration was 0.1 s. Adapted from [67].

#### 2.4.3. Structural and conformational study of Valinomycin

Valinomycin was first described by Brockmann [114] and synthesized by Shemyakin. [115] It is a naturally occurring cyclic dodecadepsipeptide antibiotic that is known for drastically altering the ionic permeability of natural [116] and artificial lipid membranes. [117] This effect is based on the ability of Valinomycin to form, with high selectivity, a hydrophobic inclusion complex with potassium ions and to transport them through membranes. [118]

The solution structure and conformation of Valinomycin (Fig. 15) have been extensively described in the past. [119-122] In this context, in 1976, Glickson and co-workers decided to use this molecule as a model for investigating the intramolecular  $^1\text{H}$  nuclear Overhauser effect in peptides and depsipeptides, and then to evaluate various models that were proposed for the conformation of Valinomycin. 1D NOE difference

experiments on Valinomycin in DMSO- $d_6$  were carried out at 90 MHz ( $^1\text{H}$ ) (FT mode) and 250 MHz ( $^1\text{H}$ ) (fast passage method). [51, 52] They observed positive NOEs at the lower frequency and negative ones at the higher frequency. (Fig. 16) The signs and magnitudes of the NOEs at 90 MHz and 250 MHz clearly demonstrated that the negative NOEs resulted from a dipolar relaxation mechanism in combination with a long molecular correlation time, and not from exchange modulation of scalar coupling, since this latter effect would not explain the positive NOEs observed at 90 MHz. At 250 MHz operating frequency, a long correlation time due to the size of Valinomycin (MW = 1111 g mol $^{-1}$ ) dissolved in a relatively viscous solvent such as neat DMSO- $d_6$  at 30°C switched Valinomycin from the fast to the slow tumbling regime, allowing the detection of negative NOE enhancements.

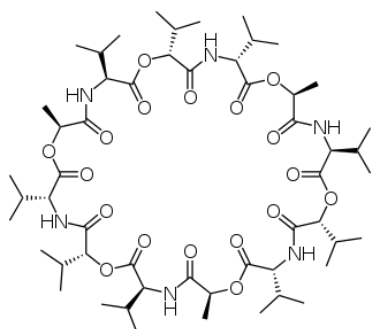


Fig. 15. Chemical structure of Valinomycin.

Because the intramolecular NOE is a sensitive probe of spatial proximity of nuclei, Glickson and co-workers collected enough conformational information from NOE data of Valinomycin at 250 MHz to assess the previously proposed conformational models of Valinomycin in DMSO- $d_6$ . They concluded that the conformation of Valinomycin was different in non-polar solvents and in highly polar solvents such as DMSO- $d_6$ . The “pore” and “core” conformations of Valinomycin detected in non-polar solvents were not maintained in DMSO- $d_6$ . Their NOE data analysis also

indicated that the C1 model of Patel and Tonelli published in 1973 [122] was the most consistent with all the spectral NMR data, NOE and  $^3J_{\text{NHCH}}$  values recorded in DMSO- $d_6$ .

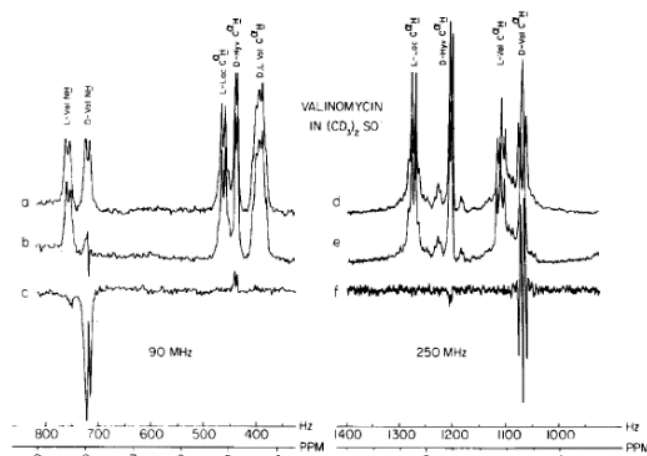


Fig. 16. NOE measurements of Valinomycin in  $(\text{CD}_3)_2\text{SO}$  at 90 MHz by FT-NMR: a) control spectrum, b) spectrum obtained after low power presaturation of D-Val  $\text{NH}$  resonance, c) difference spectrum (spectrum **b** minus spectrum **a** multiplied by a factor of 2.0). NOE measurements at 250 MHz by correlation NMR: d) control spectrum (secondary rf 100 Hz to high field of D-Val  $\text{NH}$  resonance), e) spectrum obtained with saturation of D-Val  $\text{C}\alpha\text{H}$  resonance, f) difference spectrum (spectrum **e** minus spectrum **d** multiplied by a factor of 3.1). Adapted from [52].

### 2.5. Dimethylsulfoxide- $d_6$ (DMSO- $d_6$ )/water blend

The physical properties of DMSO-water blends have been thoroughly studied for more than 50 years. [19, 44, 123-134] Some of the unexpected properties of this blend have been attributed to a very strong molecular cross interaction through hydrogen bonds. [127-129] One of the remarkable properties of DMSO-water blends is their high viscosity compared to those of the pure components. [19, 131, 132] At 25°C, a maximum viscosity of 3.764 cP is measured for a DMSO/water (6.5: 3.5  $\chi/\chi$ ;  $\chi$ : molar fraction) mixture, while pure DMSO and water have viscosities respectively equal to 2.003 and 0.898 cP. [19] Even though the viscosity of the binary solvent mixture at 25°C may be sufficient for the observation of negative NOE enhancements, another advantage of this solvent blend is its great increase in

viscosity upon temperature decrease. For instance, 3- and 10-fold increases in viscosity are achieved respectively for a 30% molar fraction of DMSO in water at 0°C ( $\eta = 9.1$  cP) and -25°C ( $\eta = 32$  cP) compared to 25°C [129] and the freezing point falls down to -130°C. [123, 134]. As a result, the sign and intensity of NOEs can be effectively modulated simply by changing the experiment temperature over a wide range from -130°C to room temperature and even higher. [7] This ability to control the size and number of NOEs turns out to be extremely useful in structural and conformational studies, in particular when several NMR distance constraints are necessary to define three-dimensional structures accurately. [135] So far, many studies have been published taking advantage of the viscosity of DMSO/H<sub>2</sub>O or D<sub>2</sub>O blends for manipulating the NOE intensity in NMR structural and conformational investigations. [47-49, 59, 77, 80, 81, 83, 88, 93, 135-160]

Another advantage of DMSO-*d*<sub>6</sub>/D<sub>2</sub>O blends over other viscous solvents is the high isotopic enrichment (> 99.8%) possible. Other viscous solvents employed (e.g. tetramethylene-*d*<sub>8</sub> sulfone or ethylene glycol-*d*<sub>6</sub>) are commercially obtainable only at a somewhat lower enrichment level (98%), which results in intense residual resonances in the <sup>1</sup>H NMR spectra. Besides, DMSO-*d*<sub>6</sub> and D<sub>2</sub>O are relatively affordable, allowing their routine use. This blend, also called a cryoprotective or cryosolvent [44, 138, 139, 143, 145] due to its low freezing point, mimics water behaviour even at sub-zero temperatures, and is therefore especially appropriate for biomolecular investigations. [44, 59, 80, 81, 141, 143, 146-151, 161, 162] A high value of dielectric constant favours the solubilisation of a wide variety of polar or moderately apolar compounds, provided that the molecule of interest is initially dissolved in the solvent DMSO-*d*<sub>6</sub> or H<sub>2</sub>O (or D<sub>2</sub>O) alone. NMR sample tube preparation, field locking and shimming are easy operations, in contrast to

what happens with other solvents that are highly viscous at room temperature.

In 1987, Fesik *et al.* used the approach of enhancing the negative NOEs of sucrose dissolved in a DMSO-*d*<sub>6</sub>/D<sub>2</sub>O (2:1 v/v) blend by reducing the temperature from 40°C to 0°C. [137] They illustrated how easily the NOE sign can be modulated in 2D NOESY spectra (Fig. 17) recorded at 300 MHz (<sup>1</sup>H). At 40°C and 25°C, the NOEs were positive. In contrast, at 0°C, the NOEs became largely negative because the blend viscosity was three times higher than that measured at 25°C. [129] At 0°C,  $\omega\tau_C$  of sucrose was estimated at from 5 to 10, corresponding to a slow-motion regime and an isotropic tumbling time more reminiscent of a large molecule for which  $\tau_C$  would be from 2 to 5 ns in usual conditions of solvent and temperature.

The authors highlighted the potential to observe large negative NOEs under viscous conditions for structure elucidation and conformational analysis.

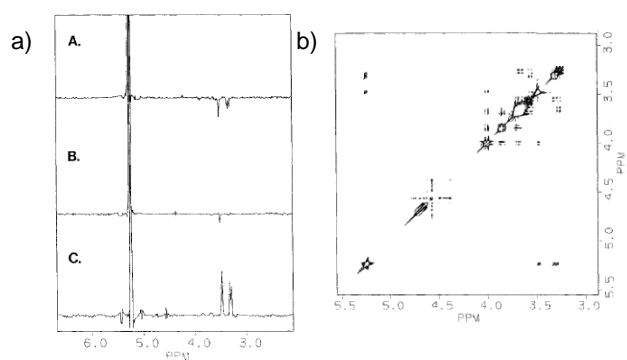


**Fig. 17.** a) Cross-sections of a 2D NOE spectrum of sucrose along the first dimension at the frequency of the anomeric proton of glucose at (A) 40 °C, (B) 25 °C and (C) 0 °C. b) Pure absorption 2D NOE contour map of 10 mM sucrose in DMSO-*d*<sub>6</sub>/D<sub>2</sub>O (2: 1 v/v) at 0 °C. Adapted from [137].

In 1987, Fesik *et al.* also considered the DMSO-*d*<sub>6</sub>/H<sub>2</sub>O (2:1 v/v) blend for the measurement of negative NOEs, with the intent of determining the 3D structure of a cyclic peptide (Fig. 18) designed to inhibit human renin, for the treatment of

hypertension. This study involved 2D NOESY experiments, molecular modelling and molecular dynamics calculations. [135] At 30°C and 500 MHz, the 3-4 fold increase of the blend viscosity compared to that of water alone [19] enhanced the magnitude of the observed positive cross peaks (diagonal peaks phased to be positive as well) from NOESY spectra. 3D structures of this strained cyclic peptide were determined by several molecular modelling techniques integrating proton-proton distances from a quantitative analysis of 2D NOE data and dihedral angles from spin-spin coupling constants. The calculations of interproton distances were accomplished by considering the cross peak and diagonal peak volumes from the 2D NOE spectra, taking multispin effects such as spin diffusion into account in the analysis. [163] They then assumed that the enhancement magnitude for two spins  $i$  and  $j$  after a mixing time  $\tau_m$  was proportional to the cross-relaxation rate, which in turn depends on  $\frac{1}{r_{ij}^6}$ , to give the proton-proton distances. Their 3D structures showed a stable conformation for the macrocyclic ring of the peptide, and the existence of a *cis*-Phe-Ala peptide bond. The authors tried to identify regions of the peptide probably influenced by motional averaging by means of a molecular dynamics trajectory of the cyclic peptide. The resulting distance and angular fluctuations in the cyclic part were very small (i.e. root mean square fluctuations of less than 0.15 Å), highlighting the low probability of a change in the ring pucker of the molecule. In contrast, the noncyclic part of the peptide of the molecule showed considerable flexibility. From the conformational information collected over the study, the authors explained the inability of this cyclic peptide to inhibit human renin by the presence of the *cis* Phe-Ala peptide bond. A computer-generated model of the active site of human renin and the docking of a larger, active, macrocyclic (12 or 14 members) peptide containing a

*trans* Phe-Ala peptide bond were invoked to explain the inactivity of peptide 1.

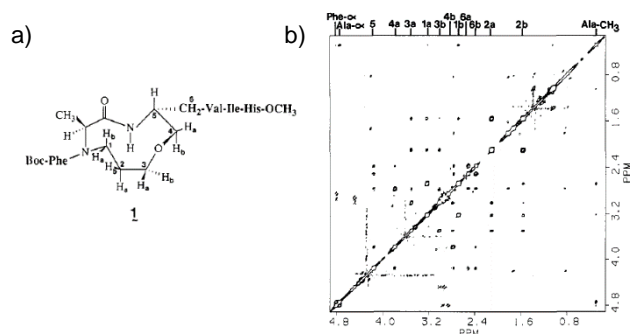


**Fig. 18.** a) Structure of the cyclic peptide 1. b) Portion of a two-dimensional NOE contour map obtained in DMSO- $d_6$ /D $_2$ O (2:1 v/v) at 500 MHz. The assignments of the protons of the macrocyclic ring are given at the top of the plot. Adapted from [135].

In 1988, Nieto *et al.* reported another example of the manipulation of NOE sign and intensity by means of an appropriate increase of the DMSO/water mixture viscosity. [140] They investigated the use of DMSO/H $_2$ O mixtures and water media for investigating sequential H $\alpha$ NH NOEs in three linear peptides of different length: GGRA, LH-RH (10 aa) and Ribonuclease S peptide (20 aa), by means of transient NOESY experiments, at 295 K and 360 MHz ( $^1$ H). They deduced relative internal mobilities from the number, the intensity and the sign of interresidue NOEs, measured at a long mixing time value of 800 ms since small molecules present slow NOE buildup rates. [164] Interresidue NOEs for very small flexible peptides are often difficult to detect owing to conformational averaging [74, 136] and an unhelpful molecular correlation time. [165] The high molecular tumbling rate of GGRA (MW = 359.38 g mol $^{-1}$ ,  $\omega\tau_c < 1$ ) in water at room temperature was responsible for negative NOE cross peaks (positive NOEs) in the NOESY spectra. However, adding DMSO- $d_6$  to water (DMSO- $d_6$ /H $_2$ O; 4:1 v/v) made the observation of positive NOE cross peaks (negative NOEs) possible at the same temperature and magnetic field due to

the increase of the global correlation time  $\tau_C$  of GGRA with the increase of the medium viscosity (Fig. 19 and 20). [19, 131, 132] In comparison, the detection of negative NOEs was possible by using DMSO- $d_6$  (at room temperature for a MW > 700 g mol<sup>-1</sup> ( $\omega\tau_C > 1$ ) from 300 MHz to higher operation frequencies.

In water, LH-RH and S-peptide NOESY spectra display almost fully negative NOE enhancements respectively at 295 K and 297 K. The more the temperature decreases, the more the water viscosity increases, causing the increase of  $\tau_C$  responsible for negative NOEs (Fig. 20).

The authors demonstrated that comprehensive or almost comprehensive sets of sequential H $\alpha$ -NH NOEs can be observed in suitable conditions, which allow sequential assignment of NMR spectra of linear peptides without solution structure. The intensities and signs of the observed NOEs also allow access to relative chain mobilities of the peptides.

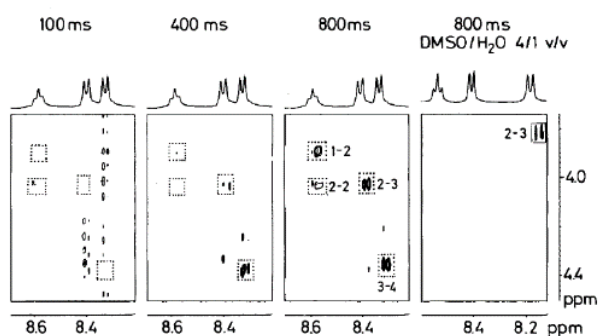


**Fig. 19.** Influence of mixing time and solvent composition on the NOESY spectrum of GGRA (20 mM, 295 K, pH 3.5). (—) Negative NOE; (\*\*\*) positive NOE. Adapted from [140].

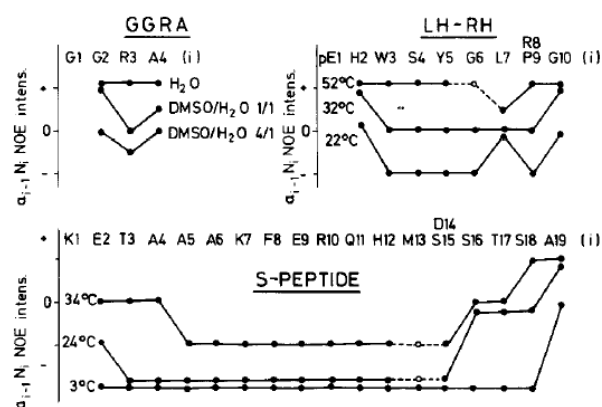


**Fig. 20.**  $\alpha_N$  NOE intensity-sequence profiles of GGRA, LH-RH and RNase S-peptide under various experimental conditions. The NOE connecting residues 14-15 of S-peptide was not seen under any conditions due to the proximity of the D14 H $\alpha$  signal to the irradiated solvent line. NOEs showing reduced intensity for the same reason are shown by open circles. Adapted from [140].

Studies of the application of DMSO- $d_6$ /water blends as cryoprotective mixtures in the determination of bioactive conformations of small linear peptides are described in section 2.12.1.

## 2.6. Ethylene glycol (EG)

EG and its deuterated forms, EG- $d_4$  and EG- $d_6$ , are highly viscous solvents (EG:  $\eta = 17$  cP at 25°C, EG- $d_6$ :  $\eta = 19.9$  cP at 15°C) [21] with a melting point of -12.5°C [44]. In addition, they have a high dissolution power for a large variety of polar compounds owing to the high dielectric constant value ( $\epsilon = 41.8$  at 20°C). [44] Nonetheless, EG- $d_4$  and EG- $d_6$  are quite expensive, and only commercially available at a relatively low enrichment level (98%) which leaves intense residual resonances in <sup>1</sup>H NMR spectra.

Bothner-By *et al.* described in 1978 for the first time the use of EG- $d_6$  for the study of the nature and the extent of spin diffusion in medium-sized molecules, by comparing several idealized limiting models that allowed the calculation of the expected degree of spin diffusion with experimental NOE data. [208] The authors studied the specificity of homonuclear NOE enhancements in the Gramicidin-S (GS)

peptide, by means of steady-state NOE difference spectroscopy (fast passage method) [249-251] at 250 MHz ( $^1\text{H}$ ) and 25°C since the structure and conformation of GS had been well established by NMR and other techniques [54-56, 63, 71, 84, 86, 200, 208-226] including theoretical investigations. [227-229] In neat EG- $d_6$  and  $\text{CD}_3\text{OD}/\text{EG}-d_6$  (25:75, 50:50, 75:25 v/v) binary mixtures, the overall correlation time of the GS backbone was considerably changed (calculated as 14 ns at 25°C in neat EG- $d_6$  according the Debye-Stokes relation), [230] preponderantly due to the high viscosity of EG- $d_6$ . [21] At such long  $\tau_C$  values, proton cross-relaxation behaviour is similar to that of moderate-sized proteins (molecular weight from 10000 to 20000  $\text{g mol}^{-1}$ ) in water, and yields negative NOE enhancements, so that spin diffusion may occur, as was found for the protons of the phenylalanine ring. The relative simplicity of the proton spectrum allowed the authors to observe the effect of irradiation of distinct well-known proton resonances on the intensities of the phenylalanine ring protons (Fig. 21).

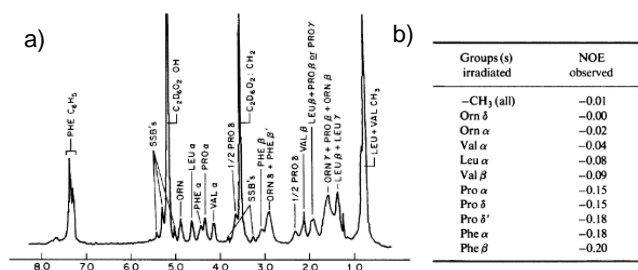


**Fig. 21.** a) 250 MHz proton spectrum of spectrum of gramicidin-S in deuterated ethylene glycol solution. b) Interproton NOE on the D-Phe ring proton signal of gramicidin-S in solution EG- $d_6$ . Adapted from [208].

Theoretical calculation of the NOE and spin diffusion effects expected requires exact geometries and conformational dynamics of GS, and would have involved a heavy computational load. However, the use of simplified ideal models (sequential chain of spins, isolated "islands", two

islands in weak contact and single bridging proton), made it possible to highlight qualitatively the specificity of the effects observed in GS. In particular, the structural and conformational study suggested that there was fast and efficient spin diffusion within closely connected "islands" of protons, and less efficient spin-diffusion between islands. The results were compatible with the accepted solution conformation of GS. [227] The authors highlighted the fact that when  $\sqrt{\omega\tau_C}$  exceeds 25, proton cross-relaxation may become very active, and the possibility of observing selective effects, with the goal of structural and conformational elucidation in particular, may be elusive in large molecules like proteins. Their structured hydrophobic cores will have residues in close contact, so that spin diffusion within the core will probably be fast and extensive. However, side chains with shorter  $\tau_C$  than the overall  $\tau_C$  of the molecule will have fewer close contacts, so they will probably exhibit specific effects. It may be difficult, nonetheless, to find and assign unique resonances to be irradiated (or inverted) in such large and complex molecules. These pitfalls are more easily overcome for small and medium-sized molecules.

In 1986, ethylene glycol- $d_6$  was also considered by LaMar and co-workers for enhancing negative nuclear Overhauser effects, in particular for resonance and structure assignments of paramagnetic heme derivatives in solution. [231] In low-spin ferric complexes, the pattern of heme hyperfine shifted resonances, as sensitive to substituents, has delivered information on the type of  $\pi$  electron distribution [232] and has been used as a model for understanding the heme methyl shift pattern in low-spin ferric hemoproteins. [233] In both cases, isotopic labelling was the only method available at that time for obtaining unambiguous assignments. [232, 233] However, this method was commonly difficult to set up,

time-consuming, and expensive. The nuclear Overhauser effect, [5] showed great promise at that time in accessing supplemental or alternative assignments in proteins, for instance. This could be applied to hemin derivatives, under specific conditions, [69] avoiding several other pitfalls. First was the observation of small or null NOEs at high magnetic field, because of specific reorientation correlation times in the intermediate motion regime. The second was the substantial paramagnetic leakage in the system (iron(III),  $S = 1/2$ ), [234] and the last was that hemin, like all porphyrin and chlorophyll complexes, tends to aggregate strongly. [235] This last problem was dealt with by using very low concentrations in solution, but this complicated even more the detection of small NOEs.

To address these issues, the authors demonstrated that the viscosity of EG- $d_6$  reduced the tumbling rate of the monomeric complex of protohemin-bis cyanide (Fig. 22a) from the intermediate to the extremely slow motion limit in which relevant negative NOE enhancements were readily observed not only by means of saturation of individual resonances, but also by 2D NOE methods. [164] Furthermore, rapidly relaxing paramagnetic complexes did not hamper the observation of relevant negative NOEs.

1D and 2D NOE experiments were performed on protohemin-bis cyanide in methanol- $d_4$  (low viscosity) and in ethylene glycol- $d_6$  (high viscosity). Fig. 22bA shows the 500 MHz proton reference spectrum of protohemin-bis cyanide dissolved in methanol. Saturation for 250 ms of the 3-CH<sub>3</sub> resonance did not yield a useful NOE difference spectrum (Fig. 22bB), indicating that the NOEs were insignificant either because of the rapid motion of the complex in this non-viscous solvent, or because of the paramagnetic leakage, or both. This may be explained by considering that the hemin correlation time value of around 0.14 ns is consistent with the

intermediate motion limit ( $\omega\tau_C \sim 0.4$ ). In contrast, dissolving the hemin complex in EG- $d_6$  (viscosity 30 times greater than methanol- $d_4$ ,  $\omega\tau_C \gg 1$ , slow-motion regime) gave the 500 MHz proton reference spectrum illustrated in Fig. 22bC. Saturation for 250 ms of the 3-CH<sub>3</sub> resonance (Fig. 22bD) created clear NOEs to all expected protons in the vicinity, the 4-vinyl H $\beta$ (*cis*), vinyl H $\beta$ (*trans*), and  $\alpha$ -*meso*-H. This showed that only the rapid reorientation, and not the “paramagnetic leakage,” interferes with the use of NOEs for peak assignments in low-spin ferric hemes.

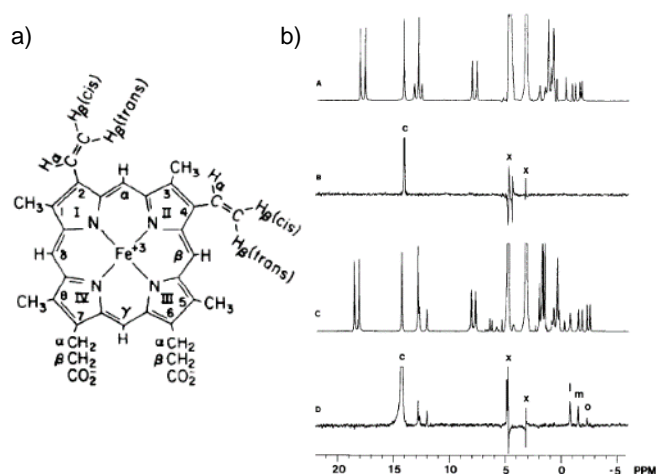


**Fig. 22.** a) Structure of protohemin b) (A) Control <sup>1</sup>H NMR spectrum of 2 mM protohemin-bis cyanide in methanol. (B) NOE difference spectrum at 500 MHz which results from saturation of the 3-CH<sub>3</sub> (peak c) in methanol. No detectable NOEs are observed. Solvent resonances are indicated by X. (C) Control <sup>1</sup>H NMR spectrum of 2 mM protohemin-bis cyanide in ethylene glycol- $d_6$ . (D) NOE difference spectrum resulting from saturation of the 3-CH<sub>3</sub> (peak c) in ethylene glycol, yielding NOEs to the  $\alpha$ -*meso*-H (peak 1), 4-vinyl-H $\beta$  (*trans*) (peak m), and 4-vinyl-H $\beta$  (*cis*) (peak o). A small amount of off-resonance saturation is seen around the 3-CH<sub>3</sub>. Adapted from [231].

NOE enhancements of protohemin-bis cyanide, which were undetectable in a low viscosity solvent such as methanol, were easily observed by means of 1D and 2D NOE techniques in a highly viscous solvent such as ethylene glycol- $d_6$ . The detection of NOE enhancements in highly

viscous solvents opened the way to complete resonance assignments in characterized species, and structure elucidation for unknown complex natural derivatives of hemin.

Two years later, La Mar and co-workers undertook an NMR study of the molecular and electronic structure of the stable green heme extract sulfhemin C from sulfmyoglobin, at 500 MHz ( $^1\text{H}$ ) and  $30^\circ\text{C}$ , dissolved in  $\text{DMSO-}d_6$ ,  $\text{methanol-}d_4$  and in a viscous blend made of  $\text{EG-}d_6$  and  $\text{methanol-}d_4$  (9.5:1.5 v/v). [236] A complete assignment of the proton resonances of low-spin dicyano sulfhemin C dissolved in  $\text{EG-}d_6/\text{MeOD}$  blend was accomplished by a combination of isotopic labelling, differential paramagnetic dipolar relaxation effects, and NOEs from steady-state 1D NOE difference spectroscopy (Fig. 23). They demonstrated that all the functional groups of the precursor hemin were conserved, with the exception of the saturation of pyrrole B to form a cyclic thiolene. The combination of NOEs (detectable in a viscous solvent) and metal-centred relaxation was enough to establish the assignment of the spectra, opening the way to spectral assignment of natural low-spin ferric chlorin complexes.

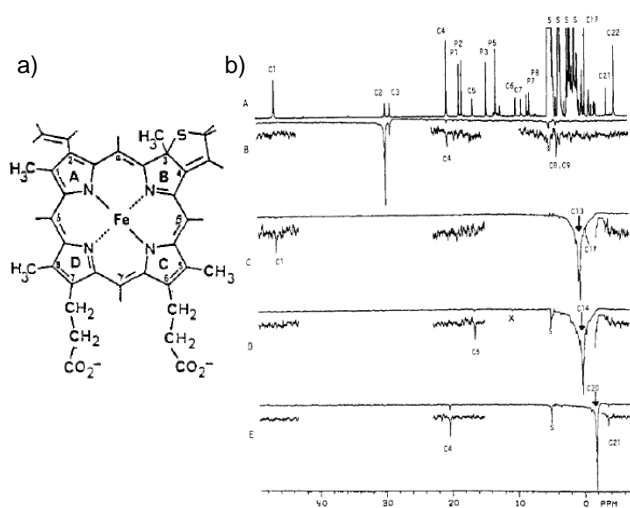


**Fig. 23.** a) Structure of low-spin dicyanosulfhemin C, b) (A) 500-MHz  $^1\text{H}$  NMR spectrum of 3 mM dicyanosulfhemin C (peaks C $i$ ) in 95% ethylene-glycol/5% methanol- $d_4$ . Dicyanoprotohem (peaks P $i$ ) and solvents (peaks S) are also present. NOE difference spectra follow: (B) Irradiation of the more

downfield 6- $\text{H}_a$ , (peak C2) yields NOEs to the geminal 6- $\text{H}_\alpha$  (C3) and 6- $\text{H}_\beta$ 's (C8, C9). (C) Irradiation of the *meso*-H peak C $_{13}$  yields an NOE to the 1- $\text{CH}_3$  (peak C $_1$ ), identifying it as the  $\delta$ -*meso*-H; the 8- $\text{CH}_3$  (peak C $_{17}$ ) exhibits off-resonance effects. (D) Saturation of the *meso*-H peak C $_{14}$  shows NOE connectivity with the 2- $\text{H}_\alpha$  (peak C $_5$ ), identifying it as the  $\alpha$ -*meso*-H. (E) Saturation of the *meso*-H peak C $_{20}$  produces an intensity change in the 5- $\text{CH}_3$  (peak C $_4$ ) and 4- $\text{H}_\alpha$  (peak C $_{21}$ ), assigning it as the  $\beta$ -*meso*-H. Reproduced from [236].

In 1993, Landis and co-workers considered ethylene glycol- $d_6$  as a viscous solvent for investigation of the structural features that explain the observed high enantioselectivity of hydrogenation of methyl (*Z*)- $\alpha$ -acetamidocinnamate (MAC) catalyzed by  $[\text{Rh}(\text{chiral bisphosphine})]^+$  complexes (Fig. 24), by means of 1D transient NOE spectroscopy, at 500 MHz ( $^1\text{H}$ ) and  $10^\circ\text{C}$ . [36] In addition to the olefinic substrate MAC, they considered its isopropyl ester (PRAC) as substrate, as well as the diolefins norbornadiene and cyclooctadiene as ligands. The authors combined the results of NOE measurements with molecular modelling and X-ray data to analyse the solution structures and energetics of several cationic rhodium complexes containing different chiral biphosphine ligands, DIPAMP, CHIRAPHOS and DIPH, (Fig. 24) since the diastereoselectivities for binding the prochiral enamide MAC to these complexes were already identified.

The authors were attached to characterize the solution structures of the catalyst-substrate intermediate, to define the features controlling the binding selectivity, and to illuminate why hydrogenation favoured the less stable intermediate diastereomer.

In  $\text{CDCl}_3$  ( $\eta = 0.596$  cP at  $25^\circ\text{C}$ ) the maximum NOE observed was about +3%, while in  $\text{EG-}d_6$  ( $\eta = 19.9$  cP at  $8.5^\circ\text{C}$ ) it was about -40%, after saturation of various resonances of  $[\text{Rh}(\text{DIPAMP})(\text{MAC})]^+$ , Fig. 25). However, in  $\text{EG-}d_6$ , line broadening was observed. Solvent viscosity has to be chosen to balance NOE enhancements against undesirable resonance line broadening and overlap.

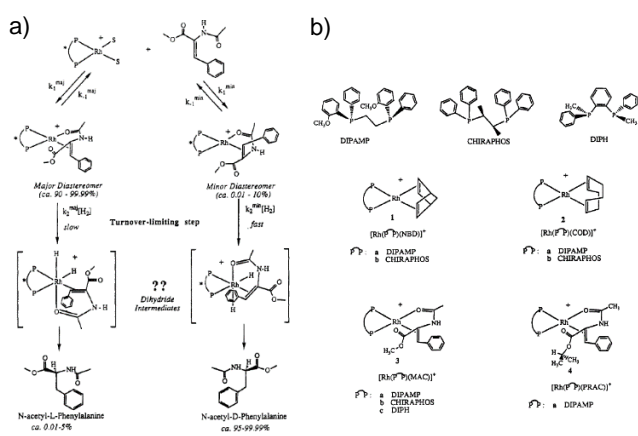


**Fig. 24.** a) Mechanistic scheme for  $[\text{Rh}(\text{chiral bisphosphine})]^+$ -catalyzed asymmetric hydrogenations of prochiral enamides. Question marks accompany the metal dihydride complexes because these proposed intermediates have not been observed experimentally. b) Structures and abbreviations of ligands and complexes examined in this work. Reproduced from [36].

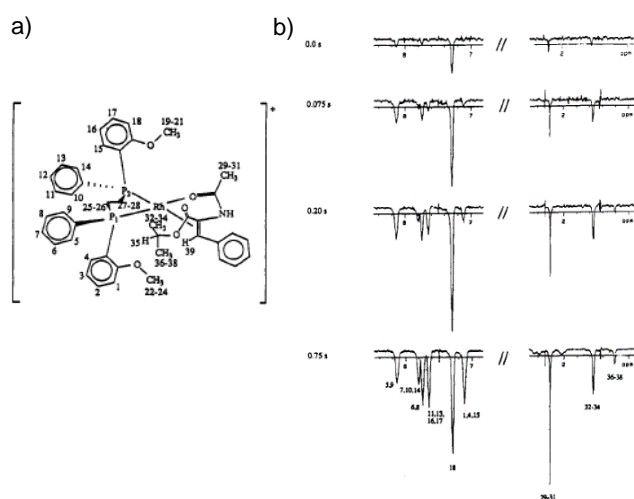


**Fig. 25.** a) Structure of  $[\text{Rh}(\text{DIPAMP})(\text{MAC})]^+$  b) One-dimensional transient NOE spectra obtained at 500 MHz with four mixing times (0.0, 0.075, 0.20, and 0.75 s) after inversion of the anisyl methoxyl resonance (protons 19-21) of 4a in ethylene glycol- $d_6$  at 10°C. Because the NOE enhancements are negative and the spectra are obtained in difference mode, the peaks grow in the direction of negative intensity. Adapted from [36].

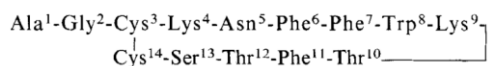
For molecular modelling computations, the SHAPES force field was employed, and for multiconformational analysis of NOE data conformers, Landis and co-workers internally developed and used the CPA (conformer population analysis) method. [35] They demonstrated that these highly selective catalysts showed substantial conformational mobility, so that

the structure could not be considered as a rigid and chiral template. Besides, the solution and solid-state structures were similar, although both molecular mechanics and NOE investigations suggested that multiple conformers could be obtained. The main enantiodiscriminating interaction occurred between the plane of the enamide ester function and the proximal arene ring of the chiral bisphosphine. Molecular mechanics computations seemed to account for the binding diastereoselectivities of the antipodal faces of MAC to the catalysts, but not for the relative reactivity of these intermediates with dihydrogen. Due to the high steric energies computed by molecular mechanics, their work left unanswered questions about the assumed six-coordinate dihydride intermediate in the catalytic asymmetric hydrogenation of prochiral enamides, and hence about the selectivity of the dihydrogen addition reaction.

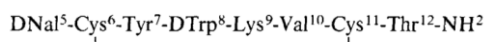
In 1994, Verheyden *et al.* assessed the influence of low temperature and high viscosity on the conformation of somatostatin (tetradecapeptide, MW= 1637.88 g/mol<sup>-1</sup>), that inhibits the release of growth hormone, insulin and glucagon, [237-239] and two agonists DC13-16 (cyclic octapeptide, MW= 1181.48 g/mol<sup>-1</sup>), and DC25-24 (linear octapeptide, MW= 1085.28 g/mol<sup>-1</sup>) (Fig. 26) by means of ethylene glycol- $d_4$  at 303 K and methanol- $d_3$  at 303 K, 243 K, and 193 K, using 2D transient NOESY spectroscopy at 500 MHz (<sup>1</sup>H). [240] Both solvents are alcohols, with similar dielectric constants, [44] thus the influence of solvent type is minimized and temperature and viscosity are the most relevant variables. In this context, they sought to determine the influence of increasing viscosity on the kinetic effect, namely the slowing down of exchange between different conformations, and of lowering temperature on the thermodynamic effect (in addition to the viscosity effect), namely the “freezing out” of the most stable conformations.

NMR experiments previous to those by Verheyden, in methanol at room temperature, revealed that native somatostatin presents a type I  $\beta$ -turn over Trp-Lys, stabilised by a hydrogen bridge between Thr<sup>10</sup> NH and Phe<sup>7</sup> C=O. [241] DC13-116, chosen for reduced flexibility due to a cysteine bridge, showed a  $\beta_{II}$ -turn/ $\beta$ -sheet structure in water, DMSO-*d*<sub>6</sub>, DMSO-*d*<sub>6</sub>/water and methanol. [76, 242, 243] DC25-24, chosen for its better sensitivity to environmental changes, due to its high flexibility, shows conformational averaging in DMSO-*d*<sub>6</sub> at 303 K and in DMSO-*d*<sub>6</sub>/water at 273 K, although at extreme low temperature (down to 193 K) in methanol the conformational freedom is reduced so DC25-24 adopts a  $\beta_{II}$ -turn/ $\beta$ -sheet structure similar to DC13-116. [243]

Somatostatin:



DC13-116:



DC25-24:

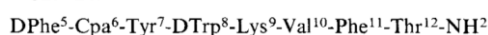


**Fig. 26.** Primary structures of somatostatin, DC13-116 and DC25-24. Reproduced from [240].

The values of <sup>3</sup>J<sub>NH-CaH</sub> coupling constants, amide proton chemical shift variations induced by temperature changes, and relevant negative NOEs suggested that in EG-*d*<sub>4</sub> at 303 K and in methanol at 243 K somatostatin is in equilibrium between a  $\beta$ -turn over Trp-Lys stabilised by a hydrogen bridge between Thr<sup>10</sup> NH and Phe<sup>7</sup> C=O, and a  $\gamma$ -turn around Trp stabilised by a H-bridge between Lys<sup>9</sup> NH and Phe<sup>7</sup> C=O. In EG-*d*<sub>4</sub> at 303K, DC13-16 adopts a  $\beta_{II}$ -turn over DTrp<sup>8</sup>-Lys<sup>8</sup> stabilised by a H-bridge between Val<sup>10</sup> NH and Tyr<sup>7</sup> C=O. In comparison, in methanol at 303 K, almost no NOEs were observed, and many more, but fewer than in EG-*d*<sub>4</sub>, at 193 K (Table 3). DC25-24 in methanol at 303 K yielded hardly any

NOEs, and again many more at 193 K but fewer than in EG-*d*<sub>4</sub> (Table 3). Nevertheless, as previously described [243], by lowering the temperature, DC25-24 evolved from conformational averaging to a predominant conformation resembling the  $\beta_{II}$ -turn/ $\beta$ -pleated sheet conformation of the cyclic DC13-116.

**Table 3.** NOEs observed between (D)Trp<sup>8</sup> and Lys<sup>9</sup>. Adapted from [240].

Somatostatin				DC13-116				DC25-24			
CD <sub>3</sub> OH 243 K		EG- <i>d</i> <sub>4</sub> 303 K		CD <sub>3</sub> OH 193 K		CD <sub>3</sub> OH 243 K		EG- <i>d</i> <sub>4</sub> 303 K		CD <sub>3</sub> OH 193 K	
Trp	Lys	Trp	Lys	$\alpha$ Trp	Lys	$\alpha$ Trp	Lys	$\alpha$ Trp	Lys	$\alpha$ Trp	Lys
NH	C $\alpha$ H	H <sub>4</sub>	C $\gamma$ H	H <sub>4</sub>	C $\alpha$ H	H <sub>1</sub>	C $\alpha$ H	H <sub>1</sub>	NH $\epsilon$	NH	NH
NH	C $\alpha$ H	H <sub>6</sub>	C $\gamma$ H	H <sub>6</sub>	NH	H <sub>1</sub>	C $\alpha$ H	H <sub>1</sub>	C $\alpha$ H	NH	H <sub>4</sub>
				H <sub>6</sub>	NH	H <sub>1</sub>	C $\delta$ H	H <sub>1</sub>	C $\delta$ H	NH	C $\alpha$ H
				NH	C $\alpha$ H	H <sub>1</sub>	C $\gamma$ H	H <sub>5</sub>	NH	NH	C $\beta$ H
						H <sub>1</sub>	NH	H <sub>6</sub>	NH	C $\alpha$ H	C $\gamma$ H
						C $\alpha$ H	C $\alpha$ H			C $\alpha$ H	C $\delta$ H
						C $\alpha$ H	C $\beta$ H			C $\alpha$ H	C $\alpha$ H
						C $\alpha$ H	C $\delta$ H			H <sub>2,6</sub>	C $\beta$ H
						NH	C $\gamma$ H			H <sub>2,6</sub>	C $\gamma$ H
						NH	C $\beta$ H			H <sub>4</sub>	C $\beta$ H
										H <sub>4</sub>	C $\epsilon$ H

The authors pointed out the observation of a larger number of positive NOESY cross peaks (negative NOEs) in ethylene glycol-*d*<sub>4</sub> at room temperature compared to methanol-*d*<sub>3</sub> at low temperature, in particular for the two agonists. This revealed that the increase in medium viscosity inducing lowering of the overall molecular correlation time is a more important factor in reducing peptide flexibility (kinetic effect) than the decrease in temperature (thermodynamic effect). Nonetheless, the linear analogue DC25-24 revealed a thermodynamic effect by the observation of the H-bridge between Val<sup>10</sup> NH and Tyr<sup>7</sup> C=O in methanol at low temperature, highlighting that reducing temperature is a relevant factor in reducing the conformational freedom of linear peptides. Hence, the authors recommended using both high viscosity and low temperature to reduce the conformational freedom of small peptides, so as to influence both the equilibrium and the kinetics of conformational exchange.

## 2.7. Ethylene glycol (EG)/water blend

Neat ethylene glycol (EG) and water have viscosities of 17 cP [21] and 0.898 cP [19] respectively at 25°C, and freezing points of ~ -12.5°C and 0°C. [44] The mixture of the two yields a viscous blend whose viscosity and freezing point depend on the proportions. The freezing point of the blend can be as low as -100°C. [44] The tendency of the solvent blend to become more viscous with increasing EG can facilitate the modulation of the sign and the intensity of NOE enhancements over a wide temperature range. The dielectric constants of 41.8 and 80.4 for EG and water respectively at 20°C [44] allow a wide variety of polar or moderately apolar compounds to be dissolved, but only if the molecule of interest is initially dissolved in one of the pure solvents, either EG or water. As with DMSO/water and DMF/water blends, the EG/water blend is also called cryoprotective, or a cryosolvent, owing to its very low freezing point and ability to mimic water behaviour even at sub-zero temperatures, especially suitable for the investigations of biomolecules. [44, 46-49, 145, 147, 157]

At equal volumes of EG and water, the dielectric constant at -20°C of 80.7 is similar to that of water at 20°C. [44] However, as pointed out earlier, deuterated ethylene glycol (EG-*d*<sub>6</sub>) is quite expensive and commercially available only at relatively low enrichment (98%), which leads to intense residual proton solvent resonances in spectra.

In 1991, complementing the use of a DMSO-*d*<sub>6</sub>/H<sub>2</sub>O cryoprotective mixture (see section 2.5), Amodeo *et al.* investigated the impact of medium viscosity on the solution conformation of the linear hexapeptide deltorphin I (Tyr-*D*-Met-Phe-His-Leu-Met-Asp-NH<sub>2</sub>) [244] in EG-*d*<sub>6</sub>/H<sub>2</sub>O blend, at 400 MHz (<sup>1</sup>H), using 2D transient NOESY experiments (mixing time from 50 to 400 ms). [145] For this purpose, the latter cryoprotective mixture was employed at 295 K, at two ratios, 5:5 v/v and 8:2 v/v, changing the solution viscosity

from 2.5 to 7 cP [245] and the dielectric constant from 60 to 50. [44]

The authors demonstrated that the medium viscosity increase from EG-*d*<sub>6</sub>/water (5:5 v/v) to EG-*d*<sub>6</sub>/water (8:5 v/v) blends was responsible for the intensity increase of the negative NOESY cross peaks, due to the reduction of the molecular overall tumbling rate. The authors reported the likely presence of two families of conformations at 295 K: a folded family consistent with the requirements of the  $\delta$  opioid receptor (~ 30%), and a fully extended family (~ 70%). [147] They ruled out a predominant role for temperature and dielectric constant, since similar conformational effects were observed regardless of the use of EG/water or DMSO/water cryoprotective mixture provided that the medium viscosity was greater than 7 cP in EG/water at 295 K or 10 cP in DMSO/water at 265 K. Folded conformers seemed favoured in high viscosity solution over disordered conformers of similar internal energy, since the latter present larger viscosity activation energies because of the number of intermolecular hydrogen bonds. In addition, the intermolecular bond breakage responsible for the loss of the enthalpic contribution is, in part, compensated by the formation of intramolecular hydrogen bonds.

The use of EG/water and DMSO-*d*<sub>6</sub>/water blends is shown to be relevant for NMR conformational investigations of neuropeptides, since their biological action occurs at synapses; they are expelled by specialized presynaptic vesicles, and reach membrane receptors positioned on the postsynaptic membrane by crossing a cleft. The intersynaptic fluid shows a viscosity greater than that of cytoplasm, [246-248] due to the ordering effect of membrane heads and unstirred layer phenomena. [249] Therefore, the viscosity of this fluid contributes, in addition to the membrane catalysis proposed by Schwyzer, [166] to overcoming the so-called entropic barrier to the transition state of peptide-receptor

interaction, by selecting ordered conformations prior to neuropeptide-receptor interaction.

D'ursi *et al.* in 2007 investigated the conformation-activity relationships of peptide T and new pseudocyclic hexapeptide analogues using three cryoprotective mixtures, EG/water, DMF/water and DMSO/water, by means of 2D NOE spectroscopy at 400 and 600 MHz ( $^1\text{H}$ ) and at 300 K, and of modelling techniques. [48]

Peptide T (ASTTTNYT), a segment (residues 185-192) of gp120, the coat protein of HIV, revealed several major biological properties *in vitro*, such as chemotactic activity, [250, 251] that motivated the authors to design simpler and possibly more active analogues containing the central residues of peptide T responsible for the chemotactic activity. The authors carried out an exhaustive NMR conformation-activity relationship (CAR) study of peptide T and its analogues in different media, supported by modelling methods since there was no consensus on the preferred solution conformation of peptide T despite several published experimental and theoretical studies. [252]

In spite of the small size of peptide T, NOESY spectra recorded in the three cryoprotective mixtures revealed a significant number of diagnostic negative NOE enhancements (Fig. 27). The pattern of NOE correlations was consistent with a preference for the peptide to adopt ordered, folded conformations in the C-terminal region. Due to the medium viscosity, the molecular tumbling rate of peptide T and its analogs was sufficiently reduced that the NOEs were negative.

**Fig. 27.** Partial NOESY spectra of peptide T in three aqueous mixtures: EG/water 80/20 v: v (left), DMF/water 80/20 v: v (centre) and DMSO/water 80/20 v: v (right) at 600 MHz. Adapted from [48]

The results of the CAR investigation were in agreement with the previous experimental conclusion that a  $\beta$ -turn conformation was one of the possible structures of peptide T but did not confirm the assumption that this was the most populated conformation. The experimental conformational analysis of peptide T, based on a "solvent scan" approach, did not solve the question of the conformational preferences of peptide T, but it did provide a firm basis on which to study the pseudocyclic analogues. Peptide T seemed to adopt a  $\gamma$ -turn in EG/water blend, a type IV  $\beta$ -turn conformation in DMF/water blend, and a type II  $\beta$ -turn conformation in DMSO/water blend. The preferred conformations of the analogues came from modelling computations, starting from the preferred conformations of peptide T. The best models arising from the  $\gamma$ -turn conformation of peptide T were those of peptides XII (DSNYSR), XIII (ETNYTK) and XVI (ESNYSR). The best models arising from the type IV  $\beta$ -turn conformation of peptide T were those of peptides XIV (KTTNYE) and XV (DSSNYR). No models with low energy could be extracted for the type II  $\beta$ -turn conformation of peptide T. The analogues with the most strongly preferred conformations were also those active in the chemotactic test. In the light of the CAR investigation, the authors described peptide T as a "chameleon" peptide. They pointed out the need (more than for any other bioactive peptide studied) to know the precise peptide environment before trying to determine the so-called bioactive conformation or the most stable conformation. This "chameleon" behaviour may be related, in part, to the high content of Thr or Ser residues, for which the side chains may favour ordered solvation. The potential role of these residues was inferred from the common orientation of their hydroxyl moieties in both peptide T and the pseudocyclic analogues.

Another examples of the use of EG/water blends as cryoprotective solutions in the conformational study of small linear peptides are detailed in section 2.12.2.

### 2.8. Phosphoric acid- $d_3$ ( $H_3PO_4-d_3$ )

Phosphoric acid- $d_3$  results from the hydrolysis of phosphorus pentoxide (a white crystalline solid) by  $D_2O$ . It easily dissolves salts and is highly viscous ( $H_3PO_4$ /water 9:1 w/w, viscosity 64,75 cP at 25°C) [22].

In 1980, Szeverenyi *et al.* investigated the NOEs of brucine- $d_2$  (MW = 396.5 g mol<sup>-1</sup>), dissolved in perdeuterated 90% phosphoric acid by means of 1D selective transient NOE difference spectroscopy, at 250 MHz (<sup>1</sup>H) and room temperature. [113] Under these operating conditions, the tumbling rate of brucine- $d_2$  slowed down considerably, thus permitting the detection of negative NOEs.

The authors experimentally measured the time-dependent NOEs of brucine- $d_2$  in  $H_3PO_4-d_3$  and compared these data with those calculated with two purposely written computer programs permitting the calculation of the time development of z magnetization after perturbations of spins by RF fields. The authors chose brucine- $d_2$  (Fig. 28) because of its well resolved proton spectrum at 250 MHz. The aromatic protons were exchanged with deuterium to ensure that the olefinic proton resonance was well resolved from all others, since this proton (n°22) was the spin of interest to invert for the transient NOE experiments.  $H_3PO_4-d_3$  was employed to promote negative NOE enhancements and spin diffusion through brucine- $d_2$  owing to its high viscosity slowing down molecular tumbling. Fig. 29 depicts the time dependence of the NOE in brucine- $d_2$  in  $H_3PO_4-d_3$ , at 250 MHz, following 74% inversion of proton 22 in 1D transient NOE difference experiments. In order to compare the experimental results and theoretical predictions, cross-relaxation rates  $\sigma_{ij}$  and

total spin-lattice relaxation rates  $\rho_i$  were calculated [5, 262] by assuming relaxation from nuclear dipolar interactions and a random field contribution from the solvent. After curve fitting, rough agreement with experimental data was obtained assuming a single rotational correlation time of 18 ns and a random field relaxation rate of 0.5 s<sup>-1</sup> (determined from the tail of the decay at long times, for which cross-relaxation is essentially over). This is consistent with brucine being a rigid, nearly spherical molecule with isotropic rotational diffusion. By using Stokes' equation, the correlation time arising from the macroscopic solvent viscosity and approximate molecular volume was predicted to be 12 ns, a value usually observed for larger molecules such as macromolecules.

The authors finally pointed out that the measurement of time-dependent NOEs may provide a practical way to determine proton distances in unknown systems subject to spin diffusion, since initial cross-relaxation rates  $\sigma_{ij}$  are proportional to the inverse sixth power of the distances between observed and inverted protons. However, the cross-relaxation rate  $\sigma_{ij}$  also depends on the molecular correlation time, so the possibility of internal motions or anisotropic reorientation may hamper data interpretation.

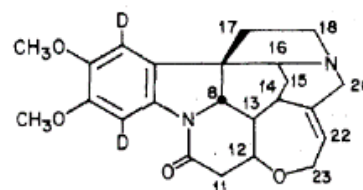
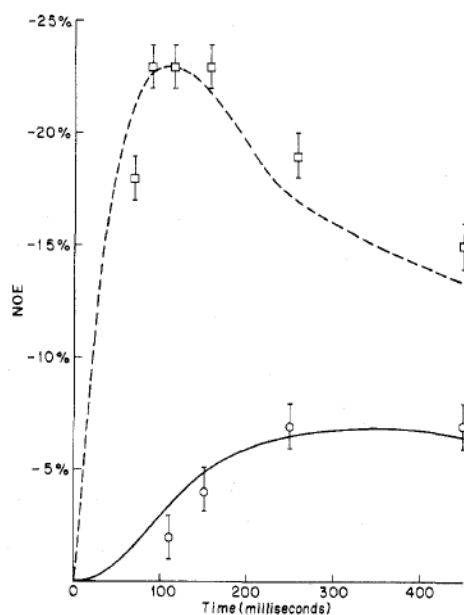


Fig. 28. Chemical structure of brucine- $d_2$ . Reproduced from [113].



**Fig. 29.** Time dependence of the nuclear Overhauser effect in brucine- $d_2$  in solution in deuteriophosphoric acid, following 74% inversion of proton 22. Solid line: calculated dependence with  $\tau_C = 18$  ns,  $\rho^* = 0.5$  s $^{-1}$  for proton 13; (o) experimental points for proton 13. Broken line: calculated dependence for combined signals from protons 14 and 20b; ( $\square$ ) experimental points for protons 14 and 20b (superimposed). Reproduced from [113].

### 2.9. Sulfolane- $d_8$

Sulfolane (2,3,4,5-tetrahydrothiophene-1,1-dioxide) is an inexpensive, colourless, non-reactive dipolar aprotic solvent with important chemical and thermal stability and unusual solvent properties. It is composed of globular molecules and has a moderately high dielectric constant ( $\epsilon = 43.4$  at 300 K) [263] and a high dipole moment ( $\mu = 4.80$  D), [24] allowing NMR investigations on a very wide variety of polar and moderately apolar organic compounds. Sulfolane is also worth considering as a viscous solvent, since it is about 5-fold more viscous ( $\eta = 10.295$  cP at 30°C) [263] than DMSO. However, unlike many other usual NMR solvents, sulfolane- $d_8$  introduces several intense residual proton multiplet resonances into spectra that may overlap with those from the molecule of interest, since it is commercially available only at a relatively low enrichment level (98%). Sulfolane- $d_8$  is also quite expensive.

In 1984, Kartha *et al.* considered sulfolane- $d_8$ , DMSO- $d_6$  and sulfolane- $d_8$ /DMSO- $d_6$  blends for a conformational study of the synthetic cyclopeptide *cyclo(L-Phe-L-Pro-D-Ala)* $_2$  (MW = 630.74 g mol $^{-1}$ ), by NMR at 300 MHz ( $^1\text{H}$ ) and 25/30°C and by X-ray crystallography (crystals grown from a solution of the peptide in DMSO/water mixture). [264] NMR data indicated that the two-*cis* backbone was the main form in solution. However, coupling constant and chemical shift data did not limit the possible backbone conformations to the two-*cis* form. Hence, additional information through the use of sulfolane- $d_8$  was sought from nuclear Overhauser enhancements by means of steady-state 1D NOE difference spectroscopy. In DMSO- $d_6$  at 25°C, no or very weak NOEs were observed among the backbone NH and C $^{\alpha}$ H protons, due to the low rotational correlation time of the peptide ( $\omega\tau_C \sim 1$ ). The use of sulfolane- $d_8$  increased the effective rotational correlation time so that NOE enhancements became negative and hence useful (Fig. 30 and Table 4).

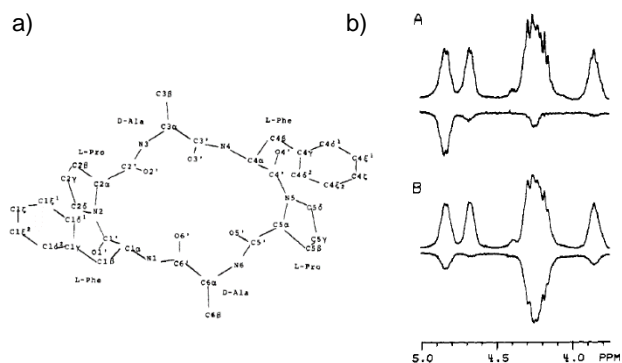


**Fig. 30.** a) Numbering scheme used for *cyclo(Phe-Pro-D-Ala)* $_2$  b) Nuclear Overhauser enhancements in *cyclo(Phe-Pro-D-Ala)* in sulfolane- $d_8$ , at 30°C at 300 MHz. Difference spectra are the lower curves. (A) Irradiation of H $^{\alpha}$ <sub>Phe(cis)</sub> at 4.84 ppm, showing NOE of H $^{\alpha}$ <sub>Pro(cis)</sub> and transfer of saturation to H $^{\alpha}$ <sub>Pro(trans)</sub>. (B) Irradiation of H $^{\alpha}$ <sub>Pro(cis)</sub> at 4.28 ppm and overlapping H $^{\alpha}$ <sub>Pro(trans)</sub> and H $^{\alpha}$ <sub>Ala(trans)</sub>, showing NOE to H $^{\alpha}$ <sub>Phe(cis)</sub>. Effect on H $^{\alpha}$ <sub>Ala(cis)</sub> may be saturation transfer from H $^{\alpha}$ <sub>Ala(trans)</sub>; no NOE is anticipated. Adapted from [264].

**Table 4.** Backbone proton-proton Overhauser enhancements in the two-*cis* form of *cyclo(Phe-Pro-D-Ala)* $_2$ , 25°C. Reproduced from [264].

Solvent <sup>a</sup>	Phe H <sub>N</sub>	Ala H <sub>N</sub>	Phe H <sub>α</sub>	Pro H <sub>α</sub>	Ala H <sub>α</sub>
S	irrad	-0.08	-0.10	-0.08	-0.30
70% S + 30% D	irrad	0	0.04	-0.03	-0.14
$(r^6/\Sigma r^6)_{av}$			-0.07	0	0.44
S	-0.08	irrad	-0.12	-0.20	-0.12
70% S + 30% D	-0.0	irrad	-0.05	-0.13	-0.08
$(r^6/\Sigma r^6)_{av}$			0	0.20	0.07 <sup>b</sup>
S	-0.12	-0.12	irrad	-0.30	-0.04
70% S + 30% D	-0.06	-0.05	irrad	-0.19	-0.03
$(r^6/\Sigma r^6)_{av}$			0.40	0	
S	0.07	-0.30	-0.30	irrad	-0.10
70% S + 30% D	0	-0.14	-0.18	irrad	-0.07
$(r^6/\Sigma r^6)_{av}$			0.56	0.0	
S	-0.25	-0.18	-0.03	-0.10	irrad
70% S + 30% D	-0.13	-0.07	-0.02	-0.05	irrad
$(r^6/\Sigma r^6)_{av}$			0	0	

<sup>a</sup>S = sulfolane, tetramethylene sulfone; D = dimethyl sulfoxide,  $(r^6/\Sigma r^6)_{av}$  is the fraction of a maximum NOE to be expected for the conformation found in the crystal. Protons within 3 Å of the observed proton are included in the sum. <sup>b</sup>For  $\psi_{D-Ala} = -60^\circ$ ,  $r^6/\Sigma r^6$  is calculated to be 0.26 if  $\varphi_{D-Ala} = -120^\circ$  and 0.47 if  $\varphi_{D-Ala} = +60^\circ$ .

The authors considered both sulfolane-*d*<sub>8</sub> and the sulfolane-*d*<sub>8</sub>/DMSO-*d*<sub>6</sub> (7:3 v/v) blend, since the latter solubilizes cyclopeptides sufficiently for <sup>13</sup>C NMR spectra acquisition. In sulfolane-*d*<sub>8</sub>, negative NOE enhancements up to -30% were obtained. Good agreement was finally reached between interproton distances determined from X-ray crystallography and steady-state 1D NOE difference experiments, indicating a similar solution conformation for the two-*cis* form of *cyclo(L-Phe-L-Pro-D-Ala)*<sub>2</sub>.

Gierasch *et al.* in 1985 also employed sulfolane-*d*<sub>8</sub> as a viscous solvent in the study of the conformation-function relationship of a synthetic hydrophobic hexapeptide *cyclo(D-Tyr(Bzl)-Gly-Ile-Leu-Gln-Pro)* (MW = 761.8 g mol<sup>-1</sup>) by means of 2D transient NOE spectroscopy, at 250 and 500 MHz (<sup>1</sup>H) and at 40°C. [265] The authors designed and synthesized this peptide as a model of the internal face of a β-turn from the protein lysozyme, so as to address biochemical problems inherent to hydrophobic environments. At that time, much of

the work carried out on polypeptide conformation dealt with isotropic aqueous solutions, while many critical biochemical functions obviously take place in anisotropic, hydrophobic environments away from bulk water, most often close to membranes.

At 250 MHz, and even more so at 500 MHz, the high viscosity of the NMR solvent allowed the overall correlation time of the cyclic hexapeptide to be increased in such a way that negative NOE cross peaks were sufficiently enhanced to allow observation of conformationally relevant data. The peptide stiffness due to the ring also favoured the NOE enhancements. Hence, intra and interresidue NOEs such as NH-NH interactions were observed between the (i + 3)<sup>th</sup> residue and the (i + 2)<sup>th</sup> residue within the β-turns: GlyNH to Tyr(Bzl)NH and LeuNH to GlnNH (Fig. 31). In contrast to the distribution of conformations that often occurs in flexible peptides, the cyclic model peptide in sulfolane-*d*<sub>8</sub> revealed the existence of a strongly preferred conformation made up of two linked β-turns, one with the same sequence Gly-Ile-Leu-Gln and geometry type I as the protein turn, and the other of geometry type II involving Gln-Pro-Tyr(Obz)-Gly (Fig. 32). A similar result was obtained when the cyclic peptide was dissolved in a chloroform/dimethylsulfoxide (98:2 v/v) blend.

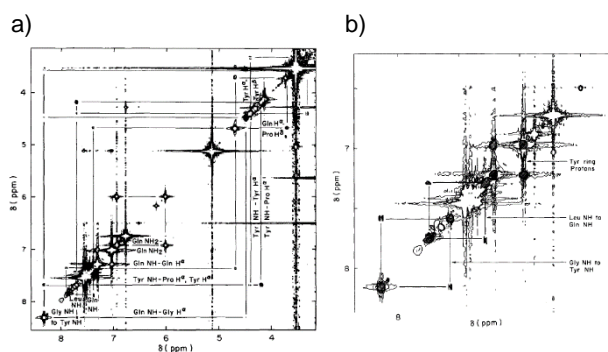


**Fig. 31.** a) Two-dimensional NOESY spectrum at 500 MHz of the cyclic hexapeptide shown in Fig 37 in sulfolane-*d*<sub>8</sub>, 5 mg/0.5 mL, 40°C. Several of the observable NOEs are labelled. This spectrum was obtained on a JEOL GX500. Parameters: 2048 points in the *F*<sub>2</sub> direction, 512 zero-filled to 1k in the *F*<sub>1</sub> direction, sweep width 5000 Hz, 64 scans, trapezoidal window, magnitude

calculation, (90- $t_1$ -90- $t_m$ -90) pulse sequence with  $t_m = 150$  ms. b) Expansion of the same data. Adapted from [265].

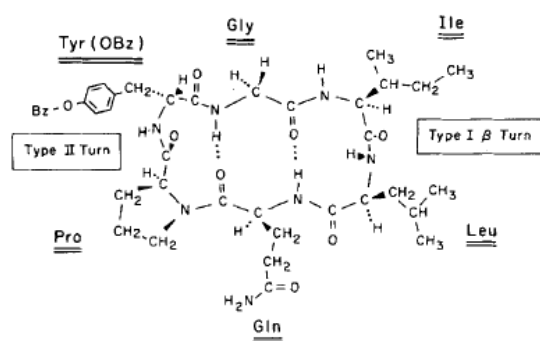


**Fig. 32.** Diagram of the proposed conformation of the cyclic hexapeptide model for the interior  $\beta$ -turn from lysozyme. Reproduced from [265].

## 2.10. Supercooled water

Supercooled water turns out to be of prime interest in the manipulation of nuclear Overhauser effects of small and medium-sized molecules at sub-zero temperatures, especially for metabolomic studies. Chemical shift values for non-labile protons of organic compounds of interest at sub-zero temperature are similar to those observed at room temperature, in contrast to what is observed with other viscous solvent systems such as DMSO/water, ethylene glycol, glycerol, glycerol carbonate, etc.

Supercooling refers to the lowering of the temperature of a liquid below its freezing point without it becoming a solid. At atmospheric pressure, the lowest freezing temperature for water was achieved in 1947, at  $-41.2^\circ\text{C}$  for  $1\ \mu\text{m}$  diameter droplets in cloud chambers. [266] Mossop published afterwards in 1955 that the lowest freezing temperature of high purity water in glass capillary tubes was  $-34.5^\circ\text{C}$  for a volume of  $0.6\ \mu\text{L}$ . [267] Chahal and Miller established in 1965 a relationship between the glass capillary tube diameter and the water freezing temperature. [268-270] Later, in 2011, the results of simulations and classical nucleation theory suggested that the temperature of crystallization of water

could reach a minimum of around  $-48^\circ\text{C}$ . [271] Interestingly, the dielectric constant of water increases nearly linearly from  $\sim 80$  at room temperature to  $\sim 95$  at  $-15^\circ\text{C}$ . This allows a wide range of polar organic compounds to dissolve. The viscosity of supercooled water also depends on temperature. For instance, the viscosity of supercooled water at  $-23.8^\circ\text{C}$  obtained by means of a capillary flow technique is 6 times higher than that of room temperature water. [269, 272-275]

To date, several NMR studies have involved supercooled water without addition of cryosolvent, either at atmospheric pressure in micro-emulsions (or reverse micelles), [276-283] in glass capillary tubes, [283-298] and in polymer gels, [299-302] or at high pressure by means of suitable NMR equipment (see section 2.11) [269, 303-312]

### 2.10.1. Micro-emulsions

The generation of micro-emulsions, or reverse micelles with smaller volumes, have been considered several times for studying the structure and dynamics of organic compounds such as synthetic polymers or proteins using analytical techniques including NMR spectroscopy. [276-283] Due to the very small volume and the absence of heterogeneous ice nucleation sites at the water interface, a water freezing temperature from  $-35$  to  $-45^\circ\text{C}$  can be reached. However, it may be quite challenging to record NMR high-resolution spectra, in particular for large molecules such as proteins, and their behaviour in contact with water may be altered. [282]

### 2.10.2. Glass capillaries

Supercooled water in glass capillary tubes has also been employed for structure and dynamics NMR studies of organic compounds such as carbohydrates, nucleic acids and/or proteins, by taking advantage of the reduction in the exchange rate of labile protons, of internal mobility, and of

reduced conformational exchange at a sub-zero temperature. [283-298] Indeed, the use of glass capillary tubes with outer diameters of 1.0 mm placed in 5 mm NMR tubes allowed -15°C to be reached. Hence, supercooled water in glass capillary tubes made it possible to obtain insights into dynamics, hydration, and cold-induced denaturation of biomolecules. [283, 288-290, 292, 293, 297, 298] By comparison, the use of conventional 5 mm NMR tubes allows a freezing temperature of -5 to -10°C to be reached for unperturbed aqueous biomolecule solutions (using filtration and centrifugation to remove free particles). [313] The use of extremely narrow capillaries (20 µm i.d.) allowed the freezing point of water to be lowered close to -35°C. [314] However, the resulting spectral sensitivity would probably be too poor for NMR studies owing to the very low amount of material of interest dissolved in the supercooled water.

### 2.10.3. Polymer gels

The handling of glass capillaries may be cumbersome and the small sample volume may result in a poor NMR sensitivity. Overcoming these problems may be possible with higher sample concentrations, but these may then give rise to problems with aggregation or precipitation of solutes. In addition, the time needed to reach the supercooled state of interest is long (-1°C per hour cooling rate is needed below -5°C). [283] An alternative way to take advantage of supercooled water is by using polymer gels such as polyacrylamide (combined or not with polyethylene glycol) or agarose gels swollen by different aqueous solutions. They were involved many times in the NMR studies of structure and dynamics of organic compounds such as peptides, proteins, nucleic acids and disaccharides in a confined environment. [299-302, 315-317]

Pastore *et al.* in 2007 used agarose gels for natural abundance NMR studies of the synthetic neuropeptide [Ala]<sup>20</sup>NPS [300] as a very flexible bioactive peptide, and of the hen egg white (HEW) lysozyme as an example of a heat-resistant protein. Agarose gel is more usually employed for the separation of biological molecules by electrophoresis, although it had already been proposed as a medium for the investigation of the effect of molecular confinement on the conformational dynamics of apomyoglobin. [316] The major issue in sample preparation is the addition of the biological material of interest to agarose powder previously dissolved in water at high temperature (60-90°). Peptide or protein solutions may suffer from the high temperature used, thus precluding structural and conformational NMR studies. In practice, solute exposure to heat lasts only a few minutes, so sample preparation is possible for the reasonably heat-resistant peptides or proteins. The very viscous hot sample solution may also be difficult to transfer into a 5 mm NMR tube. As a workaround, the authors proposed dissolving the required amount of agarose directly inside a 5 mm NMR tube and then adding the biological material solution.

Interestingly, due to the rigidity of the agarose gel, all the sugar proton resonances are too broad to be detected in liquid-state <sup>1</sup>H NMR experiments, making natural abundance NMR studies of unlabelled peptides or proteins possible. The 1D proton spectrum of HEW lysozyme in a 1.5% agarose gel, at pH = 6.5 and 25°C, is very similar to that recorded in bulk water at pH = 1.9 (Fig. 33). The encapsulation of lysozyme in the gel does not change its 3D structure.

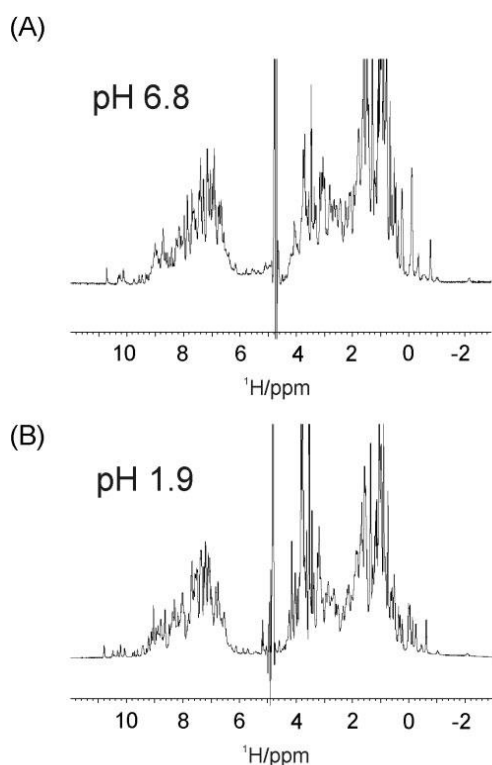


**Fig. 33.** NMR spectra of HEW lysozyme in 1.5% agarose gel at 25°C. (A) 600 MHz  $^1\text{H}$  1D spectrum of 1.5 mM HEW lysozyme in phosphate buffer at pH 6.8. (B) 600 MHz  $^1\text{H}$  1D spectrum of 1.7 mM HEW lysozyme at pH 1.9. Adapted from [300].

[Ala]<sup>20</sup>NPS belongs to a family of flexible peptides with little or no structure in water. Structure-activity relationship studies to determine the main requirements for biological activity have been exhaustively undertaken in the past. [320, 321] However, conformational inducement was not clearly explored. Pastore *et al.* posited that confinement of NPS in agarose gel might induce some degree of folding, as observed for enkephalin in PAG. [299] They investigated [Ala]<sup>20</sup>NPS in agarose gel at two different concentrations (1.5% and 4%) and with addition of a crowding agent, at low temperature, and in bulk water, at room temperature. They observed once again that the gel was  $^1\text{H}$  NMR transparent at both concentrations. The two proton NMR spectra were almost identical, suggesting that the gel pore size was too large to induce the desired folding of the peptide. Adding a known crowding agent such as Ficoll 400 to the agarose gel

did not give rise to substantial peptide structure. [322] However, the agarose gel did allow relevant negative NOE enhancements to be observed as a result of the increased viscosity of supercooled water at sub-zero temperature. At -8°C the 600 MHz  $^1\text{H}$  NOESY spectrum of NPS dissolved in 1.5% agarose gel revealed a great improvement in the intensity and number of NOE cross peaks compared to that recorded at 25°C (Fig. 34). The apparent induction of structure in [Ala]<sup>20</sup>NPS at -8°C is full of promise for future NMR studies of many types of flexible peptides such as hormones. Reaching sub-zero temperatures by means of agarose gels, without adding chemicals or increasing pressure, offers potential insights into dynamics, hydration, cold denaturation, hydrogen/deuterium exchange rates, or fast exchanging process of labile protons of biomolecules. In addition, agarose gels seem to be more practical to use than capillary tube bundles. [283-298]

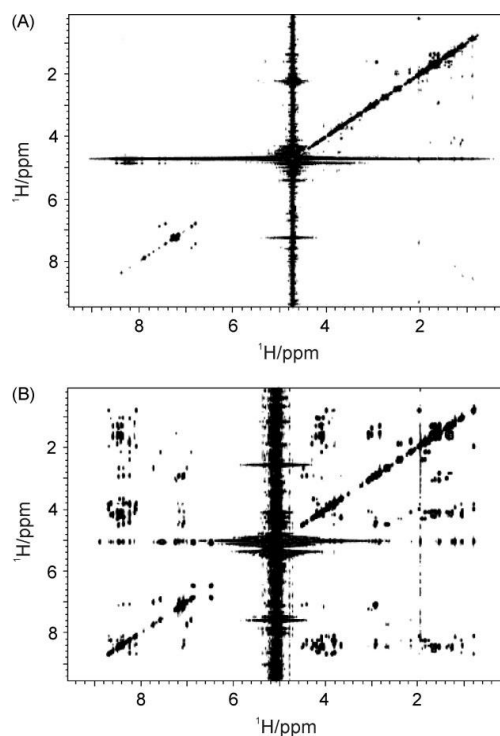


**Fig. 34.** Comparison of 600 MHz  $^1\text{H}$  NOESY spectra of a natural abundance sample of [Ala]<sup>20</sup>NPS dissolved in 40 mM phosphate buffer at pH 6.8 and embedded in a 1.5% agarose gel. (A)  $^1\text{H}$  NOESY spectrum at 25°C with a

mixing time of 400 ms. (B)  $^1\text{H}$  NOESY spectrum at  $-8^\circ\text{C}$  with a mixing time of 400 ms. Reproduced from [300].

In 2012, Spring *et al.* also considered supercooled water in agarose gel for the study of small molecules. [302] They investigated the NMR structures of  $C\alpha\text{AG}$  oligonucleotide, sucrose and tripeptide GGR all 1D and 2D homonuclear and heteronuclear experiments, at 600 MHz ( $^1\text{H}$ ), with 5 mm and 8 mm probeheads for sample preparation convenience and higher NMR sensitivity.

Sample preparation in agarose gel is relatively simple. However, as mentioned by Pastore *et al.* in 2007, [323] during this process, molecules of interest mixed with agarose powder in a water bath must survive temperatures around  $90^\circ\text{C}$  for the melting of standard agarose, and around  $65^\circ\text{C}$  for low-melting point agarose. These may turn out to be excessive for heat-sensitive proteins but are much less critical for stable small molecules such as nucleic acids, peptides or saccharides. In addition, NMR signal line sharpness can be strongly affected in the case of inhomogeneously prepared samples, owing to partially unmelted agarose or incorporation of air bubbles. The solution is to melt the sample again inside the NMR tube, then to mix it thoroughly and cool again to ambient temperature. Agarose does not chemically react with most biomolecules and organic compounds, and DNA, RNA and proteins can be recovered from agarose gels. [324, 325] The authors reported routinely reached freezing points of  $-13^\circ\text{C}$  and  $-9^\circ\text{C}$  respectively with  $\text{H}_2\text{O}$ - and  $\text{D}_2\text{O}$ -based 1% agarose gels. Changing the agarose percentage to 2% did not have any influence on the freezing point of the sample. Freezing of the sample did not break the NMR tube, allaying concerns regarding the loss of precious biomolecule samples or damage to the NMR probehead. In contrast to the use of glass capillaries, the agarose gel method allows quick

reduction of the temperature sample to  $-5^\circ\text{C}$  followed by a decrease of  $-1^\circ\text{C}$  in 10 min. [283] Interestingly, the NMR line shape of a 50 mM sucrose sample dissolved in agarose gel was similar to that obtained without gel at room temperature. Furthermore, NMR  $^1\text{H}$  and  $^{13}\text{C}$  signals from agarose gel were not visible at  $-7^\circ\text{C}$  in a standard  $^1\text{H}$ - $^{13}\text{C}$  HSQC spectrum. The authors highlighted the influence of supercooled water on the molecular tumbling of the sucrose sample (Fig. 35A) by means of 2D transient NOESY experiments recorded in  $\text{D}_2\text{O}$ -based 1% agarose gel at  $-7^\circ\text{C}$  and in bulk  $\text{D}_2\text{O}$  at  $17^\circ\text{C}$ .

It was clear from the NOESY spectrum of sucrose at  $-7^\circ\text{C}$  that longitudinal cross-relaxation was dominant, owing to the presence of full positive cross peaks corresponding to negative NOE enhancements. This may simplify the quantitative use of NOESY for structure determination of small molecules at intermediate magnetic field strengths for which NOE enhancements are usually close to zero.

The authors also probed the effect of supercooled water on the conformational dynamics of an alpha anomeric adenosine ( $\alpha\text{A}$ ) within a DNA oligonucleotide at the very low concentration of  $30\ \mu\text{M}$  (Fig. 35B). They demonstrated the presence of a weak base pair in this duplex by revealing the presence of an imino proton resonance sharpening from  $17^\circ\text{C}$  to  $-8^\circ\text{C}$  due to the reduction of base opening rates and solvent exchange at sub-zero temperatures. [326] NOESY experiments also allowed the base pair connectivity to be determined.

They also reported the reduction of labile proton exchange in supercooled water for a small disordered tripeptide GGR dissolved in 1% agarose gel prepared in  $\text{H}_2\text{O}/\text{D}_2\text{O}$  (9:1 v/v). At  $-8^\circ\text{C}$ , amide protons of G2, R3 and NH of R3 were observed, while at room temperature only the amide proton of R3 was detected.

Although sample preparation may be problematic for thermosensitive biomolecules, NMR in supercooled water

captured in agarose gel turns out to be a relatively simple and convenient method for studies of small molecules because of easy shimming, the absence of  $^1\text{H}$  and  $^{13}\text{C}$  NMR signals of agarose gel, well-resolved spectra of solutes, easy recovery of solutes, and no NMR tube breakage risk below freezing point.

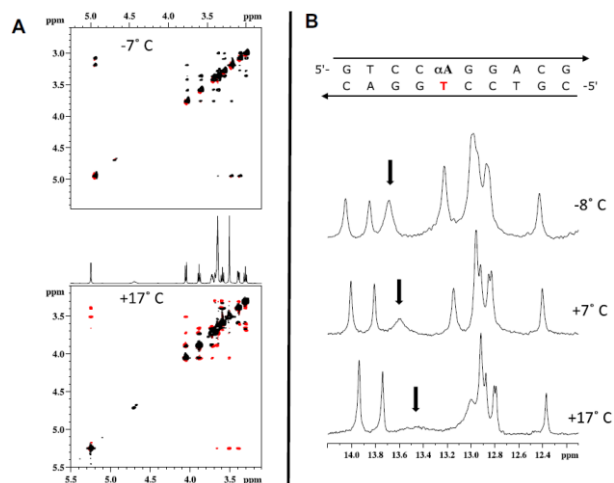


**Fig. 35.** (A) 50mM sucrose spectra from agarose gels (1%) in  $\text{D}_2\text{O}$  at 600 MHz. The top and bottom panels are phase-sensitive NOESY spectra at  $-7$  and  $+17^\circ\text{C}$ , respectively (16 scans, 512 increments,  $90^\circ$  shifted sine-squared function). Red and black peaks denote negative and positive peaks, respectively. The middle spectrum is  $^1\text{H}$  at  $+17^\circ\text{C}$ . (B)  $\text{C}\alpha\text{AG}$  oligonucleotide (30  $\mu\text{M}$  oligonucleotide, 16 000 scans 10 mM sodium phosphate, and 100 mM NaCl, pH 6.8) in 1% agarose at 600 MHz. The top panel is the sequence of  $\text{C}\alpha\text{AG}$  oligonucleotide, and the three spectra in the bottom panel are the  $^1\text{H}$  NMR imino proton region (jump and return solvent suppression). [326] The resonance noted with an arrow is the thymine imino proton base-paired with the  $\alpha\text{A}$ . Reproduced from [302].

This approach is also pertinent for structure and dynamics NMR studies of larger compounds such as carbohydrates, nucleic acids or proteins, taking advantage of the reduction of in the exchange rate of labile protons, of internal mobility, and of slow conformational exchange at sub-zero temperatures.

An example of the use of polyacrylamide gel swollen in  $\text{DMSO-}d_6/\text{water}$  cryoprotective solution in the conformational study of enkephalins is detailed in section 2.12.3.

## 2.11. Viscous solvents under high pressure

It is well known that the viscosities of liquids increase under pressure (from atmospheric to higher pressure) at a given temperature. [303, 305, 306, 310, 327-335] In addition, the use of high pressure makes it possible to extend the measurement temperature well above the boiling point and below the freezing point. [305, 306] However, pressure as an experimental variable in NMR studies, in particular for protein folding investigations, involves some unusual NMR instrumentation. [309-312, 336] Small and mid-sized molecules may show increased NOEs under viscosity enhancement promoted by increased solution pressure.

### 2.11.1. Model membrane systems in $\text{D}_2\text{O}$

$\text{D}_2\text{O}$  is a relatively low viscosity solvent ( $\eta = 1.679$  cP and 1.251 cP respectively at 10 and  $20^\circ\text{C}$ ) [337, 338]. Jonas *et al.* demonstrated the pressure dependence of the  $\text{D}_2\text{O}$  viscosity: [305] at  $10^\circ\text{C}$  and 6 kbar, the value of the viscosity of  $\text{D}_2\text{O}$  is 2.16 cP. As a result, a pressure increase may facilitate a change in sign and intensity of the NOE.

Jonas *et al.* investigated in 1990 the structure and dynamic properties of model membranes such as phospholipids in  $\text{D}_2\text{O}$ , at high pressure and by means of 2D NOESY spectroscopy, [339] since understanding biomembrane structure and function was and is still of prime interest. Phospholipid membranes show a reversible phase transition from gel to liquid-crystalline state depending on temperature. Below a specific temperature  $T_m$ , the lipid bilayers are in an ordered gel state ( $L_\beta$ ), characterized by a relatively rigid packing of their long hydrocarbon chains. Above  $T_m$ , the lipid bilayers are in a fluid-like state ( $L_\alpha$ ) with large conformational disorder along the hydrocarbon chains. The authors built a dedicated NMR probehead operating at 180 MHz ( $^1\text{H}$ ) [340] and recorded 2D phase-sensitive NOESY spectra of model membrane sonicated vesicles made of 1-palmitoyl-2-oleoyl-*sn*-glycero-3-phosphatidylcholine (POPC) and 1,2-



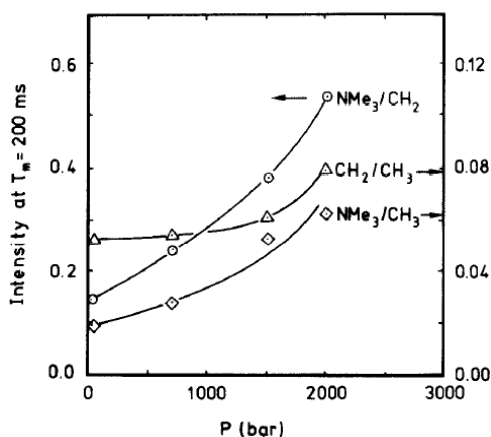


**Fig. 38.** Intensities of the CH<sub>2</sub>/CH<sub>3</sub>, CH<sub>2</sub>/NMe<sub>3</sub>, and CH<sub>3</sub>/NMe<sub>3</sub> cross peaks at a mixing time  $\tau_m = 200$  ms in sonicated vesicles of DMPC at 64°C as a function of pressure. The estimated error in the intensity is  $\pm 10\%$ . Adapted from [339].

### 2.11.2. Ethylhexylbenzoate-*d*<sub>22</sub> under high pressure

In 1993, Jonas and co-workers reported the use of liquid 2-ethylhexyl benzoate-*d*<sub>22</sub> (EHB-*d*<sub>22</sub>) as viscous solvent ( $\eta_{EHB} = 6.77$  cP at 20°C) [345] for structure and conformation investigations of 2-ethylhexyl benzoate (EHB, MW = 234.16 g mol<sup>-1</sup>, Fig. 39) at -20°C and 0°C under pressure from 1 to 3000 bar, by means of 2D NOESY experiments involving a purpose-built spectrometer operating at 180 MHz (<sup>1</sup>H), and of molecular mechanics calculations. [346]

**Fig. 39.** Chemical structure of Ethylhexylbenzoate.

The pressure increase changed the motional behaviour of the small EHB molecule in solution from a fast to a slow motion regime, causing the efficient homonuclear longitudinal cross-relaxation responsible for rapidly-growing and large positive cross peaks in phase-sensitive NOESY spectra (Fig. 40 and 41). However, resonance broadening occurred at high pressures.

The authors determined the intramolecular cross-relaxation rates of EHB by measuring cross peak buildup rates as a function of the mole fraction of EHB in EHB-*d*<sub>22</sub>, after normalizing NOE cross peak intensities. [164, 347-349]

Extrapolated cross-relaxation rates at infinite dilution were assumed to originate only from intramolecular dipolar interactions, and at a significantly greater rate than spin diffusion owing to the small values of mixing time used. At -20 and 0°C, the magnitude of the cross-peak volumes was directly proportional to the EHB concentration.

In the slow motion regime ( $\omega\tau_C \gg 1$ ), a direct correlation between cross relaxation rate and viscosity  $\eta$  to temperature ratio was described, and expressed in terms of the Debye expression [230] and of a simple function of in an isotropic situation. [350]

$$|R_{ii}^c| \propto \tau_C = KV_H \frac{\eta}{T\tau} + \tau_H$$

Here  $K$  is a parameter dependent on the ratio of the mean square intermolecular torques on the solute molecules to the intermolecular forces on the solvent molecules,  $V_H$  is the hydrodynamic volume swept out by the reorienting vector, and the correlation time  $\tau_H$  is the zero-viscosity intercept. [351]

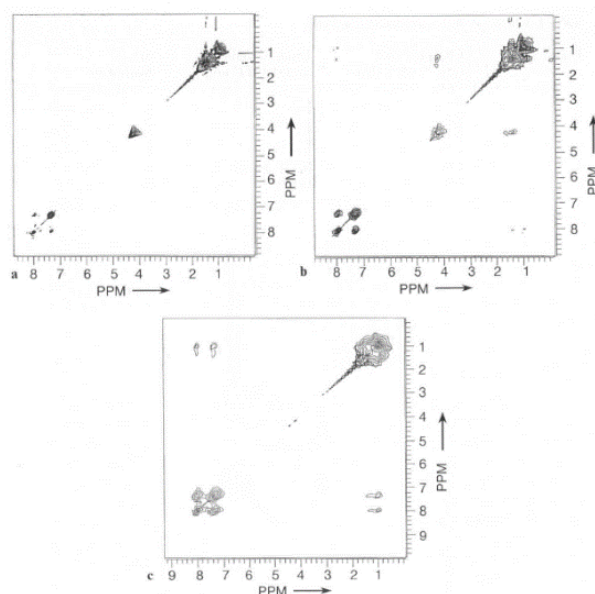


**Fig. 40.** NOESY spectra of 10% EHB in EHB-*d*<sub>22</sub> taken at 180 MHz, -20°C and (a) 500 bar; (b) 1 kbar; and (c) 1.5 kbar. The mixing time for all spectra was 75 ms. Reproduced from [346].

Insight into the time scales involved in EHB reorientation was also obtained by calculation of correlation times, since the linearity of the  $R_{ij}^C$  versus  $\frac{\eta}{\tau}$  relationship was demonstrated experimentally, proving that the overall rotation correlation time strongly influenced the intramolecular cross relaxation rates. The authors assessed the time scales of EHB overall motion to be on the order of  $\tau_C = 10^{-8}$  and  $10^{-9}$  s respectively for the rigid aromatic moiety and the flexible chain of EHB.

Intermolecular cross relaxation rates  $R_{inter}$ , the differences between rates in the neat EHB liquid and corresponding intramolecular rates, were investigated  $R_{inter}$ , and related to the inverse of the rate of translational diffusion through Torrey's translational model for relaxation. [345, 351, 352].

$$|R_{inter}^C| \propto \frac{1}{D}$$

To obtain some qualitative insights into the conformational behaviour of one or both of the chains possibly folding back to the aromatic ring of EHB, the authors combined internuclear distances calculated from intramolecular cross relaxation rates, since in the isotropic case, [350]

$$R_{ij}^C \sim -\gamma^4 \frac{\hbar^2 \tau_C}{10r_{ij}^6}$$

and the use of a molecular mechanics program involving Allinger's MM2 force field parameters. [353] MM2 calculations showed, as expected, many conformational minima for EHB, due to its high flexibility. However, under high pressure and low temperature conditions EHB revealed conformations in which one or both of the chains were bent over toward the aromatic ring, allowing substantial magnetization transfer between methyl and aromatic protons through longitudinal cross relaxation.

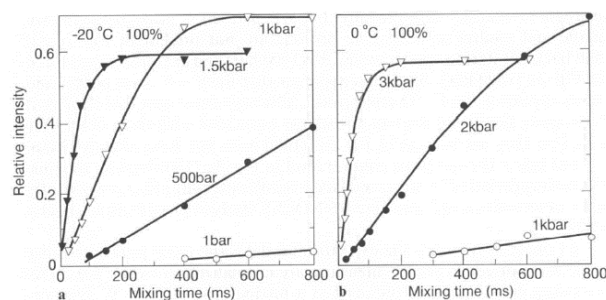


**Fig. 41.** Time dependence of the intensity for the cross peak B - F in neat EHB at -20°C (a) and 0°C (b). In (a):  $\circ$ , 1 bar;  $\bullet$ , 500 bar;  $\nabla$ , 1 kbar;  $\blacktriangledown$ , 1.5 kbar. In (b):  $\circ$ , 1 kbar;  $\bullet$ , 2 kbar;  $\nabla$ , 3 kbar. Reproduced from [346].

## 2.12. Enkephalins: a case study of the application of different viscous cryoprotective media to determine bioactive conformations

Bioactive peptides of natural origin usually have short linear sequences and high conformational flexibility in water. It is very challenging to investigate their conformations in solution since they often present a complex mixture of conformers of similar energy that are averaged on the chemical shift NMR time-scale, most of them in extended form. The bioactive conformation may be one of them, even though the solvents employed in liquid-state NMR often display physical properties radically different from those of the biological system in which the peptides are active. There is no simple way to characterize the bioactive conformation among so many possible alternatives. For addressing this issue, two distinct ways may be considered: 1) A reduction of conformational freedom of the peptide by a viscosity increase of the solubilisation medium at low temperatures, if and only if the bioactive conformation is more stable than the others. 2) Trying to mimic in solution the physicochemical features of the natural environment of the peptide, such as extracellular fluids, membranes and receptor cavities, with the intent of stabilizing a specific conformation supposed to be the one that is biologically active when in interaction with the dedicated receptor. However, another way would be to focus

on the capability of the binding site of the receptor according to its size/shape and properties to filter the bioactive conformations.

Cryoprotective solvents such as DMSO/water, DMF/water and EG/water blends have physical properties (e.g. dielectric constant) at low temperatures close to those of water at room temperature, which makes their use compatible with the study of biomolecules in solution. [44] By means of this solvent blend, unusually low temperatures for a polar environment are reachable, which may possibly stabilize certain families of conformations. Owing to the strong temperature dependence of the viscosity of the cryoprotective solvent blends, negative NOE enhancements may also be observable for medium-sized peptides by greatly slowing the molecular tumbling and may be used to characterize specific stabilized conformations. Temussi and co-workers mentioned that the action of cryosolvent blends may be compared to a kind of "conformational sieve". [145] Specifically, cryoprotective media of viscosity values from around 7 to 11 cP lead not only to a quantitative increase in all NOEs, but also to selective growth of conformationally sensitive effects involving backbone and sidechain protons. For instance, the observation of variously modulated NH-NH and long-range NOE cross peak intensities suggests an influence of viscosity on conformation populations. [145]

In addition, under these viscosity conditions at low temperatures, water is supposed to be partly ordered, [166] i.e., in a state resembling that of the medium at the interface between a membrane and the transportation fluid, at which a peptide may display some preferential conformations before its interaction with its dedicated receptor.

In this context, in order to try to delineate the bioactive conformations of linear analgesic peptides in solution, Temussi, Pavone and co-workers have now reported many examples of the use of DMSO/water, DMF/water and

EG/water blends as cryoprotective solvent mixtures for the characterization of their 3D structures by maximizing NOE enhancements. [47, 49, 83, 136, 138, 139, 142, 143, 145-147, 150, 152, 154, 156, 157, 299]

As a more specific illustration of this approach in a specific class of peptide, we describe in this section NMR structure and conformation studies of enkephalins, a well-known family of linear opioid peptides. Comparable studies of deltorphin, another linear opioid peptide, have been reported in the literature. [83, 142, 145-147, 152]

Enkephalins are endogenous brain peptides. [Met]<sup>5</sup>-enkephalin (Tyr-Gly-Gly-Phe-Met) and [Leu]<sup>5</sup>-enkephalin (Tyr-Gly-Gly-Phe-Leu) show morphine-like activity and were first isolated in 1975 from pig brain. [167] They operate at the same  $\mu$  and  $\delta$  receptor sites as natural morphine-like opiates and are involved in regulating nociception. [168] Since their discovery, although they show a high flexibility caused by the two adjacent Gly residues, scientists have tried to determine by solution NMR the bio-active conformations of these peptides in different environments, such as water, CDCl<sub>3</sub>, DMSO-*d*<sub>6</sub>, micelles, bicelles, (choline) bilayers and in particular in cryoprotective solvents such as DMF-*d*<sub>6</sub>/water, EG-*d*<sub>6</sub>/water and DMSO-*d*<sub>6</sub>/water blend. [39, 46, 136, 138, 139, 154, 169-198]

#### 2.12.1. DMSO-*d*<sub>6</sub>/water blend

In 1987, Temussi and coworkers investigated the conformational features of Met- and Leu-enkephalin by taking advantage of the increase in cryosolvent blend viscosity and the possibility of peptide conformational stabilization at low temperatures. [136, 138] 1D steady-state NOE and TOE difference spectroscopy respectively were carried out for Met- and Leu-enkephalin dissolved in DMSO-*d*<sub>6</sub>/H<sub>2</sub>O mixture with water mole fractions of 0.51 and 0.91 respectively. The medium viscosity changed from around 1 cP (viscosity of pure water) to around 4 and 2 cP respectively at room

temperature, and to approximately 10 cP at 265 K and 8 cP at 258 K. [125] These viscosity conditions should shift the value of  $\tau$  to around 4 ns for Leu- and Met- enkephalin, a range typical of small proteins.

At 265 K and 500 MHz ( $^1\text{H}$ ) in  $\text{DMSO-}d_6/\text{H}_2\text{O}$  (0.49:0.51  $\chi/\chi$ ), 1D steady-state NOE difference spectra of Met-enkephalin showed significant negative NOE enhancements of  $\sim 29\%$  and  $\sim 47\%$  after selective irradiation of the *meta* and *ortho* Tyr aromatic protons (Fig. 42a), while at 297 K in  $\text{D}_2\text{O}$ , was close to one and consequently small positive NOE enhancements of  $\sim 5\%$  and  $\sim 13\%$  were observed respectively (Fig. 42b).

The authors observed intra-residue NOEs, but it was not possible to detect any inter-residue ones in order to get insight into conformations of Leu-enkephalin in aqueous solution. In contrast, in  $\text{DMSO-}d_6/\text{H}_2\text{O}$  (0.09:0.91  $\chi/\chi$ ) blend at 258 K and 500 MHz ( $^1\text{H}$ ), the negative NOE enhancements were around  $\sim 27\%$  after selective irradiation of the *meta* Tyr aromatic protons of Leu-enkephalin (in comparison with Met-enkephalin), while at 268 K (for improved spectral resolution), the authors observed numerous intra-residue and inter-residue NOE enhancements, allowing sequential assignments (Fig. 43). In addition, small intensity long-range NOEs were also detected, potentially offering structural insights into the bioactive conformation(s) of Leu-enkephalin, though it is necessary to keep in mind that the strong head to tail electrostatic interaction may favour a mixture of disordered folded conformers for the zwitterionic enkephalin. [59]

**Fig. 42. a)** 500 MHz proton Overhauser experiments on  $1 \times 10^{-3}$  M Met<sup>5</sup>-enkephalin in  $\text{D}_2\text{O}/\text{DMSO-}d_6$  ( $\chi_{\text{DMSO}}=0.49$ ) at 265 K. (B) Normal spectrum of the aromatic region; (C, D) NOE difference spectra obtained by irradiating the Tyr<sup>1</sup> *meta* and *ortho* signals, at 6.68 and 7.02 ppm respectively. The resonances were irradiated for 1.0 s with enough power to null the peaks in 0.05 s. Recycling time was 3.5 s. A control experiment (A), irradiating at the

blank position indicated by the asterisk, was run to check the selectivity of the irradiation bandwidth, ruling out undesired spill-over effects. The difference spectra averaged 800 scans off resonance minus 800 scans on-resonance, thus showing negative effects with the same sign of the irradiated peaks.

**b)** 500 MHz proton Overhauser experiments on  $1 \times 10^{-3}$  M Met<sup>5</sup>-enkephalin in  $\text{D}_2\text{O}$  at 297 K and pH = 6.5 (uncorrected for isotope effect). (B) Normal spectrum of the aromatic region; (C, D) NOE difference spectra obtained by irradiating the Tyr<sup>1</sup> *meta* and *ortho* signals, at 6.86 and 7.15 ppm respectively. Irradiation time was 10 s, using sufficient power to saturate fully the signals in about 0.1 s; 3.5 s recycling time. Each difference spectrum represents an average of 800 scans off resonance minus 800 scans on-resonance, so that positive NOEs are shown as peaks of opposite sign with respect to those irradiated. (A) Control experiment in which a blank position, indicated by an asterisk, at about 50 Hz downfield from Phe<sup>4</sup> resonances, was irradiated. Adapted from [136]

**Fig. 43.** Truncated proton Overhauser experiments on Leu-Enkephalin at 500 MHz in the cryoprotective mixture  $\text{DMSO-}d_6/\text{H}_2\text{O}$  (0.09:0.91  $\chi/\chi$ ) at 268 K. (B, C) Difference spectra upon irradiation of the Gly<sup>2</sup> NH and Tyr<sup>1</sup> C $\alpha$ H resonances, respectively, as indicated by arrows in the reference spectrum (A). Difference spectra were obtained by applying a presaturation pulse for 1 s before measurement using a 1-1 hard pulse sequence, [199] subtracting the irradiated spectrum from the control spectrum. Reproduced from [138].

In 1988, Temussi and co-workers undertook a comparison of the temperature coefficients of amide protons chemical shift and the negative NOEs of Leu-enkephalin (LE) with those of Leu-enkephalin amide (LEA) by means of 2D transient  $^1\text{H}$  NOE spectroscopy at 277 K and 500 MHz ( $^1\text{H}$ ), in a cryoprotective  $\text{DMSO-}d_6/\text{H}_2\text{O}/\text{D}_2\text{O}$  (8:1:1 v/v/v) blend, as an attempt to characterize its potential biologically active conformation. [139] The authors sought at the same time to reach a better understanding of the head to tail electrostatic interaction of zwitterionic enkephalin, potentially responsible for disordered folded conformers. The temperature coefficients of amide protons were determined over a very wide range of temperatures (243 K to 327 K). All values for LE and LEA peptides were larger than those expected for protons involved in hydrogen bonds. Hence, all amide

protons were exposed to the cryosolvent. In this more viscous environment, several negative intra- and inter-residue NOEs were found to be particularly intense, indicating that the conformations of LE and LEA were not fully random. In addition, the authors highlighted that LE conformers probably revealed a  $\beta$ -turn of type I (or I') due to the existence of a typical inter-residue NOE between Gly<sup>2</sup> and Gly<sup>3</sup> NH (Fig. 44). However, the values of temperature coefficient and all the NOEs measured were not sufficient to imply the existence of a single folded conformation for LE or LEA. In addition, no long-range effect was observed that could support a head to tail electrostatic interaction [59] for the zwitterionic Leu-Enkephalin. This interaction was therefore inferred not to be sufficiently strong to force short distances between hydrogens of the N-terminal and C-terminal amino acids.

**Fig. 44.** Low field region of a phase-sensitive NOESY spectrum of 8 mM Leu-enkephalin in a 80:10:10 DMSO-*d*<sub>6</sub>:D<sub>2</sub>O:H<sub>2</sub>O mixture at 277 K at 500 MHz with a mixing time of 500 ms. The spectral region shown ( $\omega_1 = 0.2$  to 9.2 ppm,  $\omega_2 = 6.4$  to 9.2 ppm) contains cross peaks which manifest NOEs from amide and aromatic protons. All the effects are labelled using the one-letter codes for the residues. The circled cross peak connecting the Gly<sup>2</sup> and Gly<sup>3</sup> NH's is of diagnostic value in discriminating between type I and type II  $\beta$ -turns. Adapted from [139].

In 1998, Temussi *et al.* attempted one more time to determine the so-called bioactive conformation or family of conformations of Leu-enkephalin at 275 K, in DMSO-*d*<sub>6</sub>/water (9:1 v/v) cryoprotective mixture, at 500 MHz (<sup>1</sup>H), by means of 2D <sup>1</sup>H NOESY and <sup>1</sup>H-<sup>15</sup>N HMQC-NOESY experiments. [154] Improvement of the NMR data was essential for the structure-activity relationship study, so they used uniformly <sup>15</sup>N-labelled Leu-enkephalin, and a DMSO-*d*<sub>6</sub>/water cryoprotective blend at low temperature for collecting intense and numerous NOE enhancements that were difficult to detect in neat DMSO-*d*<sub>6</sub> or water because of the high flexibility of the peptide. Indeed, at 275 K and 500 MHz, <sup>15</sup>N-

Leu-Enkephalin dissolved in DMSO/water (9:1 v/v) presented many more NOEs than in pure DMSO-*d*<sub>6</sub>. However, negative NOE enhancements were not uniformly observed for all cross peaks, this observation probably demonstrated a possible mechanism of conformation preselection (Fig. 45) in agreement with works published by Amodeo *et al.* in 1991. [145] Nonetheless, the determination of a bioactive conformation among these structures remained an elusive goal. [143]

**Fig. 45.** Comparison between NOEs of <sup>15</sup>N-Leu-enkephalin measured in DMSO-*d*<sub>6</sub> at 298 K and in the DMSO-*d*<sub>6</sub>:H<sub>2</sub>O cryomixture at 275 K. Columns marked with \* indicate peaks obscured by presaturation of the HDO resonance, those marked with § indicate peaks affected by overlap. The parameter in the ordinate (R) is the ratio of the volume of the cross peak to the volume of the corresponding diagonal peak. Reproduced from [154].

Hence Temussi *et al.* considered a reverse strategy with respect to common practice: i) the determination of the most likely peptide conformers in solution, ii) their comparison with the shapes of rigid alkaloids, to assess whether the shape of the “message” domain is consistent with that of the rigid compounds, and iii) the use of the global shape of the opioid peptide to improve the mapping. Instead of considering NMR data to define the mixture of conformers by energy minimization (EM) and then seeking to determine the bioactive conformation from among a collection of solution conformers, they assessed the consistency of conformers resulting from EM (by means of diagnostic NOEs converted into inter-proton distances according to the method Esposito and Pastore [200]) with the shapes of two well-known alkaloid opioids, 7-spiroindanyloxymorphone (SIOM), the first selective non-peptide  $\delta_1$  opioid agonist, [201] and BW373U86, a  $\delta$  opioid agonist with a piperazinyldiphenylmethane skeleton. [202] They then checked the consistency of suitable conformers with NMR

data and energy requirements. This reverse strategy assumed, in using 3D comparison of peptide conformations with rigid moulds, that the relative positions of the T and P receptor subsites (named by Portoghese *et al.* to refer to the interaction with the aromatic rings of the Tyr<sup>1</sup> and Phe<sup>4</sup> of the enkephalins and endorphins) are crucial for selectivity and affinity of agonist and antagonists. [203-207]. Since NMR data did allow a single consensus structure to be found, they analysed the NMR data in terms of limiting canonical structures (i.e.  $\beta$ -turns and  $\gamma$ -turns for *trans* peptide bonds) and finally selected only those consistent with the requirements of  $\delta$  selective agonists and antagonists. In spite of the very flexible behaviour of Leu-enkephalin, the authors described a form of "template forcing" method that apparently was more efficient than previous methods for the prediction of a family of bioactive conformers, of which the shapes may turn out to be useful in the design of new  $\delta$ -selective opioid peptides.

#### 2.12.2. EG-*d*<sub>6</sub>/water and DMF-*d*<sub>7</sub>/water blends

Picone *et al.* in 1990 took advantage of the physical properties of biomimetic media such as EG-*d*<sub>6</sub>/water, DMF-*d*<sub>7</sub>/water and methanol-*d*<sub>4</sub>/water cryoprotective mixtures, of two neat solvents, DMF-*d*<sub>7</sub> and acetonitrile-*d*<sub>3</sub> (respectively  $\epsilon = 36.7$  and  $37.5$ ), and of an aqueous SDS micellar system, to assess the conformational preferences of [Leu]<sup>5</sup>-enkephalin (MW = 555.63 g/mol) in environments expected to be close to that in which the agonist-receptor interaction occurs, by trying to mimic the water/membrane interface. These studies were carried out by means of 2D transient NOE spectroscopy, at 500 MHz (<sup>1</sup>H) and 4°C. [46]

The authors extended previous conformational investigations of [Leu]<sup>5</sup>-enkephalin in DMSO-*d*<sub>6</sub>/water cryomixture, [138, 139] in which high viscosity and dielectric constant values at low temperature [44] induced a partial ordering of [Leu]<sup>5</sup>-enkephalin that was demonstrated by the

detection of relevant negative NOE enhancements. [44] In all the cryoprotective mixtures EG/water, DMF/water and MeOH/water, proton reassignments of [Leu]<sup>5</sup>-enkephalin were necessary since the resonance order was partially or totally changed compared to spectra acquired in neat solvents. The authors reported that the viscosity increase of EG-*d*<sub>6</sub>/water (9:1 v/v) blend, at 500 MHz and 277 K, moved [Leu]<sup>5</sup>-enkephalin from the positive NOE regime towards the negative one, in contrast to the MeOD/water blend. As a result, numerous relevant intra- and interchain negative NOEs were detected by means of 2D NOESY experiments ( $t = 300$  ms), allowing sequential and side chain resonance assignment (Fig. 46a). NOE data suggested that the EG-*d*<sub>6</sub>/water blend favoured a shift of the conformational equilibrium towards a significant fraction of folded conformers, apparently including a  $4 \rightarrow 1$   $\beta$ -turn since molecular internal motions were decoupled from tumbling by the high medium viscosity. Some similar NOEs were observed in DMF-*d*<sub>7</sub>/water blend (Fig. 46b) however others were different, in particular for the side-chain resonances, consistent with the structure-inducing effect of cryoprotective mixtures already suggested by DMSO-*d*<sub>6</sub>/water studies. [138, 139] The presence of a  $4 \rightarrow 1$   $\beta$ -turn was also suggested for [Leu]<sup>5</sup>-enkephalin in DMF-*d*<sub>7</sub>/water blend. In comparison, NOEs observed in pure DMF-*d*<sub>7</sub> and acetonitrile-*d*<sub>3</sub> were small and positive. Nonetheless, NMR data in both neat organic solvents and cryoprotective mixtures also suggested a  $4 \rightarrow 1$   $\beta$ -turn as the most probable solution structure of [Leu]<sup>5</sup>-enkephalin, whereas in SDS/water micelles the solution conformation appeared completely different, suggesting the presence of a  $5 \rightarrow 2$   $\beta$ -turn. Picone *et al.* mentioned that the existence of two different favoured conformations of [Leu]<sup>5</sup>-enkephalin may be related to their ability to be effective towards both  $\mu$  and  $\delta$  opioid receptors, contrary to other more

selective opioid peptides such as dermorphin and deltorphin. [142]

**Fig. 46.** a) Partial NOESY spectrum at 300 ms mixing time of [Leu]<sup>5</sup>enkephalin in 90% ethylene glycol/10% H<sub>2</sub>O (by vol.) at 277 K at 500 MHz, showing all the NH cross peaks. b) Partial NOESY spectrum at 300 ms mixing time of [Leu]<sup>5</sup>enkephalin in 90% dimethylformamide/10% H<sub>2</sub>O (by vol.) at 277 K at 500 MHz, showing all the NH cross peaks, labelled with standard single-letter codes for amino acids. Adapted from [46].

### 2.12.3. Polyacrylamide gel in DMSO-*d*<sub>6</sub>/water blend

In 2002, Pavone *et al.* investigated solution conformations of the highly flexible neuropeptide [Leu]<sup>5</sup>-enkephalin, <sup>15</sup>N-labelled, in cavities mimicking the synaptic cleft by means of polyacrylamide gel (PAG) swollen in water and the DMSO-*d*<sub>6</sub>/water (2:8 v/v) cryoprotective system, using 2D transient NOE experiments at 500 MHz (<sup>1</sup>H) at 273 - 293 K. [299] Signal transmission in the nervous system is controlled in synapses, by a large diversity of low molecular weight neuropeptides. The latter interact with their post-synaptic receptors with binding constants in the nanomolar concentration range. From a geometrical point of view, the pores of polyacrylamide gels (8 - 12 nm at acrylamide concentrations: 10 - 15% w/v) [318] offer a reasonable mimic of the synaptic cleft. The interaction of neuropeptides such as [Leu]<sup>5</sup>-enkephalin with post-synaptic receptors was characterized by a high entropic energy barrier resulting from the combination of low nanomolar concentration and low population of conformers. The authors demonstrated that this problem could be overcome by media of high viscosity such as cryoprotective mixtures, since these act as a "conformational sieve" so that compact, folded conformations are favoured over extended, disordered ones. [145] The use of PAG swollen with DMSO/water to mimic the physicochemical conditions of the synaptic cleft slowed the tumbling of [Leu]<sup>5</sup>-enkephalin by increasing medium viscosity, so that negative NOE enhancements were observed in <sup>15</sup>N-

edited NOESY [319] spectra at 293 K, unlike at the same temperature in bulk solution of the DMSO/water cryomixture. The number of NOESY cross peaks was similar to that seen at 273 K in DMSO /water blend. Indeed, the viscosity of the gel phase at 293 K is around 2.8 cP, twice of that of the latter cryoprotective system at the same temperature, due to the confinement effect of the small cavities. The authors then considered the use of pure water to highlight the effect of confinement in the gel pores as opposed to viscosity by preventing solvation effect of cryomixtures. In bulk water at 273 K, NOESY spectra only revealed a few cross peaks, as expected, [47] whereas in aqueous solution inside the gel phase, several NOE cross peaks were observed and their number was similar to that for NOESY spectra acquired in the DMSO/water blend (Fig. 47). By means of ROESY experiments, they discriminated between the influence of the increased viscosity in a confined environment on the rotational correlation time (influencing NOESY spectra) and the decrease of segmental mobility, since a ROESY experiment is relatively insensitive to the value of the rotational correlation time. Both NOESY and ROESY cross peaks detected in gel were more intense than in bulk solvent, demonstrating that viscosity has a distinct influence from a simple increase of (Fig. 47a). However, the intraresidue and sequential cross peaks were not sufficient for structure determination. They may originate from the increase in correlation time induced by the increase in viscosity, from the angular component of the correlation time related to internal motions, from the increase of the order parameter S<sup>2</sup>, or from a combination of these all factors. The authors mentioned that the side chains of [Leu]<sup>5</sup>-enkephalin appear much stiffer in PAG gel than in bulk water.

**Fig. 47.** a: Comparison of partial  $^{15}\text{N}$ -edited ROESY spectra of  $^{15}\text{N}$ -labelled [Leu]enkephalin in bulk water (left) with the corresponding spectrum in water hosted by gel pores (centre) and with the  $^{15}\text{N}$ -edited NOESY spectrum in bulk water (right). All spectra are recorded at 283 K at 500 MHz. Mixing times were 80 ms for the ROESY experiments and 200 ms for the NOESY experiment, typical acquisition time 12 h. Starred cross peaks originate from chemical exchange. b: Comparison of the expanded regions of the  $^{15}\text{N}$ -edited NOESY spectra of  $^{15}\text{N}$ -labelled [Leu]enkephalin in the gel pores using DMSO/water cryomixture (20/80 v/v) (left) and water (right) solutions showing also the cross peak assignments. The temperature for both spectra was 273 K. Typical acquisition time 3 h. Concentration of  $^{15}\text{N}$ -labelled enkephalin in 20 mM Na phosphate, pH 5.4, was approximately 1 mM in all cases. All spectra were recorded on a Bruker DRX-500 spectrometer equipped with an XYZ pulsed field gradient  $^1\text{H}/^{15}\text{N}$  probehead. Adapted from [299].

It is well known that PAG is valuable for inducing confinement of peptides and proteins in a small cavities, mimicking the natural environment of a cell, making NMR structural studies possible in conditions in which molecular conformations are potentially folded. Indeed, confinement in PAG is sufficient to increase the viscosity of aqueous solution without altering its composition or temperature. Peptide or protein solutions embedded in PAG offer the possibility of recording NMR spectra at sub-zero temperature with almost no degradation of spectral resolution and without any need to add co-solvents such as polyols or DMSO to lower the freezing point. However, the main limitation on the use of PAG is the  $^{15}\text{N}$  labelling of peptides or proteins needed to overcome the problems caused by intense proton signals from the flexible side chains of the gel, that obscure a large part of the proton spectrum.  $^{15}\text{N}$  labelling is routinely performed for proteins by overexpression in suitably enriched media, but it is not easy for peptides, and uniform  $^{15}\text{N}$  labelling of peptides during synthesis can be expensive.

### 3. Small molecule mixture analysis in Viscous solvents by NMR spin diffusion spectroscopy: ViscY

This part of the review reports another reason for manipulating the nuclear Overhauser effect, not for structural

or conformational analysis, but for the analysis of mixtures of small and medium-sized molecules, without physical separation, by inducing intramolecular magnetization transfer under spin diffusion conditions in viscous solvents (or solvent blends).

NMR spectroscopy plays a major role in the structure elucidation of unknown small and medium-sized organic molecules in solution, provided that the sample purity is sufficiently high, a requirement that is not always met in practice. A synthesis result containing starting materials, by-products and end products, or a therapeutic drug mixed with degradation by-products, or a natural or biotechnological extract made up of several hundred organic compounds, can often be analysed by means of simultaneous purification and NMR spectroscopy through LC-SPE-NMR or LC-SPE-MS/NMR coupling strategies. [354-357] Sensitivity issues can be addressed by such means as very high magnetic fields, ultra-cooled probe coils and preamplifiers, and sample concentration on solid adsorbents. The physical separation of mixture components can have advantages but is not always practical. Chromatography cannot be used if compounds are highly reactive, is unattractive if key molecular associations are broken by separation and may be simply too time-consuming and therefore too expensive to use. As a result, it is attractive to use NMR with no extra physical processing.

NMR investigations of mixtures are mostly limited to well-known molecule identification and quantification. Determining the structures of mixed unknown molecules is a challenging task because a global set of NMR response has to be divided into subsets, each linked to a single mixture constituent. The exercise turns out to be even more challenging when accidental strong peak overlap occurs. Being able to allocate each resonance to a specific molecule would limit the need for chromatographic separation, aid analysis of mixed unknowns, and thus significantly improve the efficiency of

synthetic and natural product chemistry. To date, the possibilities for addressing the spectral overlap issue by NMR have been explored in a limited number of directions.

i) The translational diffusion coefficient ( $D$ ) is characteristic of a given compound in solution and reflects its mobility. The 1D NMR spectrum of a mixture can be divided into subspectra for individual species by using  $D$  as discriminating factor, using the 2D DOSY method. [358-361] However,  $D$  values are only weakly discriminating, even though experimental tricks can improve the resolving power in particular cases, e.g. by loading the sample with a chromatographic solid phase, or by interacting the molecules of interest with soluble polymers, lanthanide shift reagents, or micelles. [362-371]

ii) Multi-quantum spectroscopy coupled (or not) with broadband homonuclear decoupling / pure shift NMR, ultrafast data acquisition, sparse sampling, and tensor decomposition methods can all help separate the spectra of mixed compounds. [372-376]

iii) As has already been explained, the use of viscous solvents under appropriate conditions decreases the tumbling rate of small and medium-sized compounds in solution, [18, 25, 28, 29, 208, 296, 377-383] so that the longitudinal cross-relaxation regime causes spin diffusion over entire molecules. As a result, the resonances of different species can be distinguished according to their ability to share magnetization through intramolecular spin diffusion. All  $^1\text{H}$  resonances within the same compound can correlate together in a 2D NOESY spectrum, allowing the extraction of the individual  $^1\text{H}$  NMR spectra of mixture constituents. In 2008, Simpson and co-workers first described the use of a high-viscosity solvent, CTFEP, for organic mixture separation *via* 1D and 2D NOESY spectroscopy. [377] The use of supercooled water (in narrow capillaries) as a means to tailor the rotational dynamics of small molecules was described in 2012 by the

same team for identifying small metabolites in mixtures. [296] Lameiras *et al.* have reported original outcomes in the area of mixture analysis by NMR using glycerol and glycerol carbonate (in 2011), DMSO/glycerol (in 2016), DMSO/water (in 2017), sucrose solution and agarose gel (in 2019), and sulfolane-based solvents (in 2020) as viscous solvents for  $^1\text{H}$  and  $^{19}\text{F}$  spin diffusion promotion. [378-383] Lameiras and co-workers also introduced original experimental protocols deriving from 1D and 2D selective  $^1\text{H}$ - $^1\text{H}$  NOESY and  $^1\text{H}$ - $^{19}\text{F}$  HOESY experiments.

In 2020, Pedinielli *et al.* proposed the term *ViscY* for NMR methods in which *Viscous* solvents encourage the individualization of mixture constituents by NMR spin diffusion spectroscopy. [383]

Here we report the main NMR studies of small and medium-sized molecule mixtures dissolved in viscous media.

### 3.1. Chlorotrifluoroethylene polymer (CTFEP)

As reported in section 2.2, CTFEP is a hydrogen-free and highly viscous oil. [18] When mixed with an organic solvent such as chloroform or dichloromethane, it easily dissolves non- or weakly polar compounds. The resulting solvent blend at reduced temperature provides the conditions needed for the negative NOE regime that promotes spin diffusion for small molecules, as observed in NOESY spectra recorded with long mixing times.

In 2008, Simpson *et al.* considered CTFEP mixed with  $\text{CDCl}_3$  (8:2 v/v) for the spectral editing of organic mixtures. [377] The authors investigated first a mixture of brucine (MW = 394.45 g mol $^{-1}$ ), strychnine (MW = 334.41 g mol $^{-1}$ ) and cholesteryl acetate (MW = 428.69 g mol $^{-1}$ ) at 500 MHz ( $^1\text{H}$ ), then a mixture composed of hexadecanophenone (MW = 316.53 g mol $^{-1}$ ) and phenanthrene (MW = 178.23 g mol $^{-1}$ ) in the 265 - 300 K temperature range, by means of 1D steady-state and 2D NOESY spectroscopy.

As expected, in pure  $\text{CDCl}_3$  at 288 K and 500 MHz all the small molecules of the first mixture gave rise to negative NOESY cross peaks from pairs of protons sufficiently close to each other (Fig. 48.A). In contrast, the same mixture dissolved in CTFEP/chloroform at 288 K and 500 MHz yielded many more positive NOESY cross peaks, revealing that spin diffusion was active. From  $\sim -30$  to  $-90\%$  NOE enhancements were readily reached and spread throughout each molecule in the mixture (Fig. 48.B).  $-100\%$  NOE enhancements were observed for both molecules at 268 K. Spin diffusion was already so active at 288 K that considering one specific resolved  $^1\text{H}$  resonance from the NOESY spectrum, even at one extremity of a molecule, made possible the extraction of a subspectrum (slice or row) similar to the spectrum of the isolated pure compound. Relayed NOE correlations were detected over a distance of  $\sim 18\text{-}19 \text{ \AA}$ , or  $\sim 15$  bonds, whereas in conventional NOESY spectra in non-viscous solvents only interproton correlations corresponding to distances of  $< 5\text{-}6 \text{ \AA}$  are usually observed. Hence, a complete  $^1\text{H}$  spectrum was extracted from the NOESY experiment for each molecule of the mixture, permitting compound by compound spectral discrimination. However, spectral editing by 2D transient NOE spectroscopy in viscous media has the drawback of low spectral resolution, resulting from the influence of the solvent viscosity on transverse relaxation times and hence the reduced resolution of 2D NOESY spectra. The use of CTFEP/  $\text{CDCl}_3$  gave rise to a 2- to 3-fold reduction in spectral resolution compared to 1D conventional proton spectra of the mixture in  $\text{CDCl}_3$  at 288 K. It is also important to take into account the influence on spectral broadening of the size and rigidity of the molecules studied, as well as temperature and solvent blend composition, at a specific magnetic field strength. Finding the correct temperature can turn out to be challenging.

The authors also demonstrated the efficiency of their spectral editing approach for very flexible molecules, by considering a mixture composed of hexadecanophenone and phenanthrene. Small and extremely flexible molecules such as hexadecanophenone would seem not be good candidates for spin diffusion due to local motions within the linear chain. However, in CTFEP / $\text{CDCl}_3$  (9:1 v/v), a 100% negative NOE enhancement was observed at 268 K for hexadecanophenone, enabling spectral editing even though the spectral resolution was degraded (Fig. 49). Due to its structural rigidity, phenanthrene showed around 100% negative NOE enhancement at the higher temperature of 278 K in the same solvent blend. As a result, all resonances of hexadecanophenone and phenanthrene were successfully extracted from a NOESY spectrum. Interestingly, long-range NOE correlations were observed over distances up to  $25 \text{ \AA}$ . Simpson and co-workers emphasised that if spin diffusion could give rise to correlations over such long distances in an extremely flexible molecule, the spectral editing approach should be applicable to the vast majority of apolar compounds.

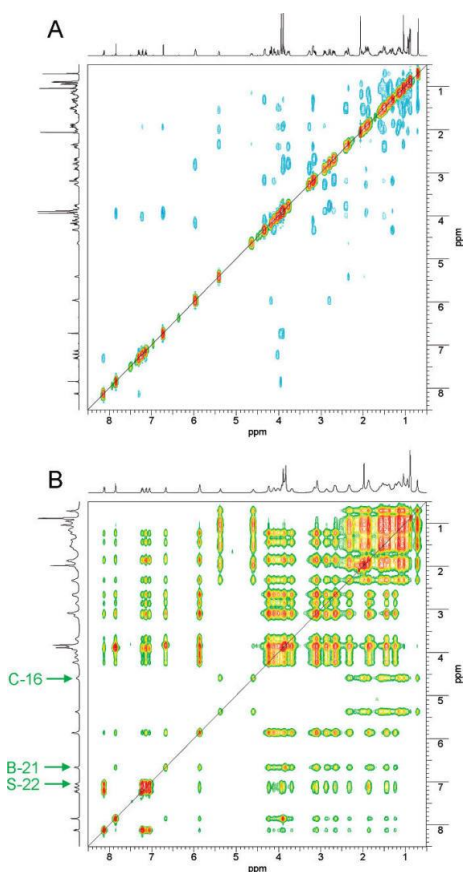


**Fig. 48.** NOESY spectra of brucine, strychnine, and cholesteryl acetate. Both spectra were obtained at 288 K with a mixing time of 1 s at 500 MHz. (A) is dissolved in chloroform-*d*. (B) is dissolved in 80:20 CTFEP/chloroform-*d*. Numbers correlate to the protons for which spectral slices were extracted. Adapted from [377].

In some situations,  $^1\text{H}$  spectral overlap hampers NOESY-based editing of spectra of mixtures. An alternative is to take advantage of the wide chemical shift dispersion of  $^{13}\text{C}$  by considering HSQC-NOESY experiments if the available sample amount is sufficient. In CTFEP/ $\text{CDCl}_3$  (8:2 v/v), all protons should correlate with all other protons and all other protonated carbons within the molecule. This was observed for cholesteryl acetate, as demonstrated in Fig. 50. Each horizontal slice extracted at a given carbon chemical shift produced a complete  $^1\text{H}$  spectrum of cholesteryl acetate, and a vertical slice produced the carbon spectrum restricted to protonated carbons.

The authors reported that the strategy to follow for inducing spin diffusion by means of the CTFEP/ $\text{CDCl}_3$  mixture was to start with the 8:2 composition ratio, to consider long NOESY mixing times, and to cool the sample if necessary down to 258-263 K with stable temperature regulation. In addition, they mentioned that the CTFEP/ $\text{CDCl}_3$  (8:2 v/v) blend was suitable for most of the molecules they studied so far. However, in cases of weak long-range NOE correlations, due to the presence of long flexible chains (alkanes, fatty acids, etc.) or extremely small molecules, they advised increasing the CTFEP proportion up to 90% to increase the viscosity. Conversely, a 70:30 ratio should only be recommended if the mixture is poorly soluble or if there is too much line broadening at 298 K in the 80:20 blend, e.g. owing to the presence of large or rigid molecules. For investigating a wide range of molecules with varying sizes and chain length, the user would have to consider several different CTFEP/ $\text{CDCl}_3$  combinations at different temperatures. In addition, the biggest problem with spectral editing using CTFEP/ $\text{CDCl}_3$  solvent blends is the limited mixture solubility for polar compounds; CTFEP is completely immiscible with water and  $\text{DMSO-}d_6$ .

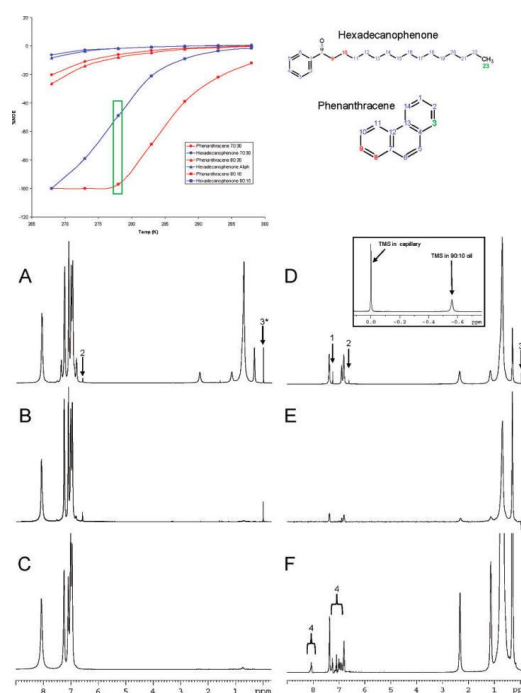


**Fig. 49.** Top left: plots of the relative % NOE observed with varying oil:chloroform ratios and temperatures for a mixture of phenanthrene and hexadecanophenone at 500 MHz. Top right: chemical structures. Unless otherwise stated, all spectra were acquired at 278 K (see green box on plot, top left) and in 90:10 oil/chloroform. (A) Mixture, (B) phenanthrene, (C) phenanthrene extracted from the NOESY spectrum, (D) hexadecanophenone, (E) hexadecanophenone extracted from the NOESY, and (F) hexadecanophenone in 80:20 oil/chloroform at 268 K acquired via the steady-state NOE method. 1, chloroform in external lock capillary; 2, chloroform in oil; 3, TMS in internal lock capillary; 4, artefacts from incomplete subtraction. Adapted from [377].

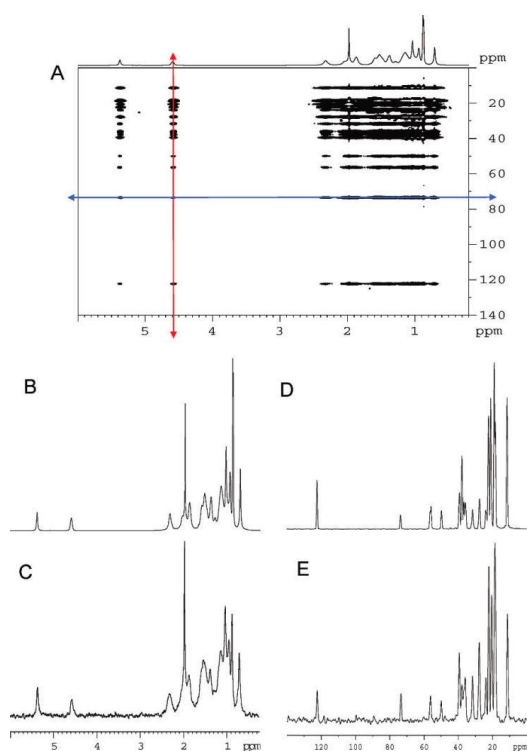


**Fig. 50.** (A) 2D HSCQ-NOESY spectra of cholesteryl acetate, (B)  $^1\text{H}$  NMR spectra of cholesteryl acetate, (C)  $^1\text{H}$  slice extracted from the 2D HSCQ-NOESY spectrum at carbon 16 (indicated by the blue arrow), (D) protonated carbons in cholesteryl acetate (from HSCQ projection), and (E) protonated carbon slice extracted from the 2D HSCQ-NOESY spectrum at proton 16 (indicated by the red arrow). All spectra were acquired for cholesteryl acetate dissolved in 80:20 oil/chloroform at 288 K at 500 MHz. Adapted from [377].

### 3.2. Glycerol (GL) and Glycerol Carbonate (GC)

Glycerol (GL) is a by-product of industrial manufacture of biofuels, soaps and surfactants from triglycerides. [384] Glycerol production presently exceeds demand, so new developments and new markets for glycerol are being

exploited. Glycerol has many applications, for instance as a hydrophilic component in neutral surfactants and as an emulsifier in food, cosmetics and pharmaceuticals. [384] In the field of organic chemistry, one of the most interesting transformations of glycerol is the synthesis of glycerol carbonate, [23, 385] which should shortly play a central role in industrial production of solvents, lubricants and surfactants from renewable carbon sources. [23] The existence of such ton-scale markets is not inconsistent with the exploration of highly specific niche applications. GL and GC are very viscous solvents (respectively  $\eta = 934$  cP and  $85.4$  cP at  $25^\circ\text{C}$ ), [23] offering high dissolution power for a wide variety of polar compounds owing to their high dielectric constants (respectively  $\epsilon = 42.5$  [50] and  $111.5$  [386] at  $20^\circ\text{C}$ ), and may be used to manipulate the NOEs of polar medium-sized and even small molecules.

In 2011, Lameiras *et al.* assessed the use of GL and GC for the individual NMR characterization of four structurally similar polar dipeptides, Leu-Val (MW =  $230.31$  g mol $^{-1}$ ), Leu-Tyr (MW =  $294.35$  g mol $^{-1}$ ), Gly-Tyr (MW =  $238.24$  g mol $^{-1}$ ) and Ala-Tyr (MW =  $252.27$  g mol $^{-1}$ ), in a single mixture, using 1D and 2D transient NOE spectroscopy at 500 MHz ( $^1\text{H}$ ), taking advantage of spin diffusion. [378] They justified this approach by demonstrating that the individual constituents in the mixture could not be distinguished by their translational diffusion coefficients in the DOSY experiment. The main drawback of this promising “spin diffusion” method was the need to suppress the strong  $^1\text{H}$  signals of non-perdeuterated GC and GL. The cost of perdeuterated GL and GC may turn out to be prohibitive, so strong  $^1\text{H}$  NMR signals from GL and GC were suppressed by employing 1D and 2D selective NOESY experiments using excitation sculpting for “band selective acquisition” or “band selective detection” (Fig. 51).

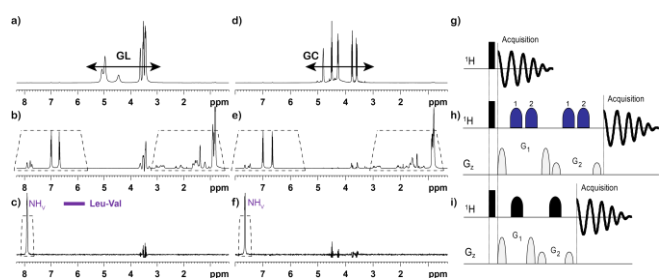


**Fig. 51.** 1D  $^1\text{H}$  spectra and NMR pulse sequences of the dipeptide test mixture in GL (a, b, c, 318 K) and in GC (d, e, f, 288 K) at 500 MHz. (a, d, g) Non-selective excitation and detection. (b, e, h) Selective detection of two resonance bands (dotted trapezium). The “1” and “2” labels on I-BURP-2 pulses respectively indicate their application to the high and low chemical shift regions. (c, f, i) Selective excitation of the valine amide proton doublet of Leu-Val (dotted trapezium) using a 20 ms, 1% truncated,  $180^\circ$  Gaussian pulse. Adapted from [378].

Since temperature is a crucial parameter in spin diffusion experiments, because it is directly related to solvent viscosity, [7, 377] the authors sought a temperature at which NOESY cross peaks were positive, well-resolved, and as intense as possible between nuclei that were not expected to be sufficiently nearby to reveal a NOE in a low-viscosity solution. The optimal temperatures of 288 and 308 K were found for for GL and GC respectively through band-selective detection 2D NOESY experiments (Figs. 52a and 52b). The authors highlighted that GL and GC made possible full intramolecular magnetization transfer through spin diffusion over distances greater than  $14 \text{ \AA}$  within each small and flexible dipeptide. In comparison, the NOESY spectrum recorded in water at 298 K displayed fewer NOE cross peaks, and these were of opposite sign (Fig. 52c). Under viscous conditions, the clustering of proton resonances allowed the identification of individual mixture constituents from their characteristic chemical shift patterns. In water, this would have required the combined use of NOESY and TOCSY (and possibly COSY) experiments, following well-established resonance assignment methods. [6]

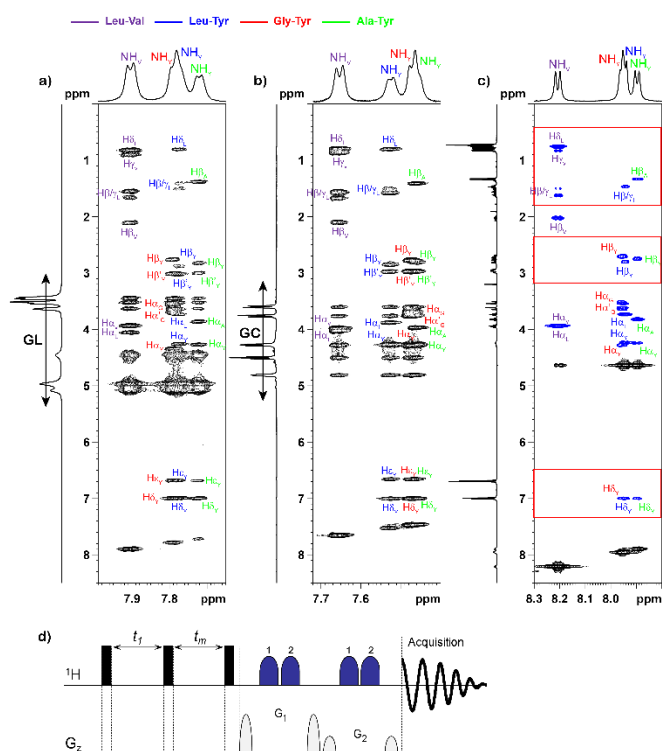


**Fig. 52.** Amide proton region of band-selective detection 2D NOESY spectra of dipeptide test mixture (a) dissolved in GL at 318 K, (b) dissolved in GC at 288 K using the pulse sequence in (d), mixing time ( $t_m$ ) = 1 s at 500 MHz. (c) Amide proton region of 2D NOESY spectrum of dipeptide test mixture dissolved in water at 298 K,  $t_m$  = 1 s. The red frames correspond to spectral regions of interest in which water as solvent has a major effect on the number and sign of observable NOESY cross peaks. Adapted from [378].

It appeared relevant for analytical purposes to gather additional structural information on mixture constituents by observing the  $\text{H}_\alpha$  proton resonances in  $F_2$  during signal acquisition, as they were not visible in the NOESY spectrum with band selective detection. To this end, the authors applied a 1D selective NOESY pulse sequence starting with a double pulse field gradient spin echo block for the selective excitation [387, 388] of the resonance of interest, followed by a mixing period comprising two wideband adiabatic inversion pulses flanked with gradient pulses in order to prevent the reestablishment of strong GL or GC solvent signals by longitudinal relaxation during the mixing time. Fig. 53 clearly shows that the two dipeptides were distinguished in GL and

GC by selective excitation of a suitable resonance followed by spin diffusion.

The authors enhanced the NOESY experiment sensitivity by implementing a new  $F_1$  band selective  $F_1$  decoupled 2D NOESY experiment [389, 390] focusing on NH amide resonances, since these nuclei had their resonances in the same frequency band and had no mutual scalar coupling. Running this experiment in GL and GC allowed the assignment of almost all  $^1\text{H}$  resonances of LV, LY, GY and AY by taking advantage of the spin diffusion occurring during the mixing time. In addition, the authors reported that discrimination between the signals of the four dipeptides in solution was reached within a shorter global acquisition time than required for four 1D selective NOESY experiments.

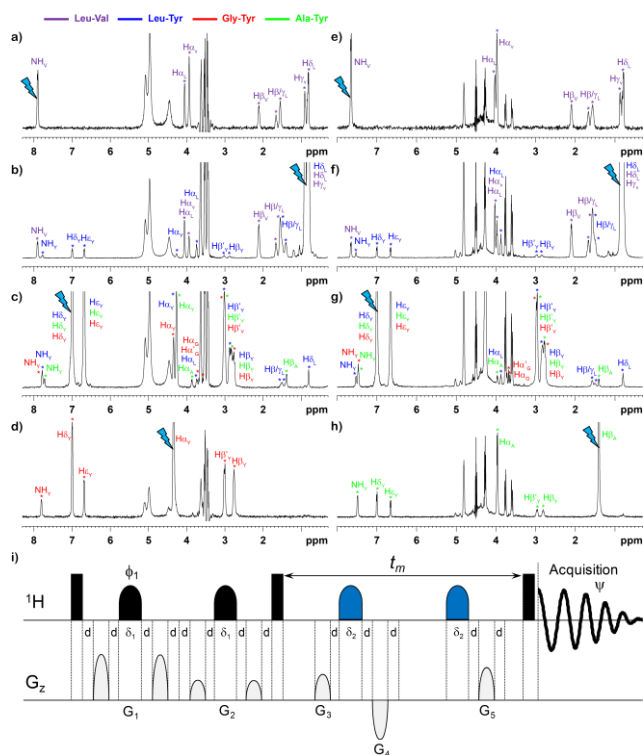


**Fig. 53.** Multi-peak selective excitation  $^1\text{H}$  1D NOESY spectra of the dipeptide test mixture in GL (a, b, c, d, 318 K) and in GC (e, f, g, h, 288 K) at 500 MHz. (i) Pulse sequence:  $\phi_1 = x, y, -x, -y, \psi = x, -x$ . The initial selective excitation was achieved by 1% truncated  $180^\circ$  Gaussian pulses with  $G_1:G_2 = 70:30$ . WURST wideband adiabatic inversion pulses of duration  $\delta_2 = 1.5$  ms were used within  $t_m$  (1 s), at 0.33 and 0.83  $t_m$ , with  $G_3:G_4:G_5 = 40:-60:50$ . The initial selective inversion pulses excited: (a, e) the  $\text{NH}_\nu(\text{LV})$  proton resonance ( $\delta_1 = 20$  ms, 8192 scans); (b, f) the  $\text{H}\delta_\nu(\text{LY})/\text{H}\delta_\nu(\text{LV})/\text{H}\nu_\nu(\text{LV})$  proton resonances ( $\delta_1$

= 5 ms, 800 scans); (c, g)  $\text{H}\delta_\nu(\text{LY})/\text{H}\delta_\nu(\text{GY})/\text{H}\delta_\nu(\text{AY})$  proton resonances ( $\delta_1 = 8$  ms, 800 scans); (d, h) respectively the  $\text{H}\alpha_\nu(\text{GY})$  and  $\text{H}\beta_\nu(\text{AY})$  proton resonances ( $\delta_1 = 50$  and 40 ms, 2048 scans). Adapted from [378].

The selective 1D and 2D NOESY experiments allowed the proton resonances to be clustered for each dipeptide in the mixture. While this might be sufficient for the identification of known molecules, it would not be sufficient for molecular structure identification due to the lack of homo- and heteronuclear  $J$ -coupling data. Homonuclear  $J$  correlation information was obtained by coupling a multiplet selective 1D NOESY block with an incremented delay and an isotropic mixing period, to build a selective 2D NOESY-TOCSY experiment. The authors used this pulse sequence to assign the  $\text{H}\alpha$  resonances of LY, GY and AY dissolved in GL and GC, previously hidden by the solvent signal, and to distinguish the side chain protons of LV and AY, located far away from the selectively excited protons  $\text{H}\delta$  of tyrosine.

Lameiras *et al.* thus demonstrated that the separation of the signals of small molecules in mixtures by NMR spectroscopy in high-viscosity solvents such as GL and GC is a viable alternative for the DOSY experiment, using magnetization transfer by spin diffusion over distances greater than 14 Å. Selective excitation and detection were employed to suppress the strong proton signals of the fully protonated solvents. GC led to the sharpest resonance lines in the narrowest frequency band. The dipeptides analysed reached a suitable NOE regime at a lower temperature in GC than in GL, which may be an advantage for the former when thermally unstable compounds are studied. The important dissolution power of both viscous solvents, and particularly of GC, has opened the way to the investigation of a large variety of polar, possibly biologically active, organic compounds.

### 3.3. Supercooled water

As mentioned earlier in this review (see part 2.10), the temperature dependence of supercooled water viscosity allows negative NOE enhancements to be increased by lowering the molecular tumbling rate, given a sufficiently strong magnetic field, a sufficiently high molecular weight (or rigidity) of the compound of interest, and a sufficiently low temperature.

Farooq *et al.* in 2012 considered supercooled water inside glass capillary tubes as a new approach to metabolite identification and structure validation. [296] The authors assessed their method with a standard mixture of three well-known molecules in D<sub>2</sub>O with overlapping proton resonances, before applying it to the assignment of metabolite signals in a worm tissue extract. Exploiting the increase of the water viscosity at sub-zero temperature, they took advantage of the nuclear Overhauser effect enhancement for structure determination of some of the metabolites in mixture.

The need for metabolite identification in complex fluids is increasing with the use of metabolomic studies in medical and environmental sciences. [391-394] In-depth metabolic profiling often relies on NMR, since it offers a non-invasive way to obtain information on mixture composition. Generally, accurate molecular identification in mixtures is achieved by 2D NMR experiments such as total correlation spectroscopy (TOCSY), [395] or selective TOCSY [393, 396, 397] and combination methods, [398] using spin connectivity through scalar couplings. New advances in NMR data processing such as covariance or indirect covariance, [399] and enhanced spectral resolution with the existence of high magnetic fields, favour metabolomics studies. However, these studies are usually carried out at room temperature, which limits intramolecular cross-relaxation due to the fast tumbling of most metabolites. 1D or 2D NOE spectroscopy may therefore be neglected even though spatial information

may be crucial for the identification of metabolites with similar proton resonance patterns, or for unprotonated nuclei in compounds such as nucleosides/nucleotides for which NMR experiments based on *J*-coupling are insufficient.

The authors proposed to solve this problem by exploiting the increased viscosity of supercooled water in a glass capillary tube (1.4 mm i.d.), at -15°C and 600 MHz (<sup>1</sup>H), to investigate a model mixture of adenosine triphosphate (ATP, MW = 507.18 g mol<sup>-1</sup>), sucrose (MW = 342.30 g mol<sup>-1</sup>), and glutathione (MW = 307.32 g mol<sup>-1</sup>), representing a range of structural rigidity and mobility with some <sup>1</sup>H resonance overlap. At -15°C, the viscosity of water is 3-4 times higher than at room temperature. [269, 272-275] Under these conditions, the molecular dynamics of the three selected compounds were slowed down so that spin diffusion occurred, facilitating molecular structure identification (Fig. 54). Full intramolecular magnetization transfer was reached for ATP, in particular between the ribose and the purine base, because of its structural rigidity. Even with a long NOESY mixing time, complete transfer remained elusive for glutathione owing to its structural plasticity. In the case of sucrose, through-space correlations between fructose and glucose were readily observed at -15°C. For instance, the anomeric proton showed correlations with other protons in both sugars. However, no complete set of correlations was detected for any given proton at -15°C.

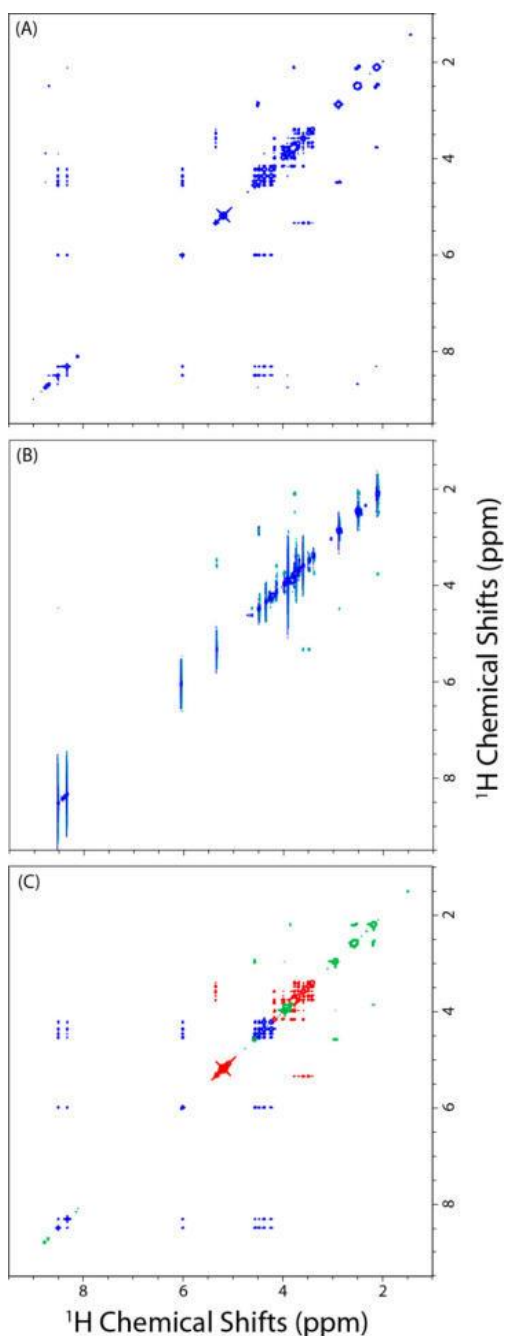


**Fig. 54.** (A) 2D NOESY spectrum of a three component mixture comprised of glutathione, sucrose, and ATP acquired with a mixing time of 600 ms at  $-15\text{ }^{\circ}\text{C}$  at 600 MHz. (B) 2D NOESY spectrum of the same sample acquired using an identical mixing time at  $25\text{ }^{\circ}\text{C}$ . (C) An overlay of 2D NOESY spectra of the three components obtained separately using the same mixing time at  $-15\text{ }^{\circ}\text{C}$ ; green corresponds to the glutathione, red to sucrose, and blue to ATP. Adapted from [296].

Appropriate slices along the  $F_2$  axis extracted from the NOESY spectrum at  $-15\text{ }^{\circ}\text{C}$  produced a complete  $^1\text{H}$  spectrum for ATP, and incomplete  $^1\text{H}$  spectra for glutathione and

sucrose molecules. All three  $^1\text{H}$  patterns were similar to those extracted from slices of the NOESY spectrum recorded under the same operating conditions for the separate, pure components of this mixture (Fig. 55). Very flexible molecules such as glutathione may be studied in supercooled water at a lower temperature than  $-15\text{ }^{\circ}\text{C}$ , to enhance spin diffusion further, by using extremely narrow capillaries. However, the extremely low detectable active volume may prevent this approach because of the much lower S/N ratio.

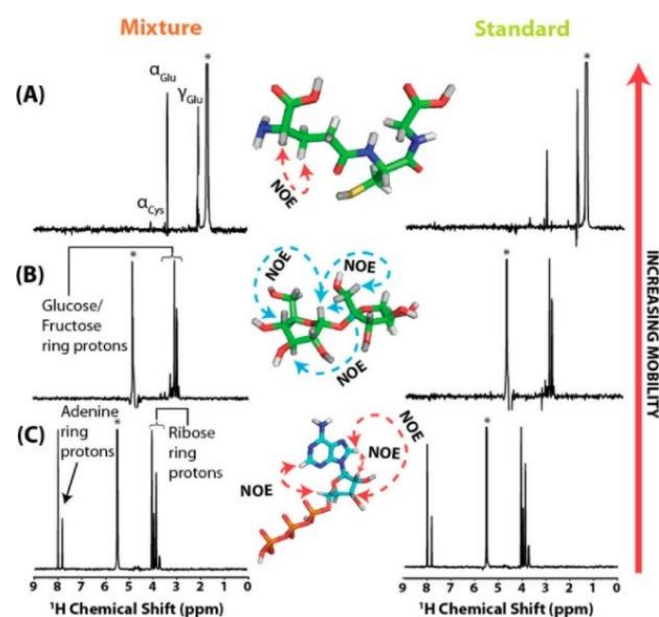


**Fig. 55.** Series of 1D slices of glutathione (A), sucrose (B), and ATP (C) obtained from the NOESY spectrum of the mixture (left) compared to those obtained from NOESY spectra of the standards alone (right) at identical temperatures ( $-15\text{ }^{\circ}\text{C}$ ) and mixing times (600 ms) and sliced at identical resonances (denoted by \*). The sliced resonances correspond to the  $\beta$  proton of the glutamine residue in glutathione, the anomeric proton of sucrose, and the anomeric proton of the ribose in ATP. Adapted from [296].

Farooq *et al.* demonstrated that NOE spectroscopy in supercooled water complements existing NMR-based metabolomics methods, especially for rigid metabolites such as saccharides, nucleosides and nucleotides for which  $^1\text{H}$  cross-relaxation acts efficiently at sub-zero temperature. Using it, molecular mixture deconvolution and identification in a congested  $^1\text{H}$  NOESY spectrum may be easier. From a

practical point of view, the use of a single glass tube (1.4 mm i.d.) corresponds to a volume of about 30  $\mu\text{L}$ . Most metabolomic studies require 5 mm NMR tubes, corresponding to an active volume of at least 550  $\mu\text{L}$ , depending on the type of probehead. Removing 30  $\mu\text{L}$  from the 5 mm NMR tube is not an issue. The supercooled water approach should be easily combinable with other metabolomics NMR experiments.

Farooq *et al.* also applied the supercooled water approach for the extraction and the spectral editing of components of a worm tissue extract by means of 2D NOESY and TOCSY experiments at  $-15^{\circ}\text{C}$ . Only minor loss in spectral resolution was observed due to the slow molecular motion regime at sub-zero temperature. The preservation of the chemical shift values of metabolites in supercooled water turned out to be an advantage over other viscous aqueous cryosolvent systems, [44] making possible mixture deconvolution using metabolite spectral databases for structure assignments without the need to re-acquire hundreds of NMR spectra of standard compounds. The authors emphasized the importance of combining NOESY and TOCSY spectra recorded in supercooled water when proton overlap in 1D  $^1\text{H}$  spectra hampers metabolite structure determination. They clearly identified nucleoside/nucleotide, tyrosine and phenylalanine amino acid, and maltose molecules by these means, an achievement that would have not been possible with NOESY and TOCSY spectra recorded at room temperature.

### 3.4. Dimethylsulfoxide- $d_6$ (DMSO- $d_6$ ) blends

#### 3.4.1. Dimethylsulfoxide- $d_6$ (DMSO- $d_6$ )/Glycerol (GL) and DMSO- $d_6$ /Glycerol- $d_8$ (GL- $d_8$ ) blends

Neat DMSO and Glycerol (GL) have viscosities of 2.2 cP and 1412 cP respectively at  $20^{\circ}\text{C}$ , [50] and melting points of  $18.52^{\circ}\text{C}$  and  $18.2^{\circ}\text{C}$ . [400]. Their mixture produces a viscous binary solvent system whose properties depend on

composition and for which the melting point can reach sub-zero temperatures. The higher the amount of GL, the more viscous is the solvent blend, making it easy to control the NOE enhancement for spin diffusion-based mixture analysis. [50] In addition, the values of the dielectric constant of 46.02 and 42.5 at  $20^{\circ}\text{C}$  for DMSO and GL respectively indicate a high dissolution ability for polar and apolar compounds. [50] GL- $d_8$  is moderately expensive and is only commercially accessible at a relatively low  $^2\text{H}$  enrichment level (98%), which results in intense residual  $^1\text{H}$  solvent resonances in the spectra.

Lameiras *et al.* reported in 2016 the use of DMSO- $d_6$ /GL and DMSO- $d_6$ /GL- $d_8$  blends as new high-viscosity solvents for NMR investigations of complex mixtures, [379] since other previously reported viscous solvents such as polymeric fluorinated oils [377] were inappropriate for the dissolution of polar molecules and pure glycerol was not appropriate for the study of low polarity compounds. [378] The authors focused on evaluating the DMSO- $d_6$ /GL (8:2 v/v) blend in discriminating between the signals of the mixed dipeptides Leu-Val, Leu-Tyr, Gly-Tyr, and Ala-Tyr (the mixture described in section 3.2), at 288 K and 500 MHz, ( $^1\text{H}$ ) and on evaluating the DMSO- $d_6$ /GL- $d_8$  (5:5 v/v) blend in separating the signals of mixed  $\beta$ -ionone (MW = 192.30 g mol $^{-1}$ ), ( $\pm$ )-citronellal (MW = 154.25 g mol $^{-1}$ ), (+)-limonene (MW = 136.23 g mol $^{-1}$ ), and flavone (MW = 222.24 g mol $^{-1}$ ), at 268 K and 600 MHz ( $^1\text{H}$ ), using homonuclear 1D and 2D selective NOESY, 2D selective NOESY-COSY, NOESY-TOCSY experiments, and heteronuclear 2D  $^1\text{H}$ - $^{13}\text{C}$  and  $^1\text{H}$ - $^{15}\text{N}$  HSQC-NOESY. The first use of a selective 2D NOESY-COSY experiment was also reported.

*Study of the polar mixture made of Leu-Val, Leu-Tyr, Gly-Tyr, and Ala-Tyr in DMSO- $d_6$ /GL (8:2 v/v)*

Fully protonated GL was chosen instead of GL- $d_8$  in this study, to prevent chemical exchange of its  $^2\text{H}$  nuclei with the amide protons of the dipeptides, so that the latter could be seen by NMR. Elimination of GL  $^1\text{H}$  NMR signals was required for the detection of mixture components. This was accomplished using selective pulses incorporated in an excitation sculpting sequence. [387] The authors focused on finding the temperature giving the best compromise between spin diffusion (as many intense positive NOESY cross peaks as possible) and overall spectral resolution. [377, 378] Sample cooling was necessary for observing positive NOESY cross peaks. Band-selective detection 2D NOESY spectra enabled Lameiras *et al.* to determine that the spectrum showed correlations at very long distance for each dipeptide (spin diffusion observed over distances greater than 14 Å) at 288 K (Fig. 56).

The authors used 1D selective NOESY experiments for the detection of all proton resonances during signal acquisition to avoid the loss of  $\text{H}_\alpha$  proton resonances in  $F_2$  when 2D band-selective NOESY spectra were recorded, as previously explained in section 3.2. Selective excitation of chosen proton resonances allowed the signals of each dipeptide to be identified, using the highly effective spin diffusion (over distances greater than 14 Å). Lameiras *et al.* then resorted to a more time-efficient approach using a single  $F_1$  band selective  $F_1$  decoupled 2D NOESY experiment (first described in section 3.2). NH amide resonances were still the initial sources of magnetization after the initial band selective excitation step. The doublet of each dipeptide amide proton was collapsed into a singlet of greater intensity using a selective echo and a nonselective echo, both flanked by gradient pulses, during  $t_1$ . The mixing time block, using wideband inversion pulses to prevent the resurgence of GL signals, let spin diffusion act throughout the proton network of each dipeptide.

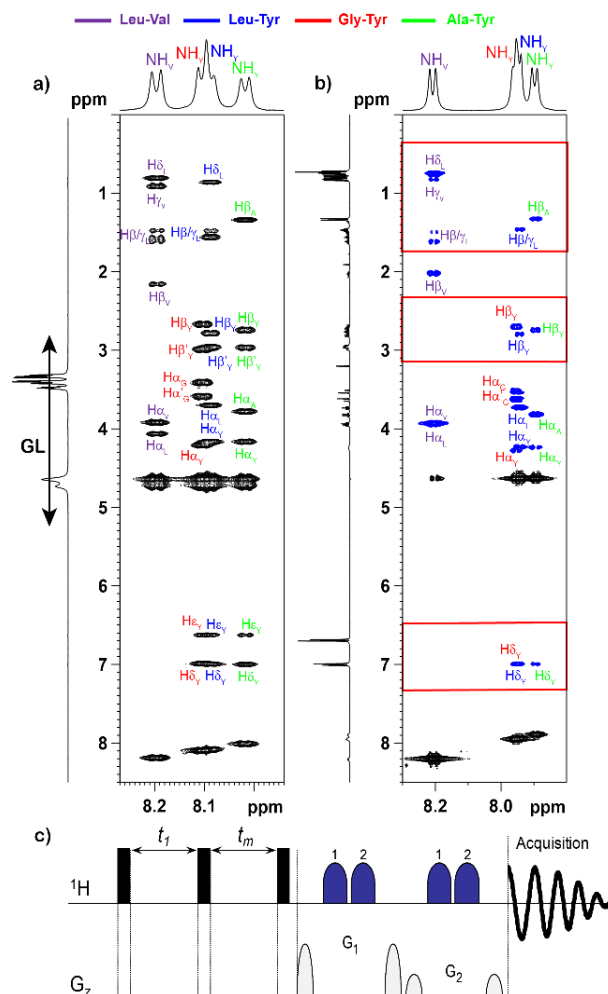


**Fig. 56.** Amide proton region of band-selective detection 2D NOESY spectra of a dipeptide test mixture at 500 MHz (a) dissolved in DMSO- $d_6$ /GL (8:2, v/v) at 288 K, mixing time ( $t_m$ ) = 1 s, using the pulse sequence in part c. (b) Amide proton region of 2D NOESY spectrum of dipeptide test mixture dissolved in water at 298 K,  $t_m$  = 1 s. The red frames correspond to spectral regions of interest, in which water as solvent has a major effect on the number and sign of observable NOESY cross peaks. Reproduced from [379].

### 3.4.1.1. Study of a low polarity mixture of $\beta$ -lonone, ( $\pm$ )-Citronellal, (+)-Limonene, and Flavone in DMSO- $d_6$ /GL- $d_8$ (5:5 v/v).

The authors chose a temperature of 268 K as giving full spin diffusion (over distances greater than 13 Å) for all mixture components, even for the very flexible ( $\pm$ )-citronellal, with acceptable spectral resolution, by means of conventional 2D NOESY experiments at 600 MHz ( $^1\text{H}$ ). Fig. 57 shows four NOE cross peak patterns, one for each mixture constituent.

In particular, the (+)-limonene pattern could be traced out, starting from the ethylenic H<sub>4</sub> et H<sub>8</sub> at 4.59 and 5.26 ppm (Fig. 57, in red).

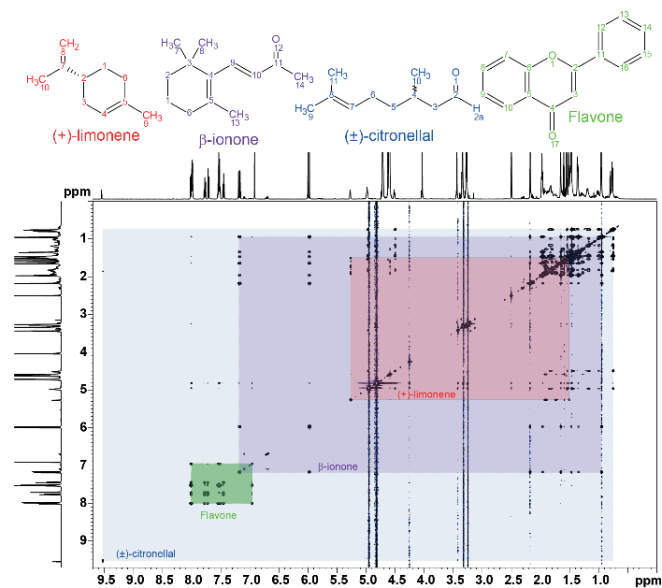


**Fig. 57.** 2D <sup>1</sup>H NOESY spectrum of β-ionone, (±)-citronellal, (+)-limonene, and flavone dissolved in DMSO-*d*<sub>6</sub>/GL-*d*<sub>8</sub> (5:5, v/v) at 268 K at 600 MHz, *t*<sub>m</sub> = 1 s. Reproduced from [379].

The authors reported the unambiguous assignment of all proton resonances, a task made challenging by resonance overlap, particularly in the region from 0.6 to 2.2 ppm. They used 1D selective NOESY experiments to group together the proton resonances of individual mixture components. At least one proton resonance was sufficiently resolved for selective excitation of each of β-ionone, (±)-citronellal, (+)-limonene, and flavone in DMSO-*d*<sub>6</sub>/GL-*d*<sub>8</sub> (5:5, v/v) blend. Even though this binary solvent was perdeuterated, strong GL residual proton signals remained. [387] The 1D selective NOESY pulse sequence formerly described for the model dipeptide mixture solved this issue. Though some loss in spectral resolution was observed at 268 K, separation of the signals of β-ionone, (±)-citronellal, (+)-limonene, and flavone was achieved using spin diffusion over distances greater than 13 Å. Fig. 58 shows a comparison of the 1D selective NOESY spectrum in DMSO-*d*<sub>6</sub>/GL-*d*<sub>8</sub> blend with the conventional 1D

proton spectrum in pure DMSO-*d*<sub>6</sub> of each of the mixture components. Again at least one proton resonance was sufficiently resolved for selective excitation of each compound. In particular, spin diffusion gave rise to full magnetization transfer over all protons of (±)-citronellal, the most flexible compound in the mixture.

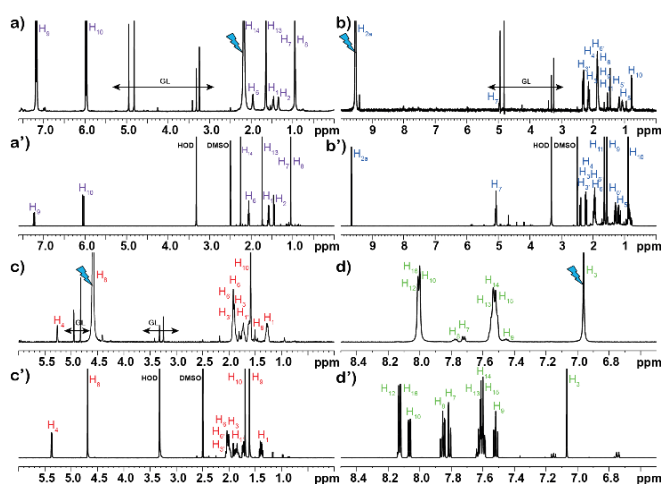


**Fig. 58.** Comparison at 600 MHz of 1D proton selective NOESY spectra of β-ionone, (±)-citronellal, (+)-limonene, and flavone mixture dissolved in DMSO-*d*<sub>6</sub>/GL-*d*<sub>8</sub> (5:5, v/v), *t*<sub>m</sub> = 1 s, at 268 K (pulse sequence in Fig. 53) with the conventional 1D proton spectrum of each compound of the mixture dissolved in DMSO-*d*<sub>6</sub> at 298 K. The initial selective inversion pulses excited: (a) the CH<sub>3</sub>(14) (β-ionone) proton resonance, (b) the CHO(2a) ((±)-citronellal) proton resonance, (c) CH<sub>2</sub>(8) ((+)-limonene) proton resonance, (d) the H(3) (flavone) proton resonance. Conventional 1D proton spectra of each compound of the mixture dissolved in DMSO-*d*<sub>6</sub> at 298 K: (a') β-ionone, (b') (±)-citronellal, (c') (+)-limonene, and (d') flavone. Reproduced from [379].

In other more complex mixtures, one or more components of interest may not reveal resolved proton resonances due to spectral overlap. Involving <sup>13</sup>C nuclei, that have a wider range of chemical shift, offers a workaround in such a situation by coupling the HSQC experiment with the NOE magnetization transfer. A 2D <sup>1</sup>H-<sup>13</sup>C HSQC-NOESY spectrum was acquired at 268 K for the same mixture in DMSO-*d*<sub>6</sub>/GL-*d*<sub>8</sub> (5:5 v/v) blend. A suitable choice of four horizontal slices through resolved carbon resonances produced the complete proton

spectrum of each mixture component. These spectra were compared to the 1D selective NOESY spectra: the proton resonance patterns were similar, as expected. Separation of the signals of the mixture components was also achieved by taking selected vertical slices from the 2D HSQC-NOESY spectrum, so as to yield the four  $^{13}\text{C}$  chemical shift patterns of the protonated carbons.

#### 3.4.1.2. Through-bond chemical shift correlations of $\beta$ -ionone, ( $\pm$ )-Citronella, (+)-Limonene, and Flavone mixed in DMSO- $d_6$ /GL- $d_8$ (5:5 v/v)

Selective 1D NOESY, 2D NOESY, and 2D HSQC-NOESY spectra readily permitted the clustering of resonance lines coming from the same compound. This can be enough to elucidate the structure of well-known mixture components. However, structure elucidation, and even just identification, of organic compounds usually requires additional NMR data based on  $J$ -coupling. In this context, Lameiras *et al.* implemented a multiplet-selective 2D NOESY-COSY experiment and reused the multiplet-selective NOESY-TOCSY experiment [378] for the characterization of the spin systems that belong to each constituent of the mixture (Figs. 59c and d). The authors recorded both spectra of  $\beta$ -ionone dissolved in DMSO- $d_6$ /GL- $d_8$  (5:5 v/v) blend, at 268 K and 600 MHz, starting from selective excitation of the acetyl protons at 2.18 ppm (Figs. 59a and b). The magnetization transferred by spin diffusion throughout the  $\beta$ -ionone structure was sufficient for the 2D NOESY-COSY experiment to reveal relevant  $^3J$  coupling between the ethylenic protons and the cyclohexene protons. The 2D NOESY-TOCSY spectrum confirmed the identification of the spin system around the cyclohexene ring. The 2D selective NOESY-COSY and NOESY-TOCSY experiments made it possible to assign fully the  $^1\text{H}$  resonances of  $\beta$ -ionone, and opened the

way to structure elucidation through the determination of the  $^1\text{H}$ - $^1\text{H}$  coupling networks of individual components in mixtures.

Lameiras *et al.* described in 2016 for the first time the use of high-viscosity binary solvents such as DMSO- $d_6$ /GL and DMSO- $d_6$ /GL- $d_8$  blends for identifying individual polar and apolar components of mixtures by spin diffusion observed over distances greater than 13 Å, using homonuclear 1D selective NOESY, 2D selective NOESY, NOESY-COSY, NOESY-TOCSY, and heteronuclear 2D HSQC-NOESY experiments, at 268 K and 600 MHz.

The authors stressed that handling DMSO- $d_6$ /GL and DMSO- $d_6$ /GL- $d_8$  has advantages over other viscous solvents previously reported in the literature, such as pure GL or GC, [378] These are easier sample preparation, control of spin diffusion over a larger range of temperature (starting at 248 K), and easier main field locking and shimming due to the high DMSO- $d_6$  content in both solvent blends. They also allow a very wide variety of low- and high-polarity compounds to be dissolved. DMSO- $d_6$ /GL and DMSO- $d_6$ /GL- $d_8$  are, respectively, recommended for the analysis of biological molecules for which labile proton exchange with solvent has to be avoided, and for the study of organic compounds for which labile protons are not crucial to their structure elucidation. Large compounds will necessitate a low proportion of GL/GL- $d_8$  in DMSO- $d_6$  while small compounds will require more GL (or GL- $d_8$ ), up to 50%, to achieve spin diffusion from 298 to 248 K.

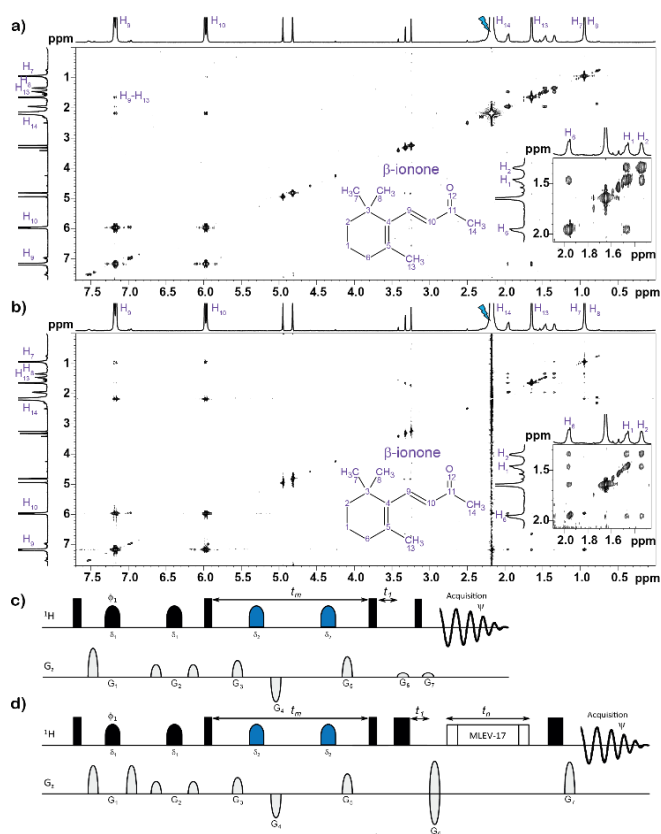


**Fig. 59.** Multiplet-selective  $^1\text{H}$  (a) NOESY-COSY and (b) NOESY-TOCSY spectra of  $\beta$ -ionone, ( $\pm$ )-citronellal, (+)-limonene, and flavone mixture dissolved in  $\text{DMSO-}d_6/\text{GL-}d_3$  (5:5, v/v) at 268 K,  $t_m = 1$  s, at 600 MHz. (c) NOESY-COSY and (d) NOESY-TOCSY pulse sequences:  $\phi_1 = x, y, -x, -y$ ,  $\psi = x, -x$ . For both 2D experiments, the initial selective  $180^\circ$  pulses had a Gaussian shape and were applied to the  $\text{CH}_3(14)$  ( $\beta$ -ionone) proton resonance. Adapted from [379].

### 3.4.2. Dimethylsulfoxide- $d_6$ ( $\text{DMSO-}d_6$ )/ethylene Glycol (EG) blend

As mentioned earlier in this review, pure DMSO and ethylene glycol (EG) have viscosities of 2.20 cP at  $20^\circ\text{C}$  [50] and 17 cP at  $25^\circ\text{C}$  [21] respectively, and freezing points of  $18.52^\circ\text{C}$  [400] and  $-12.5^\circ\text{C}$ . [44] Their mixture produces a viscous binary solvent blend whose properties depend on composition and for which the freezing point can reach sub-zero temperatures. The ability of these solvent blends to become more viscous at sub-zero temperatures as the fraction of EG increases facilitates the manipulation of the sign and the intensity of NOE enhancements over a wide range of temperature, for discriminating between the signals

of organic molecules in mixtures by spin diffusion. The dielectric constants of 46.02 and 41.9 respectively for DMSO [50] and EG [44] at  $20^\circ\text{C}$  indicate possible dissolution of a wide variety of polar or moderately apolar compounds. Furthermore, compared to other highly viscous solvents such as GL and GC, NMR sample tube preparation, main field locking and shimming are easier. EG- $d_6$  can be employed instead of EG, but EG- $d_6$  is quite expensive and is commercially available only at relatively low enrichment (98%), which gives rise to intense residual proton solvent resonances in spectra.

We report for the first time in this review the use of a  $\text{DMSO-}d_6/\text{EG}$  blend as a new viscous solvent blend for the NMR study of a mixture of polar compounds, using spin diffusion. We describe the discrimination of Leu-Val, Leu-Tyr, Gly-Tyr, and Ala-Tyr dipeptide signals in the model mixture investigated in sections 3.2 and 3.4.1, at 268 K and 500 MHz ( $^1\text{H}$ ), employing homonuclear selective 1D NOESY, selective 2D NOESY-COSY, and heteronuclear 2D  $^1\text{H-}^{15}\text{N}$  HSQC-NOESY experiments.

We first determined through band-selective detection 2D NOESY that 268 K was a temperature at which spin diffusion was efficient and spectral resolution sufficient for further studies. [377, 378] Spin diffusion was observed over distances greater than  $14 \text{ \AA}$ , and allowed the signals of the mixed peptides to be distinguished because the chemical shift pattern of each amino acid was predictable (Fig. 60a). In contrast, at 298 K and 500 MHz in water the four dipeptides produced negative NOE cross peaks (blue correlation peaks in the usual NOESY spectrum, Fig. 60b), showing the absence of spin diffusion. [6]

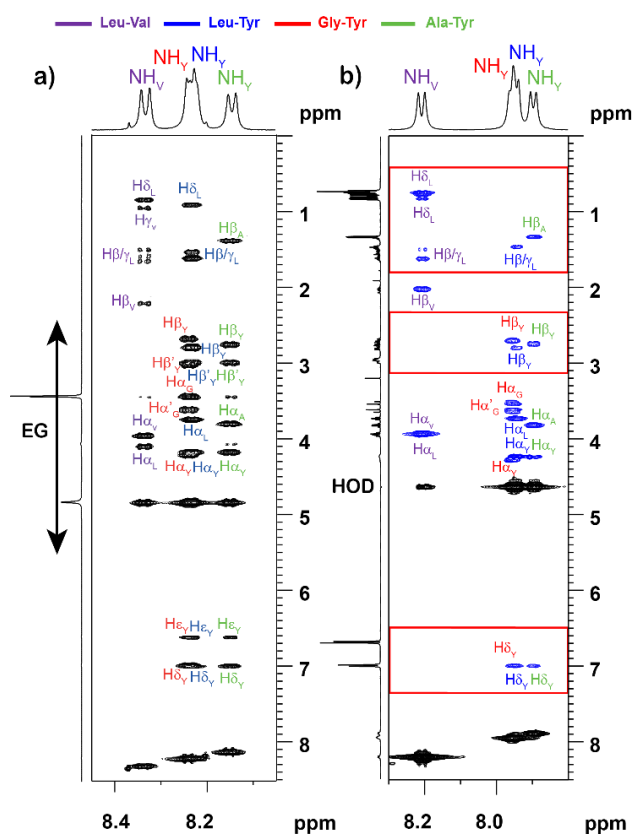


**Fig. 60.** Amide proton region of band-selective detection 2D NOESY spectra of a dipeptide test mixture at 500 MHz (a) dissolved in DMSO-*d*<sub>6</sub>/EG (7:3, v/v) at 268 K, mixing time ( $t_m$ ) = 1 s, using the pulse sequence in part c. (b) Amide proton region of 2D NOESY spectrum of dipeptide test mixture dissolved in water at 298 K,  $t_m$  = 1 s. The red frames correspond to spectral regions of interest in which water as solvent has a major effect on the number and sign of observable NOESY cross peaks.

A suitable set of 1D selective NOESY experiment (Fig. 61) enabled us to distinguish between the dipeptides. Full magnetization transfer was effective over all dipeptides (over distances greater than 14 Å).

We also employed a less time-consuming method, as described earlier, for discriminating between the signals of the dipeptides by means of an  $F_1$  band-selective  $F_1$  decoupled 2D NOESY experiment (Fig. 62). NH amide resonances were the initial source of magnetization, after the initial band selective excitation step. The mixing time block, using wideband inversion pulses to prevent the resurgence of the EG signal, let spin diffusion extend throughout the proton network of each molecule.

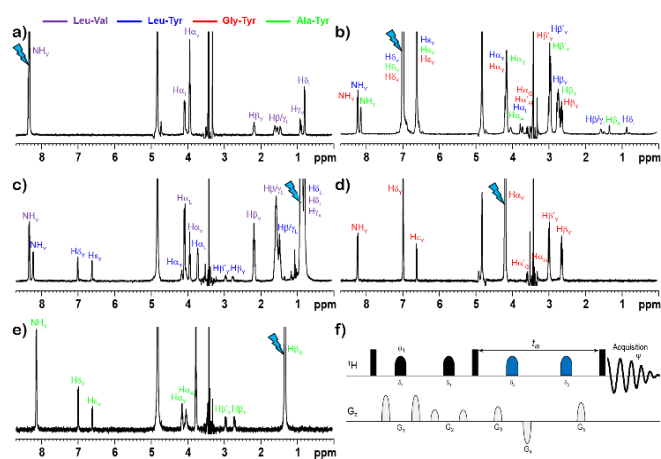


**Fig. 61.** Multiplet-selective excitation 1D NOESY spectra of the dipeptide test mixture in DMSO-*d*<sub>6</sub>/EG (7:3 v/v) (a, b, c, d, e, 268 K) at 500 MHz (<sup>1</sup>H),  $t_m$  = 1 s. (f) Pulse sequence:  $\phi_1 = x, y, -x, -y, \psi = x, -x$ . The initial selective inversion pulses excited: (a) the NH<sub>V</sub>(LV) proton resonance (experiment time (expt) = 444.85 min); (b) H $\delta_V$ (LY)/H $\delta_V$ (GY)/H $\delta_V$ (AY) proton resonances (expt = 56.98 min); (c) the H $\delta_L$ (LY) /H $\delta_L$ (LV)/H $\delta_V$ (LV) proton resonances (expt = 57.05 min); (d) the H $\alpha_V$ (GY) proton resonance (expt = 149.83 min). (e) the H $\beta_A$ (AY) proton resonance (expt = 147.50 min).

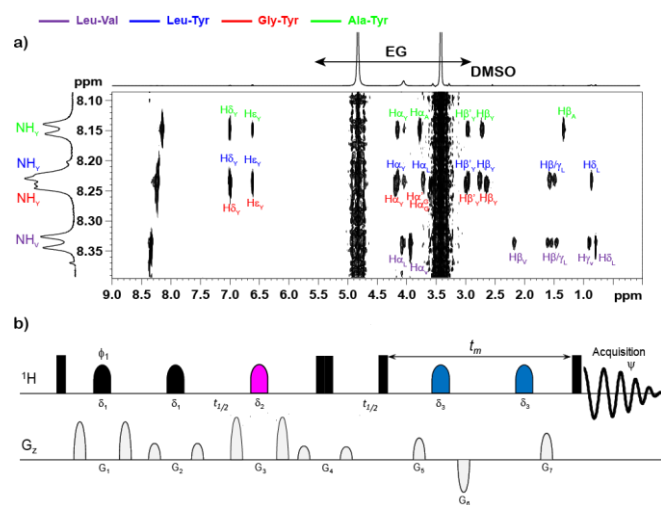


**Fig. 62.** (a)  $F_1$  band selective  $F_1$  decoupled 2D NOESY spectrum of the dipeptide test mixture in DMSO-*d*<sub>6</sub>/EG (7:3 v/v) at 268 K, at 500 MHz (<sup>1</sup>H), (256 scans per  $t_1$  value, expt = 437 min,  $t_m$  = 1 s). (b) Pulse sequence:  $\phi_1 = x, y, -x, -y, \psi = x, -x$ . The initial selective 180° pulses had Gaussian shape and were applied to the four NH amide proton resonances.

Full access to a complete spectrum for each molecule in the mixture, starting from a single <sup>15</sup>N resonance for each, was provided by hyphenation of the HSQC and NOESY pulse sequences. The 2D <sup>1</sup>H-<sup>15</sup>N HSQC-NOESY spectra of

our model dipeptide mixture acquired at 268 K and 600 MHz, in DMSO-*d*<sub>6</sub>/EG (7:3 v/v), showed that all protons of each dipeptide of the mixture were able to correlate with all other protons, and protonated nitrogen, by spin diffusion under viscous conditions, (Fig. 63). Appropriate choice of horizontal slices through nitrogen resonances then made it possible to extract the complete proton spectrum of each dipeptide.

We have demonstrated that the DMSO-*d*<sub>6</sub>/EG solvent blend is also useful for separating the signals of polar mixture components by spin diffusion. DMSO-*d*<sub>6</sub>/EG also provides valuable benefits compared to other viscous solvents such as GL and GC in terms of NMR sample preparation, selection of the range of measurement temperature, and easy main field locking and shimming. Separation of the signals of individual components a polar Leu-Val, Leu-Tyr, Gly-Tyr, and Ala-Tyr mixture in DMSO-*d*<sub>6</sub>/EG (7:3 v/v) was successfully accomplished at 268 K by selective 1D, 2D <sup>1</sup>H NOESY and <sup>1</sup>H-<sup>15</sup>N HSQC experiments. <sup>15</sup>N nuclei were used as chemical shift markers to enhance spectrum readability, but their low natural abundance caused lower sensitivity.

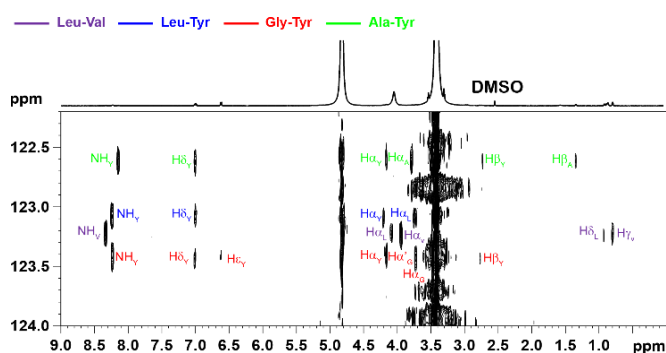


**Fig. 63.** a) 2D <sup>1</sup>H-<sup>15</sup>N HSQC-NOESY spectrum of the dipeptide test mixture (10 mM) dissolved in DMSO-*d*<sub>6</sub>/EG (7:3 v/v), at 268 K, *t*<sub>m</sub> = 1 s, at 600 MHz (<sup>1</sup>H).

### 3.4.3. Dimethylsulfoxide-*d*<sub>6</sub> (DMSO-*d*<sub>6</sub>)/water blend

As previously reported in section 2.5, the physical properties of DMSO-water blends have been thoroughly investigated for more than 50 years. [19, 44, 123-134] Due to the very strong interaction between the two solvents through

hydrogen bonding, [127-129] the viscosity of DMSO-water blends are higher than those of the individual pure solvents. [19, 131, 132] In addition, the viscosity of this solvent blend, which depends on the proportions, increases considerably with reduction in temperature. For example, multiplication of the viscosity by factors of 3 and 10 compared to ambient temperature ( $\eta = 3.8$  cP) is achieved for 30% mole fraction of DMSO in water at 0°C ( $\eta = 9.1$  cP) and -25°C ( $\eta = 32$  cP) respectively, [129] with melting points dropping down to -130°C. [123, 133, 134]. Consequently, the sign and the size of intramolecular NOE enhancements may be efficiently controlled by simply changing the sample temperature over a wide range from -130°C to room temperature and even higher. [7]. This ability to manipulate NOE enhancements turns out to be tremendously useful in NMR investigations of mixtures.

In 2017, Lameiras *et al.* reported the use of viscous DMSO-*d*<sub>6</sub>/water blends for the analysis of two mixtures respectively constituted of polar and moderately apolar compounds, by means of homo- and heteronuclear NMR, [380] since other viscous solvents previously described such as perfluorinated oils [377] were inappropriate for the dissolution of polar compounds and glycerol was not suitable for low polarity compounds. [378] The authors focused on the assessment of DMSO-*d*<sub>6</sub>/H<sub>2</sub>O (7:3 v/v), at 268 K and 500 MHz (<sup>1</sup>H), in discriminating between the signals of Leu-Val, Leu-Tyr, Gly-Tyr and Ala-Tyr dipeptides (the model mixture previously investigated in sections 3.2 and 3.4), and of DMSO-*d*<sub>6</sub>/H<sub>2</sub>O (8:2 v/v) blend, at 238 K, in the study of a synthetic difluorinated dinucleotide, <sup>2</sup><sub>α</sub>F<sup>3</sup><sub>α</sub>F<sup>T</sup> (MW = 566.40 g mol<sup>-1</sup>, chemical structure in Fig. 64).

For analysing mixtures of a large variety of polar and moderately apolar compounds by NMR, the authors mention some advantages of and advice regarding the use of DMSO-

$d_6$ /water. The main advantage of these blends is their low viscosity at room temperature, [19, 125, 129, 131, 132, 147] permitting easy introduction of the sample into an NMR tube, unlike glycerol or glycerol carbonate. Adding water to DMSO- $d_6$  allows working at or below room temperature, which is particularly suitable for thermo-sensitive molecules. The lowest melting point of DMSO/water blends is close to 228 K, at 30% (v/v) of water in DMSO- $d_6$ . As described earlier, the high proportion of DMSO- $d_6$  enables use of routine spectrometer tools such as automatic field-locking and shimming. In addition, the water signal is readily removed using common suppression tools such as excitation sculpting. [401] Changing the proportion of water in DMSO- $d_6$  between 10 and 30% enabled the authors to control spin diffusion efficiency and thus to enable separation of the signals of a large range of high-polarity and moderately low-polarity molecules. The authors recommend the use of DMSO- $d_6$ /H<sub>2</sub>O blend for the analysis of biologically active molecules, to prevent loss of labile protons such as amides through exchange with D<sub>2</sub>O. DMSO- $d_6$ /D<sub>2</sub>O blends are preferable for organic compounds in which labile protons are not needed to for structure elucidation. Mid-sized compounds require only a low proportion of water in DMSO- $d_6$ , while smaller compounds require up to 30%, to control spin diffusion between 298 and 238 K.

$F_1$  encoding of chemical shifts of nuclei other than  $^1\text{H}$  may be useful to avoid strong proton resonance overlap in the study of complex mixtures. Under spin diffusion conditions, 2D  $^1\text{H}$ - $^{13}\text{C}$  HSQC-NOESY spectra can reveal  $^1\text{H}$  and  $^{13}\text{C}$  chemical shift lists for every mixture constituent. [379] The authors extended this approach to 2D  $^1\text{H}$ - $^{15}\text{N}$  HSQC-NOESY. They also involved  $^{19}\text{F}$  nuclei in spin diffusion experiments. The  $^{19}\text{F}$  nucleus has 100% natural abundance and a high magnetogyric ratio ( $\gamma(^{19}\text{F})/\gamma(^1\text{H}) = 0.941$ ). They implemented

this original approach to mixture analysis and exemplified it *via* 1D and 2D  $^1\text{H}$ - $^{19}\text{F}$  HOESY experiments.

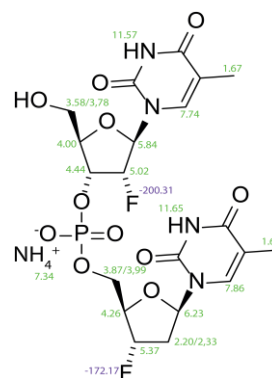


**Fig. 64.** Chemical structure of the synthetic difluorinated dinucleotide,  $2'\alpha\text{F-Tp}3'\alpha\text{F-T}$ . Reproduced from [380].

#### 3.4.3.1. Study of the Leu-Val, Leu-Tyr, Gly-Tyr, and Ala-Tyr mixture in DMSO- $d_6$ /H<sub>2</sub>O (7:3 v/v)

The NOESY spectrum of this dipeptide mixture recorded at 268 K and 500 MHz revealed full magnetization exchange through intramolecular spin diffusion from NH for each dipeptide, without significant signal broadening (Fig. 65). Consequently, the signals of all the peptides in the mixture were readily distinguished.

The authors also used the detection of all the mixture component resonances during signal acquisition *via* 1D selective NOESY experiments. [378, 379] A suitable set of proton resonances was chosen to excite selectively in order to differentiate between signals of the different dipeptides. Full magnetization exchange was observed over distances greater than 14 Å. The 2D  $^1\text{H}$ - $^{13}\text{C}$  and  $^1\text{H}$ - $^{15}\text{N}$  HSQC-NOESY spectra of the dipeptide test mixture acquired at 268 K at 600 MHz in DMSO- $d_6$ /H<sub>2</sub>O (7:3 v/v) blend showed that under viscous conditions, all the protons of each dipeptide, and protonated carbon and protonated nitrogens, were correlated, by spin diffusion. A set of slices through carbon resonances or nitrogen resonances made it possible to produce a

complete proton spectrum for each dipeptide. The four spectra were similar to those of the pure dipeptides.

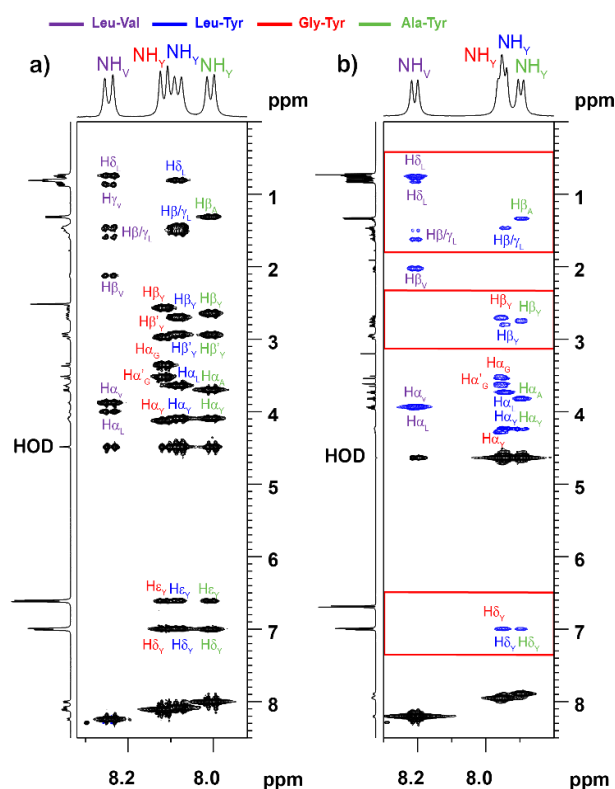


**Fig. 65.** Amide proton region of 2D NOESY spectra of a dipeptide test mixture (10 mM), mixing time ( $t_m$ ) = 1 s, at 500 MHz ( $^1\text{H}$ ), a) dissolved in  $\text{DMSO-}d_6/\text{H}_2\text{O}$  (7:3 v/v), at 268 K, b) dissolved in  $\text{H}_2\text{O}/\text{D}_2\text{O}$  (9:1 v/v), at 298 K. The red frames correspond to spectral regions of interest in which water as solvent has a major effect on the number and sign of observable NOESY cross peaks. Reproduced from [380].

#### 3.4.3.2. ${}^{2'}\alpha\text{F}T\text{p}3'\alpha\text{F}T$ in $\text{DMSO-}d_6/\text{H}_2\text{O}$ (8:2 v/v) blend

Lameiras *et al.* extended the simplification of mixture investigation by using  ${}^{19}\text{F}$  NMR spectroscopy. The incorporation of fluorine in organic compounds offers a variety of useful properties, in polymer and material sciences and in therapeutic agents, making the study of fluorine-containing compounds in mixtures important. [402, 403]

Spin diffusion in the heteronuclear NMR experiments just described only involved the  ${}^1\text{H}$  nuclei of the compounds of interest. In contrast, here the  ${}^{19}\text{F}$  nucleus is integrated into the spin network within which magnetization is exchanged by longitudinal cross relaxation under high viscosity conditions. A synthetic difluorinated dinucleotide,  ${}^{2'}\alpha\text{F}T\text{p}3'\alpha\text{F}T$  (Fig. 64) was

selected to exemplify this approach by means of HOESY experiments. Spectra were recorded in  $\text{DMSO-}d_6/\text{H}_2\text{O}$  instead of  $\text{DMSO-}d_6/\text{D}_2\text{O}$ , to prevent the exchange of the NH protons with  $\text{D}_2\text{O}$ .

The authors first set the temperature that offered the best compromise between spin diffusion and spectral resolution using 2D  ${}^1\text{H-}{}^1\text{H}$  NOESY and  ${}^1\text{H-}{}^{19}\text{F}$  HOESY spectra from 268 to 238 K, with excitation sculpting for water signal suppression. [401] Full magnetization transfer was clearly visible at 238 K over all the  ${}^{2'}\alpha\text{F}T\text{p}3'\alpha\text{F}T$   ${}^1\text{H}$  and  ${}^{19}\text{F}$  nuclei, over distances of greater than 18 Å (Fig. 66). The  ${}^1\text{H}$  and  ${}^{19}\text{F}$  spectra of the  ${}^{2'}\alpha\text{F}T\text{p}3'\alpha\text{F}T$  molecule were readily obtained by extraction of a suitable collection of rows and columns. As usual, the extracted spectra were comparable to the conventional 1D  ${}^1\text{H}$  and  ${}^{19}\text{F}$  spectra. Nevertheless,  ${}^1\text{H}$  resonance overlap may hamper structure elucidation in the investigation of complex mixtures of fluorinated compounds.

The authors proposed a workaround by selectively exciting a single  ${}^{19}\text{F}$  resonance, implementing a dedicated NMR pulse sequence made up of a double pulsed field gradient spin echo block followed by a 1D HOESY block (Fig. 67). Each of the  ${}^{19}\text{F}$  nuclei resonating at -172.19 and -200.31 ppm exchanged its magnetization with all the protons of the compound. Conversely, selective excitation of a  ${}^1\text{H}$  resonance revealed the chemical shifts of the  ${}^{19}\text{F}$  nuclei of the compound. Focusing on one or other NH proton resonance at 11.57 or 11.65 ppm led to the  ${}^{19}\text{F}$  spectrum of the sample.

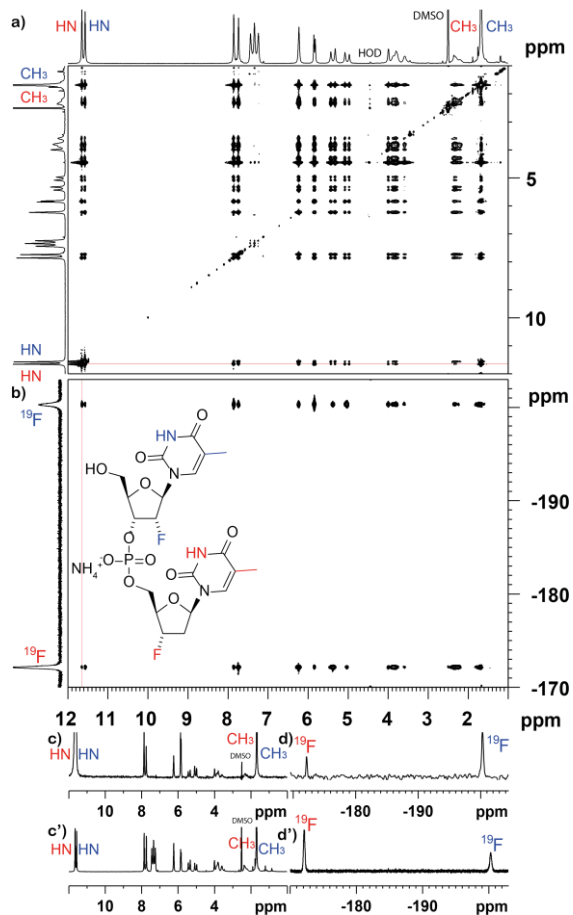


**Fig. 66.** 2D  $^1\text{H}$ - $^1\text{H}$  NOESY and  $^1\text{H}$ - $^{19}\text{F}$  HOESY spectra of  $2'\alpha\text{F-Tp}_3'\alpha\text{F-T}$  (20 mM) dissolved in  $\text{DMSO-}d_6/\text{H}_2\text{O}$  (8:2, v/v), at 238 K, mixing time ( $t_m$ ) = 1 s, at 500 MHz ( $^1\text{H}$ ). Comparison of  $^1\text{H}$  horizontal slice extracted from the 2D  $^1\text{H}$ - $^1\text{H}$  NOESY at 11.65 ppm with the conventional 1D proton spectrum (c, c', red row) and comparison of  $^{19}\text{F}$  vertical slice from the 2D  $^1\text{H}$ - $^{19}\text{F}$  HOESY at 11.65 ppm with the conventional 1D fluorine spectrum (d, d', red column). Reproduced from [380].

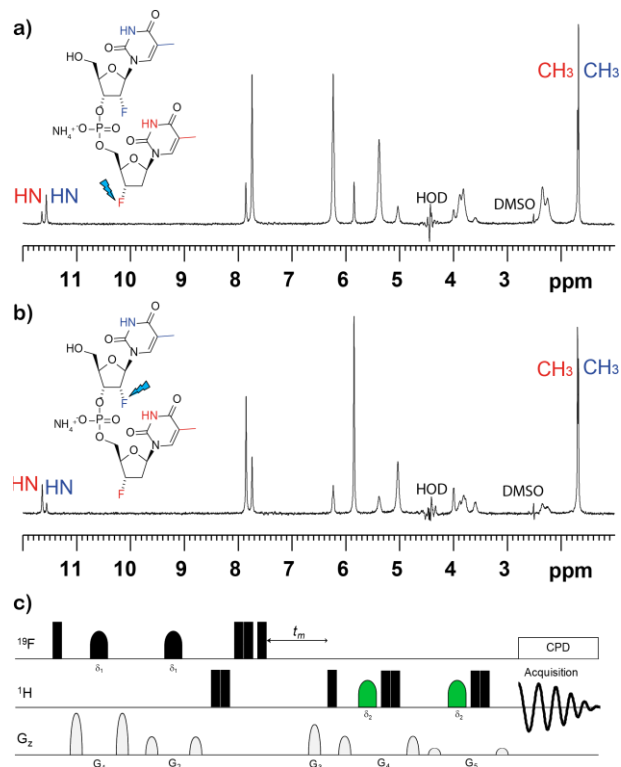


**Fig. 67.** Multiplier-selective excitation 1D  $^1\text{H}$ - $^{19}\text{F}$  HOESY spectra of  $2'\alpha\text{F-Tp}_3'\alpha\text{F-T}$  (20 mM) dissolved in  $\text{DMSO-}d_6/\text{H}_2\text{O}$  (8:2, v/v) (a, b, 238 K),  $t_m = 1$  s, at 500 MHz ( $^1\text{H}$ ). The initial selective inversion pulses excited the fluorine resonance at a) -172.17 and b) -200.31 ppm. c) Pulse sequence. Reproduced from [380].

Lameiras *et al.* demonstrated that the  $\text{DMSO-}d_6/\text{H}_2\text{O}$  solvent blend is the easiest to handle and the most efficient viscous solvent reported so far for the resolution of both polar and moderately apolar components in complex mixtures, taking advantage of  $^1\text{H}$  and  $^{19}\text{F}$  NMR spin diffusion.

### 3.5. Carbohydrate-based solutions

Lameiras *et al.* evaluated sucrose solution and agarose gels in the individual NMR characterization of the same model mixture as studied in sections 3.2 and 3.4, Leu-Val, Leu-Tyr, Gly-Tyr and Ala-Tyr, using spin diffusion in  $^1\text{H}$  selective 1D, 2D NOESY and  $^1\text{H}$ - $^{13}\text{C}/^{15}\text{N}$  2D HSQC-NOESY experiments. [381]

#### 3.5.1. Sucrose solution

Interestingly for mixture analysis, “table sugar” (i.e. sucrose) in water produces a high-viscosity medium that

leads to spin diffusion over a wide range of temperature (from room temperature downwards, the latter especially appropriate for thermally unstable bioactive molecules) due to the decrease of the molecular tumbling rate. Sucrose/water (1:1 w/w) syrup has a viscosity of around 27 cP at 283 K, [404, 405] whereas that of water at the same temperature is 1.307 cP. [338] The preparation of NMR samples is user-friendly, as the viscosity at room temperature allows easy transfer of the sample solution to the NMR tube. The cost of sample preparation is very low, since “table sugar” is a very common staple. However, the intense proton signals of non-deuterated sucrose need to be suppressed. Medium-sized compounds will require only a low concentration of sucrose in water, while smaller compounds will require more sucrose to enhance spin diffusion at room temperature and below.

Lameiras *et al.* investigated their usual test dipeptide mixture dissolved in high-viscosity sucrose solution, using  $^1\text{H}$ ,  $^1\text{H}$ - $^{13}\text{C}$  and  $^1\text{H}$ - $^{15}\text{N}$  NOESY-based spin diffusion experiments. The biggest problem of such solutions is the requirement to suppress the  $^1\text{H}$  signals of sucrose and water (Fig. 68a), since deuterated sucrose would be too expensive to produce and deuterated water would exchange with the labile amide protons of the dipeptides. As previously, the suppression of these signals can be accomplished using selective excitation and detection pulses within an excitation sculpting scheme. [387] Fig. 68b shows the efficacy of the solvent suppression that was accomplished *via* band selective detection (Fig. 68e).

Lameiras and co-workers demonstrated that using viscous sucrose solution at 283 K allows full intramolecular magnetization exchange by spin diffusion, observed over distances greater than 14 Å, throughout all these small and flexible dipeptides, using a band-selective detection NOESY experiment (Fig. 69). Clustering of proton resonances is

rapidly achievable, making it possible to distinguish the mixture constituents.

For analytical purposes, the authors also collected additional information about the structure of each mixture constituent, that was not accessible *via* band selective NOESY experiments, by observing the  $\text{H}_\alpha$  proton resonances in  $F_2$  in 1D selective NOESY experiments, [378, 379]. All the dipeptides were distinguished through spin diffusion in sucrose solution *via* selective excitation of suitable proton resonances. The authors then reused the less time-consuming approach of  $F_1$  band-selective  $F_1$ -decoupled 2D NOESY first described in section 3.2. NH amide resonances were again the initial sources of magnetization after the initial band selective excitation step. Running the latter experiment in sucrose solution made possible the assignment of all the proton resonances of Leu-Val, Leu-Tyr, Gly-Tyr and Ala-Tyr, through spin diffusion during the mixing time.

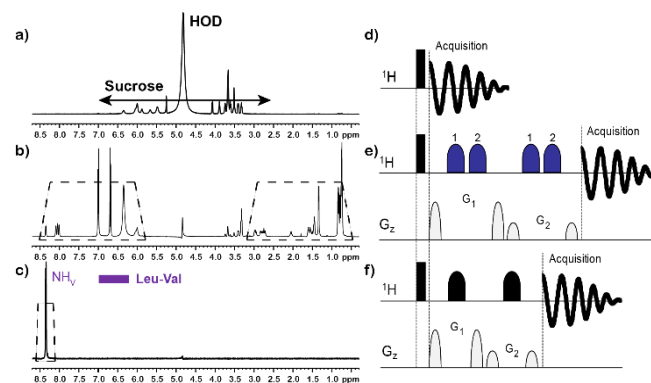


**Fig. 68.** 1D  $^1\text{H}$  spectra, at 600 MHz ( $^1\text{H}$ ), and NMR pulse sequence of the dipeptide test mixture in sucrose solution at 283 K. a, d) Non-selective excitation and detection. b, e) Selective detection of two resonance bands (dotted trapezium). The “1” and “2” labels indicate the high and low chemical shift regions respectively. c, f) Selective excitation of the valine amide proton doublet of Leu-Val (dotted trapezium) using a 10 ms, 1% truncated,  $180^\circ$  Gaussian pulse. Adapted from [381].

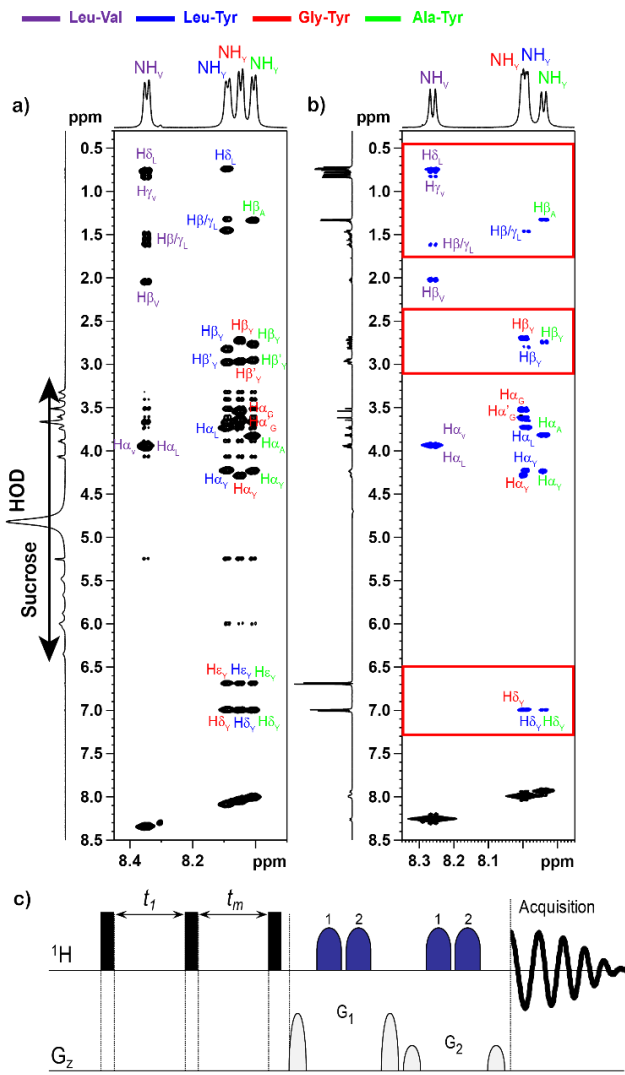


**Fig. 69.** Amide proton regions of band-selective detection 2D NOESY spectra of the dipeptide test mixture (10 mM) (a) in sucrose/H<sub>2</sub>O (5:5, w/w + 10% D<sub>2</sub>O, v/v), mixing time ( $t_m$ ) = 0.5 s, at 600 MHz (<sup>1</sup>H) using the pulse sequence in part c, at 283 K, and (b) in H<sub>2</sub>O/D<sub>2</sub>O (9:1, v/v),  $t_m$  = 0.5 s, at 600 MHz (<sup>1</sup>H), using the noesyegpph pulse sequence, at 298 K. The red frames correspond to spectral regions of interest in which water as solvent has a major effect on the number and signs of observable NOESY cross peaks. Reproduced from [381].

More complex mixtures may not show the resolved proton resonances required for selective <sup>1</sup>H NOESY experiments, because of a spectral overlap. Hyphenation of the HSQC and NOESY experiments may address this issue by exploiting the greater dispersal of <sup>13</sup>C and <sup>15</sup>N chemical shifts. 2D <sup>1</sup>H-<sup>15</sup>N HSQC-NOESY spectra of our model dipeptide mixture, acquired at 283 K and 600 MHz in sucrose solution (Fig. 70), showed that in each dipeptide spin diffusion shared

magnetization across all protons and protonated carbons or nitrogens. Appropriate slices through carbon resonances or nitrogen resonances then allowed extraction of the complete proton spectrum of each dipeptide.

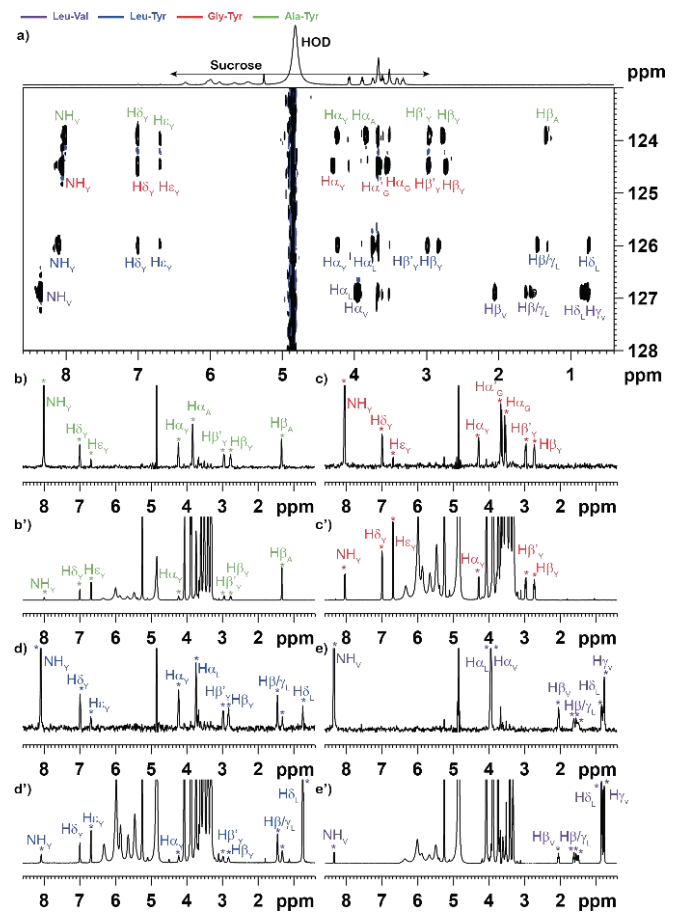


**Fig. 70.** a) 2D <sup>1</sup>H-<sup>15</sup>N HSQC-NOESY spectrum of the dipeptide test mixture (20 mM) dissolved in sucrose solution, at 283 K,  $t_m$  = 0.5 s, with solvent multiple presaturation, at 600 MHz (<sup>1</sup>H). Comparison of four <sup>1</sup>H horizontal slices extracted from the 2D <sup>1</sup>H-<sup>15</sup>N HSQC-NOESY spectrum at 123.93 (b, b', Ala-Tyr, green row), 124.49 (c, c', Gly-Tyr, red row), 126.01 (d, d', Leu-Tyr, blue row), and 126.91 ppm (e, e', Leu-Val, purple row) with the conventional 1D proton spectra of each pure dipeptide dissolved (20 mM) in sucrose solution, at 283 K, at 600 MHz (<sup>1</sup>H). Reproduced from [381].

### 3.5.2. Agarose gel

Agarose gels are usually employed for biological molecule separation by electrophoresis, but also turn out to be useful in small molecule mixture analysis. As reported in section 2.10, the main complication is sample preparation, because incorporating compounds of interest into the gel requires

mixing with agarose powder followed by solution in water at high temperature (363 K for regular agarose and around 338 K for low-melting agarose). Some peptides and proteins may be damaged because of the exposure to high temperature, impeding NMR structural and conformational studies. The heating required lasts only a few minutes, so less thermo-sensitive small molecules such as nucleic acids, peptides or saccharides can be studied. In addition, NMR peaks can be dramatically broadened, especially if samples are inhomogeneous owing to partially unmelted agarose or the presence of air bubbles. The remedy is to re-liquefy the sample inside the NMR tube, shake thoroughly, and cool again to room temperature. Freezing points of 260 K and 264 K are given in the literature for H<sub>2</sub>O- and D<sub>2</sub>O-based 1% agarose gels respectively, [302] reducing the temperature range over which spin diffusion may be used compared to sucrose solution. Consequently, agarose gel is recommended for investigating rigid small or mid-sized compounds in mixtures, as these have higher correlation times than very flexible small compounds.

As previously noted, [300, 302] owing to the rapid transverse relaxation of protons in agarose gel, agarose proton resonances are not normally observable (Fig. 71). This is undoubtedly the biggest advantage of this medium in polar mixture analysis, as there is only the residual HOD signal to suppress.

Lameiras *et al.* also first showed with band-selective detection 2D NOESY experiments that at 273 K, spin diffusion was efficient and spectral resolution sufficient for further studies. [377, 378] Spin diffusion was detected over distances greater than 14 Å for Leu-Tyr, Gly-Tyr and Ala-Tyr owing to the rigidity of their aromatic components. However, the flexibility of the Leu-Val peptide in agarose gel at 273 K prevented observation of magnetization transfer over the entire molecule and only positive NOEs were observed. Spin

diffusion was sufficiently efficient in agarose gel at 273 K to group together all proton resonances of the Tyr-based dipeptides, allow them to be distinguished; the proton resonance pattern of Leu-Val was then inferred by elimination. “and early gelation might happen” has been removed.

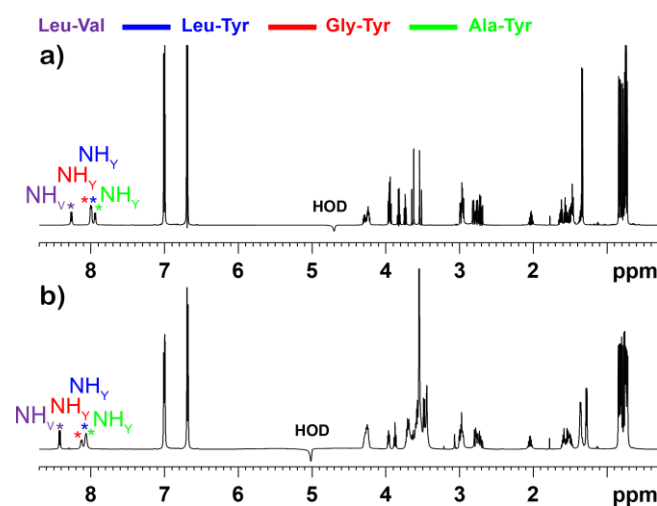


**Fig. 71.** 1D <sup>1</sup>H spectra of the dipeptide test mixture (10 mM) dissolved a) in H<sub>2</sub>O/D<sub>2</sub>O (9:1, v/v), at 298 K, at 600 MHz (<sup>1</sup>H) and b) in agarose gel 1%, at 273 K, at 600 MHz (<sup>1</sup>H) with water suppression using excitation sculpting. Reproduced from [381].

The authors reused the 1D selective NOESY experiment described earlier to emphasise the difference in behaviour between the different dipeptides in agarose gel. Fig. 72 shows that all the Tyr-based dipeptides could be distinguished through spin diffusion by selective excitation of suitable proton resonances. Owing to their different molecular tumbling rates, Leu-Tyr and Leu-Val show respectively negative (active spin diffusion, positive peaks) and positive (negative peaks) NOEs. The NOE sign therefore distinguishes the two sets of signals. A complete proton assignment of Gly-Tyr was obtained by comparing the 1D NOESY spectra.

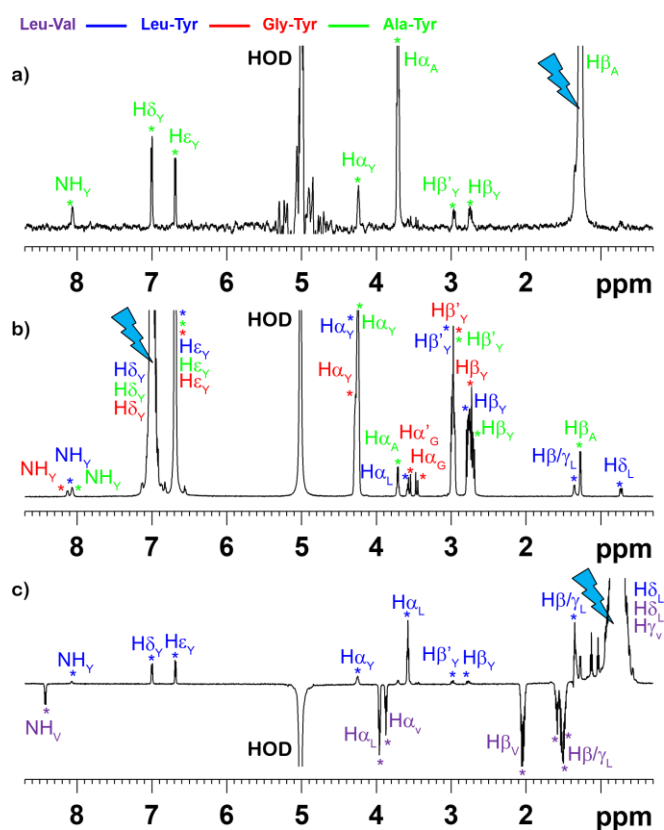


**Fig. 72.** Multiplet selective excitation 1D  $^1\text{H}$  NOESY spectra of the dipeptide test mixture (10 mM) dissolved in agarose gel 1% (a, b, c, 273 K),  $t_m = 0.5$  s, at 600 MHz ( $^1\text{H}$ ). The initial selective inversion pulses excite: a) the  $\text{H}\beta_\gamma(\text{A}\gamma)$  proton resonance; b) the  $\text{H}\delta_\gamma(\text{L}\gamma)/\text{H}\delta_\gamma(\text{G}\gamma)/\text{H}\delta_\gamma(\text{A}\gamma)$  proton resonances; c) the  $\text{H}\delta_\text{L}(\text{L}\gamma)/\text{H}\delta_\text{L}(\text{L}\gamma)/\text{H}\gamma_\text{V}(\text{L}\gamma)$  proton resonances. Adapted from [381].

Lameiras *et al.* thus established that using sucrose solution and agarose gel allows the signals of mixed polar constituents to be distinguished through NMR spin diffusion. They highlighted some advantages of sucrose solutions over agarose gel - spin diffusion occurs over a larger range of temperature, NMR sample preparation, with no heating required, is easy and well-suited to thermo-sensitive molecules - but noted that agarose gel has the significant advantage of not showing strong solvent proton signals owing to fast transverse relaxation. Medium-sized compounds only require a small quantity of sucrose in water, while smaller compounds require more, up to 50% (w/w), to promote spin diffusion at and below room temperature. Agarose gel may be an appropriate alternative to sucrose

solution for investigating small rigid or medium-sized compounds in mixtures showing relatively long correlation times.

Discrimination between Leu-Val, Leu-Tyr, Gly-Tyr and Ala-Tyr signals in a mixture was accomplished at 283 K and 273 K in sucrose solution and agarose gel respectively, via selective 1D, 2D  $^1\text{H}$ - $^1\text{H}$  NOESY experiments.  $^1\text{H}$ - $^{13}\text{C}$  and  $^1\text{H}$ - $^{15}\text{N}$  HSQC-NOESY experiments were employed for sucrose solution since  $^{13}\text{C}$  and  $^{15}\text{N}$  offer a wider chemical shift range than  $^1\text{H}$ , improving spectrum readability.

### 3.6. Sulfolane blends

Sulfolane is an inexpensive, non-reactive dipolar aprotic solvent with interesting chemical, thermal and physical properties. It is composed of globular molecules and has a moderately high dielectric constant ( $\epsilon = 43.4$  at 300 K) [406] and a high dipole moment ( $\mu = 4.80$  D), responsible for its ability to dissolve a very large variety of polar and moderately apolar organic molecules. [407] Sulfolane is fully miscible with water, other polar, and aromatic organic solvents. Its freezing point is significantly reduced, to sub-zero temperatures, after adding water (50% v/v, 256 K) or DMSO- $d_6$  (30% v/v, 238 K). [383] This is particularly helpful for thermo-sensitive molecules. Owing to the increase in viscosity of these binary solvents with decreasing temperature, dissolved species can show spin diffusion at room temperature and below. [408] At room temperature the viscosities of both blends are reasonably small, although neat sulfolane has a value of 10.29 cP at 303 K, [409] greater than 0.898 cP for water and 2.007 cP for DMSO- $d_6$  at 298 K [19] Sulfolane is thus convenient for NMR sample preparation, in contrast to the high-viscosity alternatives glycerol ( $\eta = 934$  cP at 298 K) and glycerol carbonate ( $\eta = 85.4$  cP at 298 K). [23] The major experimental drawback of using both sulfolane-based blends is the appearance of intense proton signals,

from non-deuterated sulfolane and water, that need to be suppressed. This is readily accomplished *via* selective excitation and detection pulses in a DPGFSE sequence (Fig. 73). [383, 410]

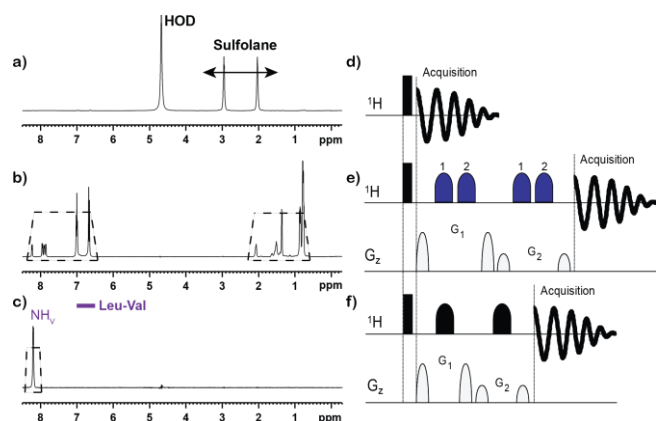


**Fig. 73.** 1D proton spectra and NMR pulse sequence for the dipeptide test mixture Leu-Val, Leu-Tyr, Gly-Tyr and Ala-Tyr (20 mM) dissolved in sulfolane/H<sub>2</sub>O/D<sub>2</sub>O (5:4:1 v/v/v), at 258 K, at 500 MHz (<sup>1</sup>H). a, d) Non-selective excitation and detection. b, e) Selective detection of two resonance bands (dotted trapezia). The “1” and “2” labels indicate the high and low chemical shift regions respectively. c, f) Selective excitation of the valine amide proton doublet of Leu-Val (dotted trapezium) using a 30 ms, 1% truncated, 180° Gaussian pulse. Reproduced from [383].

### 3.6.1. Sulfolane/dimethylsulfoxide-*d*<sub>6</sub> (DMSO-*d*<sub>6</sub>) blend

Pedinielli *et al.* investigated the use of sulfolane/DMSO-*d*<sub>6</sub> (7:3 v/v) in the individual NMR characterization of four apolar phosphorus-containing compounds (Fig. 74) by spin diffusion in selective 1D, 2D <sup>1</sup>H NOESY experiments and a 2D <sup>1</sup>H-<sup>31</sup>P HSQC-NOESY, since these four molecules show similar diffusion in neat DMSO-*d*<sub>6</sub>, owing to their comparable shape and size. [383]

The authors extended the simplification of small molecule mixture analysis *via* <sup>31</sup>P NMR spectroscopy. Phosphorus is common in synthetic intermediates and biological compounds. It has 100% natural abundance and sharp resonance peaks. [411] Its wide chemical shift range extends over about 2000 ppm, which aids discrimination of the signals of phosphorus-containing compounds in mixtures. [412] In

the slow tumbling limit, unlike <sup>19</sup>F and <sup>1</sup>H nuclei that show negative NOEs and HOEs, with homo- and heteronuclear spin diffusion, <sup>31</sup>P nuclei show only positive HOEs that tend towards zero with slower tumbling because of their particular magnetogyric ratios. [413]. Because of this limitation, to use <sup>31</sup>P nuclei as chemical shift markers requires magnetization exchange with the proton network *via* the 2D <sup>1</sup>H-<sup>31</sup>P HSQC-NOESY experiment under viscous conditions.

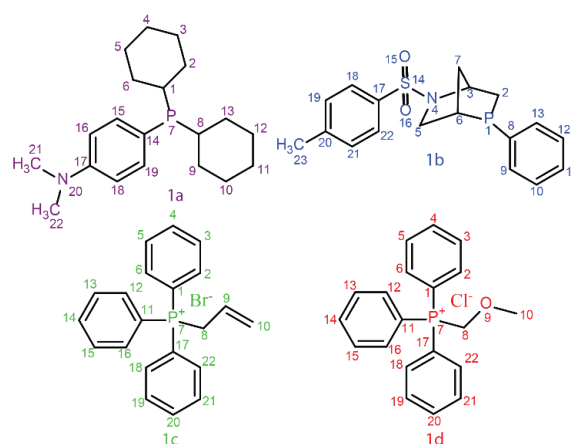


**Fig. 74.** Chemical structures of the four phosphorus-containing compounds in the mixture, 1a: dicyclohexyl (4-(*N,N*-dimethylamino)phenyl) phosphine, 1b: exophenyl Kwon [2.2.1] bicyclic phosphine, 1c: allyltriphenyl-phosphonium bromide and 1d: (methoxymethyl)triphenylphosphonium chloride. Reproduced from [383].

The authors established, *via* band-selective detection 2D NOESY (Fig. 75), at 500 MHz (<sup>1</sup>H) and <sup>1</sup>H-decoupled <sup>31</sup>P experiments at 202.46 MHz (<sup>31</sup>P), that <sup>1</sup>H spin diffusion was efficient and spectral resolution adequate for further homo- and heteronuclear NMR studies at 258 K. At this temperature, the sulfolane/DMSO-*d*<sub>6</sub> blend permits full intramolecular magnetization exchange through spin diffusion, observed over distances greater than 13 Å within each phosphorus-containing molecule (Fig. 75a), in part due to the rigidity of the cycloalkyl and aromatic parts. In contrast, the conventional 2D NOESY spectrum acquired in neat DMSO-*d*<sub>6</sub> at 298 K shows positive NOEs (Fig. 75b) due to

rapid reorientation of all the mixture components, preventing spin diffusion.

Because of resonance peak overlap in the 1D and 2D spectra, the authors used the selective 1D NOESY experiments described earlier to group proton resonances associated with the same phosphorus-containing molecule. They chose proton resonances to selectively excite to obtain the individual 1D  $^1\text{H}$  spectra of all the mixture components through spin diffusion. The authors then took advantage of the broad chemical shift range of the  $^{31}\text{P}$  nucleus by coupling 2D HSQC and NOESY experiments at 258 K (Fig. 76) [377, 379-381]. Under these *ViscY* operating conditions, each proton of every compound correlates with all other protons *via* spin diffusion after having labelled the phosphorus chemical shift in  $F_1$ . The choice of four slices through  $^{31}\text{P}$  resonances produces four whole complete spectra belonging to 1a, 1b, 1c and 1d. The authors thus demonstrated complete discrimination between the mixture components by 1D selective NOESY and 2D  $^1\text{H}$ - $^{31}\text{P}$  HSQC-NOESY experiments in the viscous sulfolane/DMSO- $d_6$  (7:3 v/v) blend at 258 K.

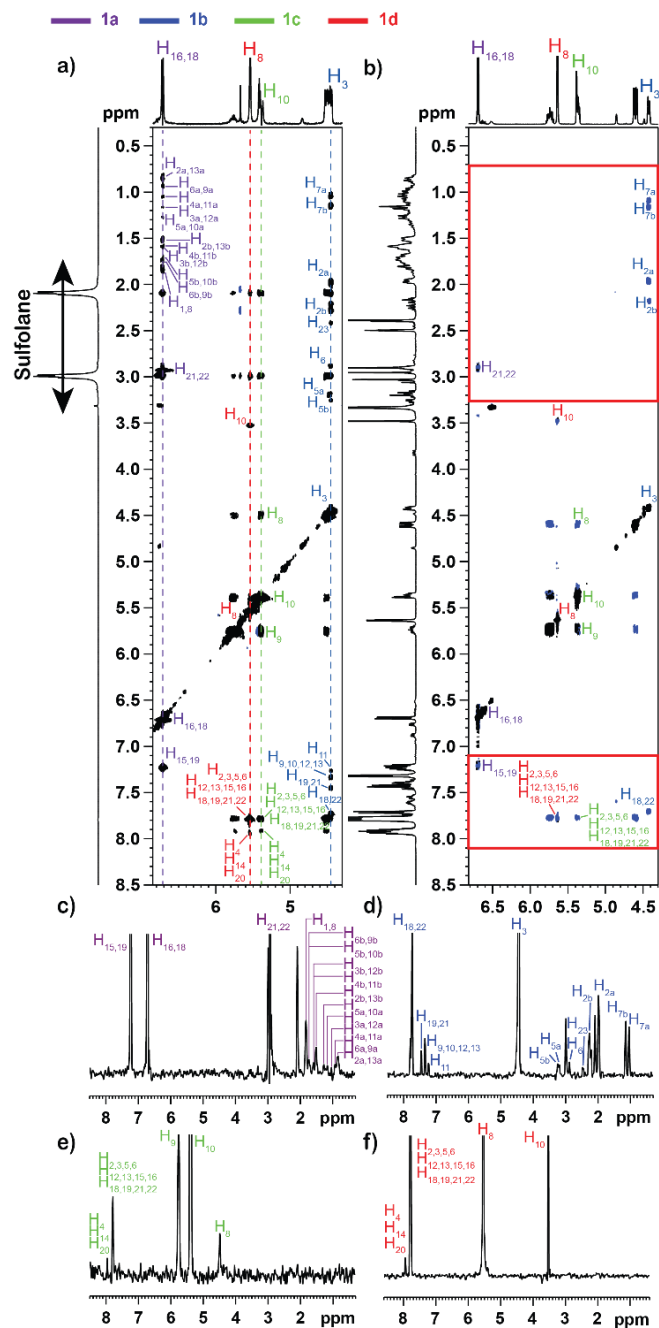


**Fig. 75.** a) Deshielded proton region of the band-selective detection 2D NOESY spectrum of the phosphorus-containing compound test mixture (20 mM) dissolved in sulfolane/DMSO- $d_6$  (7:3 v/v),  $t_m = 1$  s, at 258 K, at 500 MHz ( $^1\text{H}$ ).  $^1\text{H}$  vertical slices extracted from the 2D  $^1\text{H}$  NOESY at 6.72 ppm (c, H<sub>16,18</sub>(1a), purple dotted line), at 4.45 ppm (d, H<sub>3</sub>(1b), blue dotted line), at 5.40 ppm (e, H<sub>10</sub>(1c), green dotted line), and at 5.54 ppm (f, H<sub>8</sub>(1d), red dotted line). b) Deshielded proton region of the 2D NOESY spectrum of the same phosphorus-based compound test mixture dissolved in neat DMSO- $d_6$ ,  $t_m = 1$  s, at 298 K, at 500 MHz ( $^1\text{H}$ ). The red frames correspond to spectral regions of interest in which the solvent has a major influence on the number and signs of observable NOESY cross peaks. Reproduced from [383].

### 3.6.2. Sulfolane/water blend

Pedinielli *et al.* assessed the utility of the sulfolane/water blend in the individual NMR characterization of four dipeptides, Leu-Val, Leu-Tyr, Gly-Tyr and Ala-Tyr (as described previously), *via* spin diffusion in selective 1D and 2D  $^1\text{H}$  NOESY experiments. [383]

The authors demonstrated that the use of the sulfolane/water blend at 258 K, at 500 MHz ( $^1\text{H}$ ), allowed complete intramolecular magnetization exchange through spin diffusion over distances greater than 14 Å within each of the small and flexible dipeptides, using band-selective detection NOESY experiments (Fig. 77).

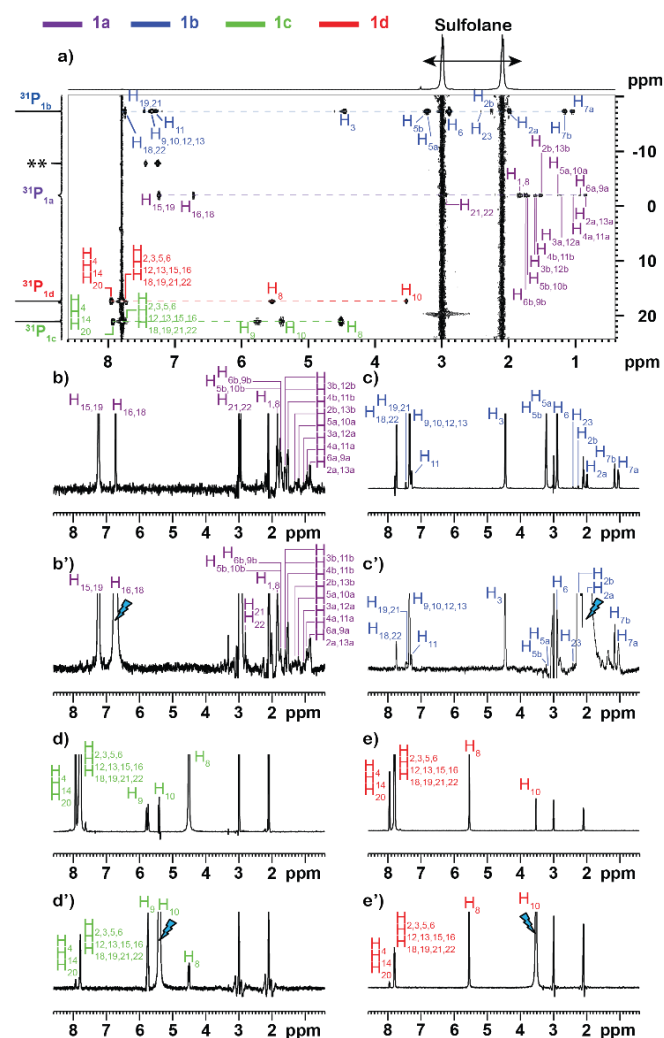
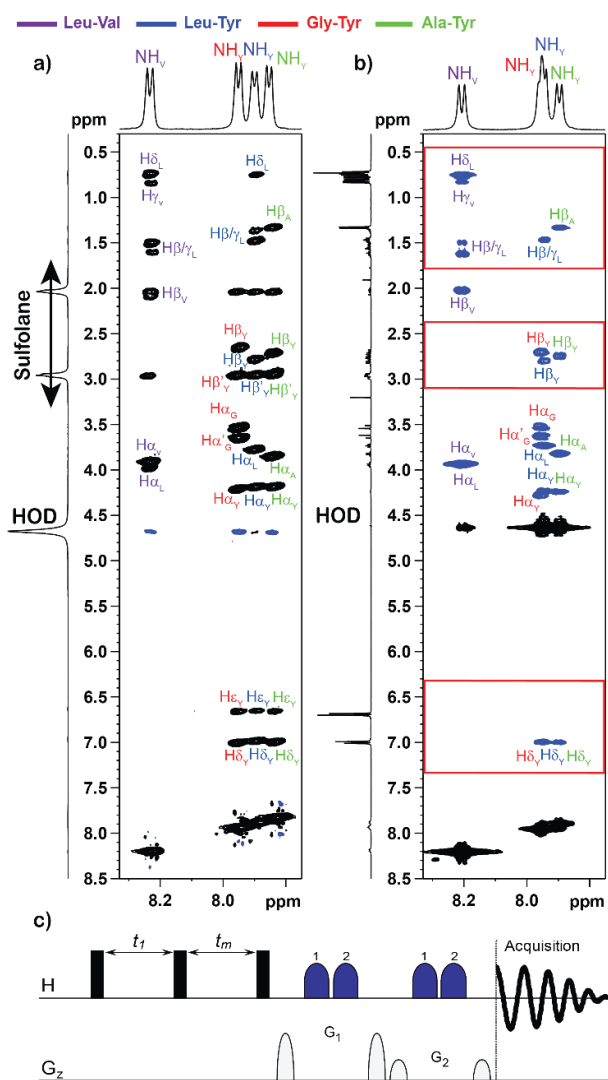


**Fig. 76.** a) 2D  $^1\text{H}$ - $^{31}\text{P}$  HSQC-NOESY spectrum of the phosphorus-based compound test mixture (20 mM) dissolved in sulfolane/ $\text{DMSO-}d_6$  (7:3 v/v),  $t_m = 1$  s, at 258 K, at 500 MHz ( $^1\text{H}$ ). Comparison of four  $^{31}\text{P}$  horizontal slices extracted from the 2D  $^1\text{H}$ - $^{31}\text{P}$  HSQC-NOESY at -2.00 (b, b', 1a, purple dotted line), -17.34 (c, c', 1b, blue dotted line), 21.01 (d, d', 1c, green dotted line), and

17.32 ppm (e, e', 1d, red dotted line) with the 1D selective NOESY spectra (selection of, b')  $\text{H}_{16,18}$ (1a), c')  $\text{H}_{2a}$ (1b), d')  $\text{H}_{10}$ (1c) and e')  $\text{H}_{10}$ (1d) protons resonances). \*\* Impurity. Reproduced from [383].

For analytical purposes, Pedinielli and co-workers again used 1D selective-NOESY experiments. [388, 410] Under viscous conditions at 258 K, all the dipeptides were differentiated by spin diffusion in sulfolane/water solution using selective excitation of suitable proton resonances. Pedinielli *et al.* also used  $F_1$  band-selective  $F_1$ -decoupled 2D NOESY to reduce experiment time. The NH resonances were the sources of magnetization after the initial band selective excitation step. Recording the latter experiment in sulfolane/water blend allowed full proton resonance assignments of Leu-Val, Leu-Tyr, Gly-Tyr and Ala-Tyr through spin diffusion.

Pedinielli *et al.* showed that viscous sulfolane/water and sulfolane/ $\text{DMSO-}d_6$  blends allow the signals of high- and low-polarity mixture constituents respectively to be distinguished through spin diffusion. They highlighted some benefits of using sulfolane-based blends compared to the high-viscosity solvents discussed earlier. Spin diffusion occurs over a wider range of temperatures, the solvent systems are suitable for thermo-sensitive molecules, and NMR sample preparation is easily carried out. Sulfolane/water is best suited to the investigation of mixtures of high-polarity molecules, while sulfolane/ $\text{DMSO-}d_6$  is most suitable for the study of mixtures of low-polarity molecules. Medium-sized compounds require a low proportion of water or  $\text{DMSO-}d_6$  in sulfolane, while smaller or more flexible compounds require more water or  $\text{DMSO-}d_6$ , up to 50% (v/v), to promote spin diffusion at room temperature and below.



proton exchange, applicability of routine NMR tools such as locking and shimming, and the need for solvent suppression necessary are indicated either positively (green tick) or negatively (red cross).

**Fig. 77.** a) Amide proton region of band-selective detection 2D NOESY spectrum of the dipeptide test mixture (20 mM) dissolved in sulfolane/H<sub>2</sub>O/D<sub>2</sub>O (5:4:1 v/v/v), mixing time ( $t_m$ ) = 1 s, at 258 K, at 500 MHz (<sup>1</sup>H), using the pulse sequence in part c. b) Amide proton region of 2D NOESY spectrum of the same dipeptide test mixture (20 mM) dissolved in H<sub>2</sub>O/D<sub>2</sub>O (9:1 v/v),  $t_m$  = 1 s, at 298 K, at 500 MHz (<sup>1</sup>H), using the noesyegpph pulse sequence. The red frames correspond to spectral regions in which water has a major effect on the number and signs of NOESY cross peaks. Reproduced from [383].

### 3.7. Overview of advantages/disadvantages of viscous solvents in molecule mixture analysis

This section offers an overview of the advantages and disadvantages of the various viscous solvents (solvent blends) described to date in the literature for mixture analysis using spin diffusion, in Table 5. Ease of sample preparation, dissolution power for high-/low-polarity compounds, solvent cost, spin diffusion efficiency, NMR spectral resolution, labile

	CTFEP/ CDCl <sub>3</sub>	Supercooled Water	Glycerol	Glycerol Carbonate	DMSO-d <sub>6</sub> / Glycerol	DMSO-d <sub>6</sub> / Glycerol-d <sub>6</sub>	DMSO-d <sub>6</sub> / Ethylene Glycol	DMSO-d <sub>6</sub> / Water	Sucrose/ Water	Agarose Gel	Sulfolane/ DMSO-d <sub>6</sub>	Sulfolane/ Water
Sample preparation	✓	✗	✗	✗	✓	✓	✓	✓	✓	✗	✓	✓
Polar compound dissolution power	✗	✓	✓	✓	✓	✓	✓	✓	✓	✓	✗	✓
Apolar compound dissolution power	✓	✗	✗	✗	✓	✓	✓	✓	✗	✗	✓	✗
Solvent cost	✗	✓	✓	✗	✓	✗	✓	✓	✓	✓	✓	✓
Efficient Spin Diffusion	278 K d > 25 Å	258 K d > ?? Å	318 K d > 14 Å	288 K d > 14 Å	288 K d > 14 Å	268 K d > 13 Å	268 K d > 14 Å	268/238 K d > 18 Å	283 K d > 14 Å	273 K d > 14 Å	258 K d > 13 Å	258 K d > 14 Å
NMR spectral resolution	✓	✓	✓	✓	✓	✓	✓	✓	✓	✓	✓	✓
Labile proton exchange	✓	✓	✓	✓	✓	✗	✓	✓	✓	✓	✓	✓
Routine NMR (lock, shimming)	✓	✓	✗	✗	✓	✓	✓	✓	✓	✓	✓	✓
Solvent suppression	✓	✓	✗	✗	✗	✓	✗	✓	✗	✓	✗	✗

**Table 5.** Overview of advantages/disadvantages of viscous solvents in molecule mixture analysis. d = distance over which spin diffusion has been reported. The size of the symbols is correlated with the strength of advantages/disadvantages.

## 4. Conclusion

This review article covers more than 40 years of NMR investigations dealing with the manipulation of the size and sign of NOE enhancements in small and medium-sized molecules by means of viscous solvents, for structure determination and mixture analysis. The NOE enhancement depends on Larmor frequency and overall rotational correlation time  $\tau_c$ , and therefore on the solution viscosity, since the latter affects  $\tau_c$ . [7] For a given magnetic field strength, increasing viscosity allows the molecular tumbling rate to be reduced. As a result, molecules enter the negative NOE regime. The maximum negative NOE of 100% is then reachable, and for long saturation (steady-state NOE) or mixing times (transient NOE), partial or full intramolecular magnetization exchange may occur through spin diffusion. In the case of very efficient spin diffusion, the determination of internuclear distances and therefore of molecular structure and conformation may be hampered. Nonetheless, we have reported the great contribution of active spin diffusion in identifying individual polar and apolar compounds in mixtures.

Negative NOE enhancements are generally found at high field (>300 MHz) for isotropically tumbling rigid mid-sized compounds ( $MW > \sim 700 \text{ g mol}^{-1}$ ) at room temperature in low-viscosity solvents ( $\eta > 2 \text{ cP}$ ) such as DMSO- $d_6$ , and are widely used for studying molecular structure and conformation. Smaller ( $MW > 150 \text{ g mol}^{-1}$ ) and/or less rigid molecules will require an increase in magnetic field or medium viscosity (or both), typically at least 500 MHz operation frequency and a solvent with minimum viscosity 7-10 cP such as room-temperature EG/water blend. For the same Larmor frequency, efficient spin diffusion (long-range NOE correlations over distances  $> 25 \text{ \AA}$ ) will require a highly viscous solvent ( $\eta > 80 \text{ cP}$ ) such as GL or GC at room temperature, or solvent blends such as DMSO- $d_6$ /GL,

DMSO- $d_6$ /water at sub-zero temperatures for mixture analysis.

## Acknowledgements

Financial support by CNRS, Conseil Regional Champagne Ardenne, Conseil General de la Marne, MESR, and EU-programme FEDER to the PIAneT CPER project is gratefully acknowledged.

## References

- [1] T.R. Carver, C.P. Slichter, Polarization of Nuclear Spins in Metals, *Phys. Rev.*, 92 (1953) 212-213.
- [2] A.W. Overhauser, Polarization of Nuclei in Metals, *Phys. Rev.*, 92 (1953) 411-415.
- [3] T.R. Carver, C.P. Slichter, Experimental verification of the overhauser nuclear polarization effect, *Phys. Rev.*, 102 (1956) 975-980.
- [4] I. Solomon, Relaxation Processes in a System of Two Spins, *Phys. Rev.*, 99 (1955) 559-565.
- [5] J.H. Noggle, R.E. Schirmer, *The Nuclear Overhauser Effect: Chemical Applications*, 1971.
- [6] K. Wüthrich, *NMR of proteins and nucleic acids*, Wiley: New York, 1986.
- [7] A. Gierer, K. Wirtz, *Molekulare Theorie der Mikrorotation*, *Z. Naturforsch., A: Phys. Sci.*, 8 (1953) 532-538.
- [8] A.A. Bothner-By, R.L. Stephens, J.M. Lee, C.D. Warren, R.W. Jeanloz, Structure Determination of a Tetrasaccharide: Transient Nuclear Overhauser Effects in the Rotating Frame, *J. Am. Chem. Soc.*, 106 (1984) 811-813.
- [9] A. Bax, D.G. Davis, Practical aspects of two-dimensional transverse NOE spectroscopy, *J. Magn. Reson.* (1969), 63 (1985) 207-213.
- [10] J.D. Mersh, J.K.M. Sanders, Diamagnetic relaxation reagents can increase the growth rates and ultimate sizes of nuclear overhauser enhancements, *J. Magn. Reson.*, 51 (1983) 345-347.
- [11] H. Mo, T.C. Pochapsky, Intermolecular interactions characterized by nuclear Overhauser effects, *Prog. Nucl. Magn. Reson. Spectrosc.*, 30 (1997) 1-38.
- [12] A. Kumar, R. Christy Rani Grace, Nuclear Overhauser Effect, in: *Encyclopedia of Spectroscopy and Spectrometry*, Elsevier, Oxford, 1999, pp. 1643-1653.
- [13] D. Neuhaus, M.P. Williamson, *The Nuclear Overhauser Effect in Structural and Conformational Analysis*. 2<sup>nd</sup> Ed., Wiley-VCH: New York, 2000.
- [14] M.P. Williamson, The Nuclear Overhauser Effect, in: G.A. Webb (Ed.) *Modern Magnetic Resonance*, Springer Netherlands: Dordrecht, 2008, pp. 409-412.
- [15] T.D.W. Claridge, Correlations Through Space: The Nuclear Overhauser Effect, in: *High-Resolution NMR Techniques in Organic Chemistry*. 3<sup>rd</sup> Ed., Elsevier Ltd., 2016, pp. 315-380.
- [16] A.M. Cases, A.C. Gómez Marigliano, C.M. Bonatti, H.N. Sólamo, Density, Viscosity, and Refractive Index of Formamide, Three Carboxylic Acids, and Formamide + Carboxylic Acid Binary Mixtures, *J. Chem. Eng. Data*, 46 (2001) 712-715.
- [17] D. Neuhaus, H.S. Rzepa, R.N. Sheppard, I.R.C. Bick, Assignment of the structure of dihydrodaphnine diacetate by nuclear Overhauser effect difference spectroscopy, *Tetrahedron Lett.*, 22 (1981) 2933-2936.

- [18] S.F. Lienin, R. Brüscheiler, R.R. Ernst, Rotational Motion of a Solute Molecule in a Highly Viscous Liquid Studied by  $^{13}\text{C}$  NMR: 1,3-Dibromoadamantane in Polymeric Chlorotrifluoroethene, *J. Magn. Reson.*, 131 (1998) 184-190.
- [19] J.M.G. Cowie, P.M. Toporowski, Association in the binary liquid system dimethyl sulphoxide - water, *Can. J. Chem.*, 39 (1961) 2240-2243.
- [20] L. Jannelli, A. Sacco, Thermodynamic and physical behavior of binary mixtures involving sulfolane II. Viscosity, dielectric constant, solid + liquid phase diagram of mixtures of benzene + sulfolane, *J. Chem. Thermodynamics*, 4 (1972) 715-722.
- [21] A.I. Artemchenko, Viscosity and structure of potassium iodide solutions in ethylene glycol, *Fiz. Khim. Rastvorov.*, (1972) 128-134.
- [22] X. Jiang, Y. Zhao, B. Hou, M. Zhang, Y. Bao, Density, viscosity, and thermal conductivity of electronic grade phosphoric acid, *J. Chem. Eng. Data*, 56 (2011) 205-211.
- [23] M.O. Sonnati, S. Amigoni, E.P. Taffin de Givenchy, T. Darmanin, O. Choulet, F. Guittard, Glycerol carbonate as a versatile building block for tomorrow: synthesis, reactivity, properties and applications, *Green Chem.*, 15 (2013) 283-306.
- [24] J.A. Riddick, W.B. Bunger, T.K. Sakano, *Organic solvents: physical properties and methods of purification*. 4<sup>th</sup> edition, John Wiley and Sons: New York, 1986.
- [25] M.P. Williamson, D.H. Williams, Manipulation of the nuclear Overhauser effect by the use of a viscous solvent: The solution conformation of the antibiotic echinomycin, *J. Chem. Soc., Chem. Commun.*, (1981) 165-166.
- [26] M.J. Waring, L.P.G. Wakelin, Echinomycin: a bifunctional intercalating antibiotic, *Nature*, 252 (1974) 653.
- [27] H.T. Cheung, J. Feeney, G.C.K. Roberts, D.H. Williams, G. Ughetto, M.J. Waring, The conformation of echinomycin in solution, *J. Am. Chem. Soc.*, 100 (1978) 46-54.
- [28] L.A. Luck, C.R. Landis, Aprotic, Viscous Solvent Mixtures for Obtaining Large, Negative NOE Enhancements in Small Inorganic and Organic Molecules: Ideal Solvent Systems for Deducing Structures by NMR Techniques, *Organometallics*, 11 (1992) 1003-1005.
- [29] C.R. Landis, L.L. Luck, J.M. Wright, Multiconformational Analysis of Solution NOE Data for the Ac-(L)Proline-(D)Alanine-NHMe Dipeptide in a Nonprotic Solvent, *J. Magn. Reson. Ser. B*, 109 (1995) 44-59.
- [30] G.D. Rose, L.M. Gierasch, J.A. Smith, Turns in Peptides and Proteins, in: J.T.E. C.B. Anfinsen, M.R. Frederic (Eds.) *Advances in Protein Chemistry*, Academic Press, 1985, pp. 1-109.
- [31] G. Pietrzynski, B. Rzeszotarska, Z. Kubica, Conformational investigation of  $\alpha,\beta$ -dehydropeptides. Part. IV.  $\beta$ -turn in saturated and  $\alpha,\beta$ -unsaturated peptides Ac-Pro-Xaa-NHCH<sub>3</sub>: NMR and IR studies, *Int. J. Pept. Protein Res.*, 40 (1992) 524-531.
- [32] M.T. Cung, M. Marraud, A. Aubry,  $\beta$ I- and  $\beta$ II-Turn Conformations in Model Dipeptides with the Pro-Xaa Sequences, *J. Am. Chem. Soc.*, 107 (1985) 7640-7647.
- [33] G.B. Liang, C.J. Rito, S.H. Gellman, Thermodynamic analysis of  $\beta$ -turn formation in Pro-Ala, Pro-Gly, and Pro-Val model peptides in methylene chloride, *J. Am. Chem. Soc.*, 114 (1992) 4440-4442.
- [34] G.B. Liang, C.J. Rito, S.H. Gellman, Variations in the turn-forming characteristics of N-acyl proline units, *Biopolymers*, 32 (1992) 293-301.
- [35] C. Landis, V.S. Allured, Elucidation of Solution Structures by Conformer Population Analysis of NOE Data, *J. Am. Chem. Soc.*, 113 (1991) 9493-9499.
- [36] J.S. Giovannetti, C.M. Kelly, C.R. Landis, Molecular Mechanics and NOE Investigations of the Solution Structures of Intermediates in the [Rh(chiral bisphosphine)]<sup>+</sup>-Catalyzed Hydrogenation of Prochiral Enamides, *J. Am. Chem. Soc.*, 115 (1993) 4040-4057.
- [37] G.V. Nikiforovich, B. Vesterman, J. Betins, L. Podins, The Space Structure of a Conformationally Labile Oligopeptide in Solution: Angiotensin, *J. Biomol. Struct. Dyn.*, 4 (1987) 1119-1135.
- [38] G.V. Nikiforovich, B.G. Vesterman, J. Betins, Combined use of spectroscopic and energy calculation methods for the determination of peptide conformation in solution, *Biophys. Chem.*, 31 (1988) 101-106.
- [39] B. Vesterman, J. Saulitis, J. Betins, E. Liepins, G.V. Nikiforovich, Dynamic space structure of the Leu-enkephalin molecule in DMSO solution, *Biochim. Biophys. Acta*, 998 (1989) 204-209.
- [40] G.V. Nikiforovich, O. Prakash, C.A. Gehrig, V.J. Hruby, Conformations of the dermenkephalin backbone in dimethyl sulfoxide solution by a new approach to the solution conformations of flexible peptides, *J. Am. Chem. Soc.*, 115 (1993) 3399-3406.
- [41] R. Brüscheiler, M. Blackledge, R.R. Ernst, Multi-conformational peptide dynamics derived from NMR data: A new search algorithm and its application to antamanide, *J. Biomol. NMR*, 1 (1991) 3-11.
- [42] T.F. Havel, K. Wüthrich, An evaluation of the combined use of nuclear magnetic resonance and distance geometry for the determination of protein conformations in solution, *J. Mol. Biol.*, 182 (1985) 281-294.
- [43] C. Yang, G. Wei, Y. Li, Densities and viscosities of *N,N*-dimethylformamide + formic acid, and + acetic acid in the temperature range from (303.15 to 353.15) K, *J. Chem. Eng. Data*, 53 (2008) 1211-1215.
- [44] P. Douzou, G.A. Petsko, Proteins at work: "stop-action" pictures at subzero temperatures, *Adv. Protein Chem.*, 36 (1984) 245-361.
- [45] F. Corradini, L. Marcheselli, L. Tassi, G. Tosi, Static dielectric constants of the *N,N*-dimethylformamide/2-methoxyethanol solvent system at various temperatures, *Can. J. Chem.*, 70 (1992) 2895-2899.
- [46] D. Picone, A. D'Ursi, A. Motta, T. Tancredi, P.A. Temussi, Conformational preferences of [Leu<sup>5</sup>]enkephalin in biomimetic media: Investigation by  $^1\text{H}$  NMR, *Eur. J. Biochem.*, 192 (1990) 433-439.
- [47] R. Spadaccini, P.A. Temussi, Natural peptide analgesics: The role of solution conformation, *Cell. Mol. Life Sci.*, 58 (2001) 1572-1582.
- [48] A. D'Ursi, G. Caliendo, E. Perissutti, V. Santagada, B. Severino, S. Albrizio, G. Bifulco, S. Spisani, P.A. Temussi, Conformation - Activity relationship of peptide T and new pseudocyclic hexapeptide analogs, *J. Pept. Sci.*, 13 (2007) 413-421.
- [49] A. Pastore, P. Temussi, When "IUPs" were "BAPs": How to study the nonconformation of intrinsically unfolded polyaminoacid chains, *Biopolymers*, 100 (2013) 592-600.
- [50] G. Angulo, M. Brucka, M. Gerecke, G. Grampp, D. Jeannerat, J. Milkiewicz, Y. Mitrev, C. Radzewicz, A. Rosspeintner, E. Vauthey, P. Wnuk, Characterization of dimethylsulfoxide/glycerol mixtures: a binary solvent system for the study of "friction-dependent" chemical reactivity, *Phys. Chem. Chem. Phys.*, 18 (2016) 18460-18469.
- [51] J.D. Glickson, S.L. Gordon, T.P. Pitner, D.G. Agresti, R. Walter, Intramolecular  $^1\text{H}$  Nuclear Overhauser Effect Study of the Solution Conformation of Valinomycin in Dimethyl Sulfoxide, *Biochemistry*, 15 (1976) 5721-5729.
- [52] T.P. Pitner, R. Walter, J.D. Glickson, Mechanism of the intramolecular  $^1\text{H}$  nuclear Overhauser effect in peptides and depsipeptides, *Biochem. Biophys. Res. Commun.*, 70 (1976) 746-751.
- [53] D.H. Williams, J.R. Kalman, Structural and Mode of Action Studies on the Antibiotic Vancomycin. Evidence from

- 270-MHz Proton Magnetic Resonance, *J. Am. Chem. Soc.*, 99 (1977) 2768-2774.
- [54] C.R. Jones, C.T. Sikakana, S. Hehir, M.C. Kuo, W.A. Gibbons, The quantitation of nuclear Overhauser effect methods for total conformational analysis of peptides in solution. Application to gramicidin S, *Biophys. J.*, 24 (1978) 815-832.
- [55] C.R. Jones, C.T. Sikakana, S.P. Hehir, W.A. Gibbons, Individual residue correlation times of peptides from proton relaxation parameters: Application to gramicidin S, *Biochem. Biophys. Res. Commun.*, 83 (1978) 1380-1387.
- [56] C.R. Jones, C.T. Sikakana, M.C. Kuo, W.A. Gibbons, Interproton Distances for the  $\beta$ -Turn Residues of the Peptide Gramicidin S Determined from Nuclear Overhauser Effect Ratios, *J. Am. Chem. Soc.*, 100 (1978) 5960-5961.
- [57] M. Kuo, W.A. Gibbons, Total assignments, including four aromatic residues, and sequence confirmation of the decapeptide tyrocidine A using difference double resonance. Qualitative nuclear overhauser effect criteria for  $\beta$  turn and antiparallel  $\beta$ -pleated sheet conformations, *J. Biol. Chem.*, 254 (1979) 6278-6287.
- [58] D.H. Williams, V. Rajananda, G. Bojesen, M.P. Williamson, Structure of the antibiotic ristocetin A, *J. Chem. Soc., Chem. Commun.*, (1979) 906-908.
- [59] T. Higashijima, J. Kobayashi, U. Nagai, T. Miyazawa, Nuclear-Magnetic-Resonance Study on Met-enkephalin and Met-enkephalin, *Eur. J. Clin. Chem. Clin. Biochem.*, 97 (1979) 43-58.
- [60] J.R. Kalman, D.H. Williams, An NMR Study of the Interaction between the Antibiotic Ristocetin A and a Cell Wall Peptide Analogue. Negative Nuclear Overhauser Effects in the Investigation of Drug Binding Sites, *J. Am. Chem. Soc.*, 102 (1980) 906-912.
- [61] J.R. Kalman, D.H. Williams, An NMR Study of the Structure of the Antibiotic Ristocetin A. The Negative Nuclear Overhauser Effect in Structure Elucidation, *J. Am. Chem. Soc.*, 102 (1980) 897-905.
- [62] G.A. Ellestad, R.A. Leese, G.O. Morton, F. Barbatschi, W.E. Gore, W.J. McGahren, I.M. Armitage, Avoparcin and Epiavoparcin, *J. Am. Chem. Soc.*, 103 (1981) 6522-6524.
- [63] D.H. Huang, R. Walter, J.D. Glickson, N.R. Krishna, Solution conformation of gramicidin S: An intramolecular nuclear Overhauser effect study, *Proc. Nat. Acad. Sci. U.S.A.*, 78 (1981) 672-675.
- [64] M.P. Williamson, D.H. Williams, Structure Revision of the Antibiotic Vancomycin. The Use of Nuclear Overhauser Effect Difference Spectroscopy, *J. Am. Chem. Soc.*, 103 (1981) 6580-6585.
- [65] C. Deleuze, W.E. Hull, Assignment and analysis of the 500 MHz  $^1\text{H}$  NMR spectra of somatostatin and the acyclic precursor ( $\text{S}^{3,14}$ -Acm)-somatostatin in dimethyl sulphoxide, *Org. Magn. Reson.*, 18 (1982) 112-116.
- [66] A.H. Hunt, Structure of the Pseudoaglycon of A35512B, *J. Am. Chem. Soc.*, 105 (1983) 4463-4468.
- [67] D.H. Williams, M.P. Williamson, D.W. Butcher, S.J. Hammond, Detailed Binding Sites of the Antibiotics Vancomycin and Ristocetin A: Determination of Intermolecular Distances in Antibiotic/Substrate Complexes by Use of the Time-Dependent NOE, *J. Am. Chem. Soc.*, 105 (1983) 1332-1339.
- [68] A.H. Hunt, M. Debono, K.E. Merkel, M. Barnhart, Structure of the Pseudoaglycon of Actaplanin, *J. Org. Chem.*, 49 (1984) 635-640.
- [69] M. Barbush, D.W. Dixon, Use of the nuclear Overhauser effect to assign  $^1\text{H}$  NMR resonances in a low-spin paramagnetic hemin, *Biochem. Biophys. Res. Commun.*, 129 (1985) 70-75.
- [70] A. Pastore, P.A. Temussi, S. Salvadori, R. Tomatis, P. Mascagni, A conformational study of the opioid peptide dermorphin by one-dimensional and two-dimensional nuclear magnetic resonance spectroscopy, *BIOPHYS. J.*, 48 (1985) 195-200.
- [71] D. Gondol, G. Van Binst, Distance determination by a two-dimensional NOE NMR study on the medium-sized peptide Gramicidin S, *Biopolymers*, 25 (1986) 977-983.
- [72] G.E. Hawkes, L.Y. Lian, E.W. Randall, K.D. Sales, E.H. Curzon, The conformation of gramicidin A in dimethylsulphoxide solution: A full analysis of the one- and two-dimensional  $^1\text{H}$ ,  $^{13}\text{C}$ , and  $^{15}\text{N}$  nuclear-magnetic-resonance spectra, *Eur. J. Biochem.*, 166 (1987) 437-445.
- [73] Z.-Y. Yan, B.N. Narasinga Rao, Influence of Nonaqueous Solvents on the Conformation of Blood Group Oligosaccharidase, *J. Am. Chem. Soc.*, 109 (1987) 7663-7669.
- [74] D. Picone, P.A. Temussi, M. Marastoni, R. Tomatis, A. Motta, A 500 MHz study of peptide T in a DMSO solution, *FEBS Lett.*, 231 (1988) 159-163.
- [75] K. Uma, H. Balaram, S. Raghothama, P. Balaram, Simultaneous observation of positive and negative nuclear overhauser effects in oligopeptides due to segmental motion, *Biochem. Biophys. Res. Commun.*, 151 (1988) 153-157.
- [76] C. Wynants, D.H. Coy, G. Van Binst, Conformational study of super-active analogues of somatostatin with reduced ring size by XXXH nmr, *Tetrahedron*, 44 (1988) 941-973.
- [77] C. Di Bello, L. Gozzini, M. Tonellato, M.G. Corradini, G. D'Auria, L. Paolillo, E. Trivellone, Mono and two-dimensional 500-MHz characterization of synthetic bombesin and related peptides in DMSO and DMSO-water, *Biopolymers*, 28 (1989) 421-440.
- [78] A. Motta, D. Picone, P.A. Temussi, M. Marastoni, R. Tomatis, Conformational analysis of peptide T and of its C-pentapeptide fragment, *Biopolymers*, 28 (1989) 479-486.
- [79] V.V. Krishnan, S.C. Shekar, A. Kumar, Simultaneous Observation of Positive and Negative NOE in Biomolecules: A Bistable Jump Model for Segmental Motion with Modulation of Internuclear Distances, *J. Am. Chem. Soc.*, 113 (1991) 7542-7550.
- [80] A. Motta, P.A. Temussi, E. Wünsch, G. Bovermann, A  $^1\text{H}$  NMR Study of Human Calcitonin in Solution, *Biochemistry*, 30 (1991) 2364-2371.
- [81] G. Saviano, P.A. Temussi, A. Motta, C.A. Maggi, P. Rovero, Conformation-Activity Relationship of Tachykinin Neurokinin A (4-10) and of Some [Xaa<sup>8</sup>] Analogues, *Biochemistry*, 30 (1991) 10175-10181.
- [82] N.J. Skelton, D.H. Williams, M.J. Rance, J.C. Ruddock, Structure Elucidation of a Novel Antibiotic of the Vancomycin Group. the Influence of Ion-Dipole Interactions on Peptide Backbone Conformation, *J. Am. Chem. Soc.*, 113 (1991) 3757-3765.
- [83] T. Tancredi, P.A. Temussi, D. Picone, P. Amodeo, R. Tomatis, S. Salvadori, M. Marastoni, V. Santagada, G. Balboni, New insights on  $\mu/\delta$  selectivity of opioid peptides: Conformational analysis of deltorphin analogues, *Biopolymers*, 31 (1991) 751-760.
- [84] C. Yu, J.F. Hwang, C.J. Yeh, L.C. Chuang, Solution Conformation of Gramicidin S Determined by Nuclear Magnetic Resonance and Distance Geometry Calculation, *J. Chin. Chem. Soc.*, 39 (1992) 231-234.
- [85] D. Duchesne, M. Naim, P. Nicolas, D. Baron, Folding trends in a flexible peptide: Two-dimensional NMR study of deltorphin-I, a  $\delta$  selective opioid heptapeptide, *Biochem. Biophys. Res. Commun.*, 195 (1993) 630-636.
- [86] Y. Xu, I.P. Sugár, N.R. Krishna, A variable target intensity-restrained global optimization (VARTIGO) procedure for determining three-dimensional structures of

- polypeptides from NOESY data: Application to gramicidin-S, *J. Biomol. NMR*, 5 (1995) 37-48.
- [87] P. Pristovšek, J. Kidrič, NMR and molecular dynamics study of muroctasin—Implications for the bioactive conformation, *Biopolymers*, 42 (1997) 659-671.
- [88] D. Picone, A. Riviaccio, O. Crescenzi, G. Caliendo, V. Santagada, E. Perissutti, S. Spisani, S. Traniello, P.A. Temussi, Peptide T revisited: Conformational mimicry of epitopes of anti-HIV proteins, *J. Pept. Sci.*, 7 (2001) 197-207.
- [89] J. Huang, Y. Yao, J. Lin, Y.H. Ye, W.Y. Sun, W.X. Tang, The solution structure of rat A $\beta$ -(1-28) and its interaction with zinc ion: Insights into the scarcity of amyloid deposition in aged rat brain, *J. Biol. Inorg. Chem.*, 9 (2004) 627-635.
- [90] L. Klauedel, A. Łęgowska, K. Brzozowski, J. Silberring, J. Wójcik, K. Rolka, Solution conformational study of nociceptin and its 1 - 13 and 1 - 11 fragments using circular dichroism and two-dimensional NMR conjunction with theoretical conformational analysis, *J. Pept. Sci.*, 10 (2004) 678-690.
- [91] H. Murakami, A. Kawabuchi, R. Matsumoto, T. Ido, N. Nakashima, A multi-mode-driven molecular shuttle: photochemically and thermally reactive azobenzene rotaxanes, *J. Am. Chem. Soc.*, 127 (2005) 15891-15899.
- [92] K. Yamada, S.S. Shinoda, H. Oku, K. Komagoe, T. Katsu, R. Katakai, Synthesis of low-hemolytic antimicrobial dehydropeptides based on gramicidin S, *J. Med. Chem.*, 49 (2006) 7592-7595.
- [93] T. Tancredi, R. Guerrini, E. Marzola, C. Trapella, G. Caló, D. Regoli, R.K. Reinscheid, V. Camarda, S. Salvadori, P.A. Temussi, Conformation-activity relationship of neuropeptide S and some structural mutants: Helicity affects their interaction with the receptor, *J. Med. Chem.*, 50 (2007) 4501-4508.
- [94] J.E. Philip, J.R. Schenck, M.P. Hargie, *Antibiotics Annual, 1956-57*, Medical Encyclopaedia Inc.: New York, 1957.
- [95] H.R. Perkins, Specificity of combination between mucopeptide precursors and vancomycin or ristocetin, *BIOCHEM. J.*, 111 (1969) 195-205.
- [96] M. Nieto, H.R. Perkins, Modifications of the acyl-*D*-alanyl-*D*-alanine terminus affecting complex-formation with Vancomycin, *BIOCHEM. J.*, 123 (1971) 789.
- [97] H.R. Perkins, M. Nieto, The chemical basis for the action of the vancomycin group of antibiotics, *Ann. N. Y. Acad. Sci.*, 235 (1974) 348-363.
- [98] D.H. Williams, B. Bardsley, The Vancomycin Group of Antibiotics and the Fight against Resistant Bacteria, *Angew. Chem. Int. Ed.*, 38 (1999) 1172-1193.
- [99] R.D. Süßmuth, The Chemistry and Biology of Vancomycin and Other Glycopeptide Antibiotic Derivatives, in: *Medicinal Chemistry of Bioactive Natural Products*, John Wiley & Sons, Inc., 2006, pp. 35-72.
- [100] B.S. Collier, The Effects of Ristocetin and von Willebrand Factor on Platelet Electrophoretic Mobility, *J. Clin. Invest.*, 61 (1978) 1168-1175.
- [101] D.H. Williams, V. Rajananda, J.R. Kalman, On the structure and mode of action of the antibiotic ristocetin A, *J. Chem. Soc., Perkin Trans. 1*, (1979) 787-792.
- [102] M.P. Williamson, D.H. Williams, A carbon-13 nuclear magnetic resonance study of ristocetins A and B and their derivatives, *J. Chem. Soc., Perkin Trans. 1*, (1981) 1483-1491.
- [103] G.M. Sheldrick, P.G. Jones, O. Kennard, D.H. Williams, G.A. Smith, Structure of vancomycin and its complex with acetyl-*D*-alanyl-*D*-alanine, *Nature*, 271 (1978) 223-225.
- [104] C. Liu, A. Bayer, S.E. Cosgrove, R.S. Daum, S.K. Fridkin, R.J. Gorwitz, S.L. Kaplan, A.W. Karchmer, D.P. Levine, B.E. Murray, J.R. M., D.A. Talan, H.F. Chambers, Clinical practice guidelines by the infectious diseases society of america for the treatment of methicillin-resistant *Staphylococcus aureus* infections in adults and children: executive summary, *Clin. Infect. Dis.*, 52 (2011) 285-292.
- [105] M.H. McCormick, W.M. Stark, G.E. Pittenger, R.C. Pittenger, J.M. McGuire, *Antibiotics Annual, 1955-56*, Medical Encyclopedia Inc.: New York, 1956.
- [106] F.J. Marshall, Structure Studies on Vancomycin, *J. Med. Chem.*, 8 (1965) 18-22.
- [107] F.J. Marshall, Additions and Corrections - Structure Studies on Vancomycin, *J. Med. Chem.*, 8 (1965) 894-894.
- [108] K.A. Smith, D.H. Williams, G.A. Smith, Structural studies on the antibiotic vancomycin; the nature of the aromatic rings, *J. Chem. Soc., Perkin Trans. 1*, (1974) 2369-2376.
- [109] G.A. Smith, K.A. Smith, D.H. Williams, Structural studies on the antibiotic vancomycin: evidence for the presence of modified phenylglycine and  $\beta$ -hydroxytyrosine units, *J. Chem. Soc., Perkin Trans. 1*, (1975) 2108-2115.
- [110] C.M. Harris, T.M. Harris, Structure of the glycopeptide antibiotic vancomycin. Evidence for an asparagine residue in the peptide, *J. Am. Chem. Soc.*, 104 (1982) 4293-4295.
- [111] A.A. Bothner-By, J.H. Noggle, Time Development of Nuclear Overhauser Effects in Multispin Systems, *J. Am. Chem. Soc.*, 101 (1979) 5152-5155.
- [112] G. Wagner, K. Wüthrich, Truncated driven nuclear overhauser effect (TOE). A new technique for studies of selective  $^1\text{H}$ - $^1\text{H}$  overhauser effects in the presence of spin diffusion, *J. Magn. Reson.* (1969), 33 (1979) 675-680.
- [113] N.M. Szeverenyi, A.A. Bothner-By, R. Bittner, Kinetics of spin diffusion in the protons of brucine-*d*2 in solution in deuteriophosphoric acid, *J. Phys. Chem.*, 84 (1980) 2880-2883.
- [114] H. Brockmann, G. Schmidt-Kastner, Valinomycin I, XXVII. Mitteil. über Antibiotica aus Actinomyceten, *Chem. Ber.*, 88 (1955) 57-61.
- [115] M.M. Shemyakin, N.A. Aldanova, E.I. Vinogradova, M.Y. Feigina, The structure and total synthesis of valinomycin, *Tetrahedron Lett.*, 4 (1963) 1921-1925.
- [116] C. Moore, B.C. Pressman, Mechanism of action of valinomycin on mitochondria, *Biochem. Biophys. Res. Commun.*, 15 (1964) 562-567.
- [117] A.A. Lev, E.P. Buzhinsky, Cation specificity of model bimolecular phospholipid membranes with incorporated valinomycin, *Cytology*, 9 (1967) 102-106.
- [118] Y.A. Ovchinnikov, Second FEBS-Ferdinand Springer lecture: Membrane active complexones. Chemistry and biological function, *FEBS Lett.*, 44 (1974) 1-21.
- [119] M.M. Shemyakin, Y.A. Ovchinnikov, V.T. Ivanov, V.K. Antonov, E.I. Vinogradova, A.M. Shkrob, G.G. Malenkov, A.V. Evstratov, I.A. Laine, E.I. Melnik, I.D. Ryabova, Cyclodepsipeptides as chemical tools for studying ionic transport through membranes, *J. Membr. Biol.*, 1 (1969) 402-430.
- [120] D.H. Haynes, A. Kowalsky, B.C. Pressman, Application of Nuclear Magnetic Resonance to the Conformational Changes in Valinomycin during Complexation, *J. Biol. Chem.*, 244 (1969) 502-505.
- [121] D.W. Urry, M. Ohnishi, Spectroscopic Approaches to Biomolecular Conformation, Urry, D. W., Ed., American Medical Association Press: Chicago, 1970.
- [122] D.J. Patel, A.E. Tonelli, Solvent-dependent conformations of valinomycin in solution, *Biochemistry*, 12 (1973) 486-496.
- [123] R.N. Havemeyer, Freezing point curve of dimethyl sulfoxide-water solutions, *J. Pharm. Sci.*, 55 (1966) 851-853.
- [124] K.J. Packer, D.J. Tomlinson, Nuclear spin relaxation and self-diffusion in the binary system, dimethylsulphoxide (DMSO)+ water, *Trans. Faraday Soc.*, 67 (1971) 1302-1314.

- [125] S.A. Schichman, R.L. Amey, Viscosity and local liquid structure in dimethyl sulfoxide-water mixtures, *J. Phys. Chem.*, 75 (1971) 98-102.
- [126] T. Tokuhira, L. Menafrá, H.H. Szmant, Contribution of relaxation and chemical shift results to the elucidation of the structure of the water-DMSO liquid system, *J. Chem. Phys.*, 61 (1974) 2275-2282.
- [127] M.F. Fox, K.P. Whittingham, Component interactions in aqueous dimethyl sulphoxide, *J. Chem. Soc., Faraday Trans. 1*, 71 (1975) 1407-1412.
- [128] H. Schott, Determination of Extent of Hydration of Water-Miscible Organic Liquids in Aqueous Solution from Viscosity Data, *J. Pharm. Sci.*, 69 (1980) 369-378.
- [129] W.M. Madigosky, R.W. Warfield, Ultrasonic measurements and liquid structure of DMSO-water mixture, *J. Chem. Phys.*, 78 (1983) 1912-1916.
- [130] A. Luzar, D. Chandler, Structure and hydrogen bond dynamics of water-dimethyl sulfoxide mixtures by computer simulations, *J. Chem. Phys.*, 98 (1993) 8160-8173.
- [131] J. Catalán, C. Díaz, F. García-Blanco, Characterization of binary solvent mixtures of DMSO with water and other cosolvents, *J. Org. Chem.*, 66 (2001) 5846-5852.
- [132] M.M. Palaiologou, I.E. Molinou, N.G. Tsierekzos, Viscosity Studies on Lithium Bromide in Water + Dimethyl Sulfoxide Mixtures at 278.15 K and 293.15 K, *J. Chem. Eng. Data*, 47 (2002) 1285-1289.
- [133] I. Plowaś, J. Świergiel, J. Jadżyn, Relative Static Permittivity of Dimethyl Sulfoxide + Water Mixtures, *J. Chem. Eng. Data*, 58 (2013) 1741-1746.
- [134] Y.-C. Wen, H.-C. Kuo, J.-L. Guo, H.-W. Jia, Nuclear Magnetic Resonance Spectroscopy Investigation on Ultralow Melting Temperature Behavior of Dimethyl Sulfoxide-Water Solutions, *J. Phys. Chem. B*, 120 (2016) 13125-13135.
- [135] S.W. Fesik, G. Bolis, H.L. Sham, E.T. Olejniczak, Structure refinement of a cyclic peptide from two-dimensional NMR data and molecular modeling, *Biochemistry*, 26 (1987) 1851-1859.
- [136] A. Motta, T. Tancredi, P.A. Temussi, Nuclear Overhauser effects in linear peptides A low-temperature 500 MHz study of Met-enkephalin, *FEBS Lett.*, 215 (1987) 215-218.
- [137] S.W. Fesik, E.T. Olejniczak, Increased NOEs for small molecules using mixed solvents, *Magn. Reson. Chem.*, 25 (1987) 1046-1048.
- [138] A. Motta, D. Picone, T. Tancredi, P.A. Temussi, NOE measurements on linear peptides in cryoprotective aqueous mixtures, *J. Magn. Reson.* (1969), 75 (1987) 364-370.
- [139] A. Motta, D. Picone, T. Tancredi, P.A. Temussi, Low temperature nmr studies of leu-enkephalins in cryoprotective solvents, *Tetrahedron*, 44 (1988) 975-990.
- [140] J.L. Nieto, M.A. Jiménez, M. Rico, J. Santoro, J. Herranz, Nuclear Overhauser effects in aqueous solution as dynamic probes in short linear peptides, *FEBS Lett.*, 239 (1988) 83-87.
- [141] T. Tancredi, G. Zanotti, F. Rossi, E. Benedetti, C. Pedone, P.A. Temussi, Comparison of the conformations of cyclolinopeptide A in the solid state and in solution, *Biopolymers*, 28 (1989) 513-523.
- [142] P.A. Temussi, D. Picone, T. Tancredi, R. Tomatis, S. Salvadori, M. Marastoni, G. Balboni, Conformational properties of deltorphin: New features of the  $\delta$ -opioid receptor, *FEBS Lett.*, 247 (1989) 283-288.
- [143] P.A. Temussi, D. Picone, M.A. Castiglione-Morelli, A. Motta, T. Tancredi, Bioactive conformation of linear peptides in solution: An elusive goal?, *Biopolymers*, 28 (1989) 91-107.
- [144] L. Mueller, S.L. Heald, J.C. Hempel, P.W. Jeffs, Determination of the Conformation of Molecular Complexes of the Ardicin Aglycon with Ac2-L-Lys-D-Ala-D-Ala and Ac-L-Ala- $\gamma$ -D-Gln-L-Lys(Ac)-D-Ala-D-Ala: An Application of Nuclear Magnetic Resonance Spectroscopy and Distance Geometry in the Modeling of Peptides, *J. Am. Chem. Soc.*, 111 (1989) 496-505.
- [145] P. Amodeo, A. Motta, D. Picone, G. Saviano, T. Tancredi, P.A. Temussi, Viscosity as a conformational sieve. NOE of linear peptides in cryoprotective mixtures, *J. Magn. Reson.* (1969), 95 (1991) 201-207.
- [146] P. Amodeo, A. Motta, T. Tancredi, S. Salvadori, R. Tomatis, D. Picone, G. Saviano, P.A. Temussi, Solution structure of deltorphin I at 265 K: a quantitative NMR study, *Pept. Res.*, 5 (1992) 48-55.
- [147] P.A. Temussi, D. Picone, G. Saviano, P. Amodeo, A. Motta, T. Tancredi, S. Salvadori, R. Tomatis, Conformational analysis of an opioid peptide in solvent media that mimic cytoplasm viscosity, *Biopolymers*, 32 (1992) 367-372.
- [148] M. Tallon, D. Ron, D. Halle, P. Amodeo, G. Saviano, P.A. Temussi, Z. Selinger, F. Naider, M. Chorev, Synthesis, biological activity, and conformational analysis of [pGlu<sup>6</sup>, N-MePhe<sup>8</sup>, Aib<sup>9</sup>] substance P (6-11): A selective agonist for the NK-3 receptor, *Biopolymers*, 33 (1993) 915-926.
- [149] L. Moroder, A. D'Ursi, D. Picone, P. Amodeo, P.A. Temussi, Solution Conformation of CCK9, a Cholecystokinin Analog, *Biochem. Biophys. Res. Commun.*, 190 (1993) 741-746.
- [150] T. Tancredi, S. Salvadori, P. Amodeo, D. Picone, L.H. Lazarus, S.D. Bryant, R. Guerrini, G. Marzola, P.A. Temussi, Conversion of Enkephalin and Dermorphin into  $\delta$ -Selective Opioid Antagonists by Single-Residue Substitution, *Eur. J. Biochem.*, 224 (1994) 241-247.
- [151] P. Amodeo, P. Rovero, G. Saviano, P.A. Temussi, Solution conformation of c-[Gln-Trp-Phe-Gly-Leu-Met], a NK-2 tachykinin antagonist, *Int. J. Pept. Protein Res.*, 44 (1994) 556-561.
- [152] O. Crescenzi, P. Amodeo, G. Cavicchioni, R. Guerrini, D. Picone, S. Salvadori, T. Tancredi, P.A. Temussi,  $\delta$ -Selective opioid peptides containing a single aromatic residue in the message domain: An NMR conformational analysis, *J. Pept. Sci.*, 2 (1996) 290-308.
- [153] G. Caliendo, P. Grieco, E. Perissutti, V. Santagada, G. Saviano, T. Tancredi, P.A. Temussi, Conformational analysis of three NK1 tripeptide antagonists: A proton nuclear magnetic resonance study, *J. Med. Chem.*, 40 (1997) 594-601.
- [154] P. Amodeo, F. Naider, D. Picone, T. Tancredi, P.A. Temussi, Conformational sampling of bioactive conformers: A low-temperature NMR study of <sup>15</sup>N-leu-enkephalin, *J. Pept. Sci.*, 4 (1998) 253-265.
- [155] A. D'Ursi, S. Albrizio, C. Fattorusso, A. Lavecchia, G. Zanotti, P.A. Temussi, Solution conformation of a potent cyclic analogue of tuftsin: Low temperature nuclear magnetic resonance study in a cryoprotective mixture, *J. Med. Chem.*, 42 (1999) 1705 - 1713.
- [156] R. Spadaccini, O. Crescenzi, D. Picone, T. Tancredi, P.A. Temussi, Solution structure of dynorphin A (1-17): A NMR study in a cryoprotective solvent mixture at 278 K, *J. Pept. Sci.*, 5 (1999) 306-312.
- [157] P. Amodeo, R. Guerrini, D. Picone, S. Salvadori, R. Spadaccini, T. Tancredi, P.A. Temussi, Solution structure of nociceptin peptides, *J. Pept. Sci.*, 8 (2002) 497-509.
- [158] Y.J. Zhang, T. Tanaka, Y. Betsumiya, R. Kusano, A. Matsuo, T. Ueda, I. Kouno, Association of tannins and related polyphenols with the cyclic peptide gramicidin S, *Chem. Pharm. Bull.*, 50 (2002) 258-262.
- [159] S. Albrizio, A. Carotenuto, C. Fattorusso, L. Moroder, D. Picone, P.A. Temussi, A. D'Ursi, Environmental mimic of receptor interaction: Conformational analysis of CCK-15 in solution, *J. Med. Chem.*, 45 (2002) 762-769.
- [160] S. Giannecchini, A. Di Fenza, A.M. D'Ursi, D. Matteucci, P. Rovero, M. Bendinelli, Antiviral activity and

- conformational features of an octapeptide derived from the membrane-proximal ectodomain of the feline immunodeficiency virus transmembrane glycoprotein, *J. Virol.*, 77 (2003) 3724-3733.
- [161] A. Motta, M.A.C. Morelli, N. Goud, P.A. Temussi, Sequential  $^1\text{H}$  NMR Assignment and Secondary Structure Determination of Salmon Calcitonin in Solution, *Biochemistry*, 28 (1989) 7996-8002.
- [162] P.A. Temussi, P. Amodio, D. Picone, T. Tancredi, Solution structure of bioactive peptides in biomimetic media, *Acta Pharma.*, 42 (1992) 323-328.
- [163] E.T. Olejniczak, R.T. Gampe Jr, S.W. Fesik, Accounting for spin diffusion in the analysis of 2D NOE data, *J. Magn. Reson.* (1969), 67 (1986) 28-41.
- [164] S. Macura, R.R. Ernst, Elucidation of cross relaxation in liquids by two-dimensional N.M.R. spectroscopy, *Mol. Phys.*, 41 (1980) 95-117.
- [165] M.D. Shenderovich, G.V. Nikiforovich, G.I. Chipens, Conformational dependence of the local nuclear overhauser effects in peptides, *J. Magn. Reson.* (1969), 59 (1984) 1-12.
- [166] D.F. Sargent, R. Schwyzer, Membrane lipid phase as catalyst for peptide-receptor interactions, *Proc. Nat. Acad. Sci. U.S.A.*, 83 (1986) 5774-5778.
- [167] J. Hughes, T.W. Smith, H.W. Kosterlitz, L.A. Fothergill, B.A. Morgan, H.R. Morris, Identification of two related pentapeptides from the brain with potent opiate agonist activity, *Nature*, 258 (1975) 577.
- [168] J.A.H. Lord, A.A. Waterfield, J. Hughes, H.W. Kosterlitz, Endogenous opioid peptides: multiple agonists and receptors, *Nature*, 267 (1977) 495.
- [169] H.E. Bleich, J.D. Cutnell, A.R. Day, Preliminary analysis of  $^1\text{H}$  and  $^{13}\text{C}$  spectral and relaxation behavior in methionine enkephalin, *Proc. Nat. Acad. Sci. U.S.A.*, 73 (1976) 2589-2593.
- [170] C. Garbay-Jaureguiberry, B.P. Roques, R. Oberlin, M. Anteunis, A.K. Lala, Preferential conformation of the endogenous opiate-like pentapeptide met-enkephalin in DMSO- $d_6$  solution determined by high field  $^1\text{H}$  NMR, *Biochem. Biophys. Res. Commun.*, 71 (1976) 558-565.
- [171] C.R. Jones, W.A. Gibbons, V. Garsky, Proton magnetic resonance studies of conformation and flexibility of enkephalin peptides, *Nature*, 262 (1976) 779-782.
- [172] B.P. Roques, C. Garbay-Jaureguiberry, R. Oberlin, M. Anteunis, A.K. Lala, Conformation of met $^5$ -enkephalin determined by high field PMR spectroscopy, *Nature*, 262 (1976) 778-779.
- [173] M. Anteunis, A.K. Lala, C. Garbay-Jaureguiberry, B.P. Roques, A Proton Magnetic Resonance Study of the Conformation of Methionine-Enkephalin as a Function of pH, *Biochemistry*, 16 (1977) 1462-1466.
- [174] H.E. Bleich, A.R. Day, R.J. Freer, J.A. Glasel, 360 MHz proton NMR spectra of active and inactive derivatives of methionine-enkephalin. Assignments, derived parameters, conformational implications, *Biochem. Biophys. Res. Commun.*, 74 (1977) 592-598.
- [175] C. Garbay-Jaureguiberry, B.P. Roques, R. Oberlin, M. Anteunis, S. Combrisson, J.Y. Lallemand,  $^1\text{H}$  and  $^{13}\text{C}$  NMR studies of conformational behaviour of Leu-enkephalin, *FEBS Lett.*, 76 (1977) 93-98.
- [176] P. Tancredi, R. Deslauriers, W.H. McGregor, E. Ralston, D. Sarantakis, R.L. Somorjai, I.C.P. Smith, A Carbon-13 Nuclear Magnetic Resonance Study of the Molecular Dynamics of Methionine-enkephalin and  $\alpha$ -Endorphin in Aqueous Solution, *Biochemistry*, 17 (1978) 2905-2914.
- [177] T. Higashijima, J. Kobayashi, U. Nagai, T. Miyazawa, Nuclear-Magnetic-Resonance Study on Met-enkephalin and Met-enkephalin: Molecular Association and Conformation, *Eur. J. Biochem.*, 97 (1979) 43-58.
- [178] B.A. Levine, D.L. Rabenstein, D. Smyth, R.J.P. Williams, Proton magnetic resonance studies on [methionine]-enkephalin and  $\beta$ -endorphin in aqueous solution, *Biochim. Biophys. Acta*, 579 (1979) 279-290.
- [179] S. Premilat, B. Maigret, Conformations of Angiotensin II and Enkephalin related to N.M.R., *Biochem. Biophys. Res. Commun.*, 91 (1979) 534-539.
- [180] E.R. Stimson, Y.C. Meinwald, H.A. Scheraga, Solution Conformation of Enkephalin. A Nuclear Magnetic Resonance Study of  $^{13}\text{C}$ -Enriched Carbonyl Carbons in [Leu $^5$ ]-enkephalin, *Biochemistry*, 18 (1979) 1661-1671.
- [181] C. Garbay-Jaureguiberry, J. Baudet, D. Florentin, B.P. Roques, Conformational analysis of linear peptides by  $^{15}\text{N}$  NMR spectroscopy using the enkephalin-related fragment Tyr-Gly-Gly-Phe as a model compound, *FEBS Lett.*, 115 (1980) 315-318.
- [182] H.C. Jarrell, W. Herbert McGregor, I.C.P. Smith, Interaction of Opioid Peptides with Model Membranes. A Carbon-13 Nuclear Magnetic Study of Enkephalin Binding to Phosphatidylserine, *Biochemistry*, 19 (1980) 385-390.
- [183] J. Kobayashi, T. Higashijima, U. Nagai, T. Miyazawa, Nuclear magnetic resonance study of side-chain conformation of tyrosyl residue in [Met $^5$ ]-enkephalin. Solvent and temperature dependence, *Biochim. Biophys. Acta*, 621 (1980) 190-203.
- [184] C. Garbay-Jaureguiberry, D. Marion, E. Fellion, B.P. Roques, Refinement of conformational preferences of Leu enkephalin and Tyr-Gly-Gly-Phe by  $^{15}\text{N}$  n.m.r. Chemical shifts and vicinal coupling constants, *Int. J. Pept. Protein Res.*, 20 (1982) 443-450.
- [185] C.A. Beretta, M. Parrilli, A. Pastore, T. Tancredi, P.A. Temussi, Experimental simulation of the environment of the  $\delta$  opioid receptor. A 500 MHz study of enkephalins in  $\text{CDCl}_3$ , *Biochem. Biophys. Res. Commun.*, 121 (1984) 456-462.
- [186] A. De Marco, L. Zetta, E. Menegatti, M. Guarneri,  $^1\text{H}$ -NMR of Met-enkephalin in AOT reverse micelles, *FEBS Lett.*, 178 (1984) 39-43.
- [187] B.A. Behnam, C.M. Deber, Evidence for a folded conformation of methionine- and leucine-enkephalin in a membrane environment, *J. Biol. Chem.*, 259 (1984) 14935-14940.
- [188] L. Zetta, A. De Marco, G. Zannoni, B. Cestaro, Evidence for a folded structure of met-enkephalin in membrane mimetic systems:  $^1\text{H}$ -nmr studies in sodiumdodecylsulfate, lyso-phosphatidylcholine, and mixed lyso-phosphatidylcholine/sulfatide micelles, *Biopolymers*, 25 (1986) 2315-2323.
- [189] G. Gupta, M.H. Sarma, R.H. Sarma, M.M. Dhingra, NOE data at 500 MHz reveal the proximity of phenyl and tyrosine rings in enkephalin, *FEBS Lett.*, 198 (1986) 245-250.
- [190] J. Belleney, G. Gacel, M.C. Fournié-Zaluski, B. Maigret, B.P. Roques,  $\delta$  Opioid Receptor Selectivity Induced by Conformational Constraints in Linear Enkephalin-Related Peptides:  $^1\text{H}$  400-MHz NMR Study and Theoretical Calculations, *Biochemistry*, 28 (1989) 7392-7400.
- [191] A. Milon, T. Miyazawa, T. Higashijima, Transferred Nuclear Overhauser Effect Analyses of Membrane-Bound Enkephalin Analogues by  $^1\text{H}$  Nuclear Magnetic Resonance: Correlation between Activities and Membrane-Bound Conformations, *Biochemistry*, 29 (1990) 65-75.
- [192] C.R. Watts, M.R. Tessmer, D.A. Kallick, Structure of Leu $^5$ -enkephalin bound to a model membrane as determined by high-resolution NMR, *Lett. Pept. Sci.*, 2 (1995) 59-70.
- [193] I. Marcotte, F. Separovic, M. Auger, S.M. Gagné, A Multidimensional  $^1\text{H}$  NMR Investigation of the Conformation of Methionine-Enkephalin in Fast-Tumbling Bicelles, *Biophys. J.*, 86 (2004) 1587-1600.

- [194] L. Zetta, A. De Marco, G. Zannoni, B. Cestaro, Evidence for a folded structure of met-enkephalin in membrane mimetic systems:  $^1\text{H}$ -nmr studies in sodiumdodecylsulfate, lyso-phosphatidylcholine, and mixed lyso-phosphatidylcholine/sulfatide micelles, *Biopolymers*, 25 (2004) 2315-2323.
- [195] B.A. Begotka, J.L. Hunsader, C. Oparaeche, J.K. Vincent, K.F. Morris, A pulsed field gradient NMR diffusion investigation of enkephalin peptide-sodium dodecyl sulfate micelle association, *Magn. Reson. Chem.*, 44 (2006) 586-593.
- [196] I. Chandrasekhar, W.F. Van Gunsteren, G. Zandomenighi, P.T.F. Williamson, B.H. Meier, Orientation and conformational preference of leucine-enkephalin at the surface of a hydrated dimyristoylphosphatidylcholine bilayer: NMR and MD simulation, *J. Am. Chem. Soc.*, 128 (2006) 159-170.
- [197] T. Kimura, Human opioid peptide Met-enkephalin binds to anionic phosphatidylserine in high preference to zwitterionic phosphatidylcholine: Natural-abundance  $^{13}\text{C}$  NMR study on the binding state in large unilamellar vesicles, *Biochemistry*, 45 (2006) 15601-15609.
- [198] A. Gayen, C. Mukhopadhyay, Evidence for effect of GM1 on opioid peptide conformation: NMR study on leucine enkephalin in ganglioside-containing isotropic phospholipid bicelles, *Langmuir*, 24 (2008) 5422-5432.
- [199] G. Marius Clore, B.J. Kimber, A.M. Gronenborn, The 1-1 hard pulse: A simple and effective method of water resonance suppression in FT  $^1\text{H}$  NMR, *J. Magn. Reson.* (1969), 54 (1983) 170-173.
- [200] G. Esposito, A. Pastore, An alternative method for distance evaluation from NOESY spectra, *J. Magn. Reson.* (1969), 76 (1988) 331-336.
- [201] P.S. Portoghese, S.T. Moe, A.E. Takemori, A selective  $\delta_1$  opioid receptor agonist derived from oxymorphone. Evidence for separate recognition sites for  $\delta_1$  opioid receptor agonists and antagonists, *J. Med. Chem.*, 36 (1993) 2572-2574.
- [202] K.J. Chang, G.C. Rigdon, J.L. Howard, R.W. McNutt, A novel, potent and selective nonpeptidic delta opioid receptor agonist BW373U86, *J. Pharmacol. Exp. Ther.*, 267 (1993) 852-857.
- [203] P.S. Portoghese, B.D. Alreja, D.L. Larson, Allylprodine analogs as receptor probes. Evidence that phenolic and nonphenolic ligands interact with different subsites on identical opioid receptors, *J. Med. Chem.*, 24 (1981) 782-787.
- [204] P.S. Portoghese, Bivalent ligands and the message-address concept in the design of selective opioid receptor antagonists, *Trends Pharmacol. Sci.*, 10 (1989) 230-235.
- [205] P.A. Temussi, S. Salvadori, P. Amodeo, C. Bianchi, R. Guerrini, R. Tomatis, L.H. Lazarus, D. Picone, T. Tancredi, Selective opioid dipeptides, *Biochem. Biophys. Res. Commun.*, 198 (1994) 933-939.
- [206] P.S. Portoghese, M. Sultana, S.T. Moe, A.E. Takemori, Synthesis of naltrexone-derived  $\delta$ -opioid antagonists. Role of conformation of the  $\delta$  address moiety, *J. Med. Chem.*, 37 (1994) 579-585.
- [207] P. Amodeo, G. Balboni, O. Crescenzi, R. Guerrini, D. Picone, S. Salvadori, T. Tancredi, P.A. Temussi, Conformational analysis of potent and very selective  $\delta$  opioid dipeptide antagonists, *FEBS Lett.*, 377 (1995) 363-367.
- [208] A.A. Bothner-By, P.E. Johner, Specificity of interproton nuclear Overhauser effects in gramicidin-S dissolved in deuterated ethylene glycol, *BIOPHYS. J.*, 24 (1978) 779-790.
- [209] R. Schwyzler, U. Ludescher, Conformational Study of Gramicidin S Using the Phthalimide Group as Nuclear Magnetic Resonance Marker, *Biochemistry*, 7 (1968) 2519-2522.
- [210] A. Stern, W.A. Gibbons, L.C. Craig, A conformational analysis of gramicidin S-A by nuclear magnetic resonance, *Proc. Nat. Acad. Sci. U.S.A.*, 61 (1968) 734-741.
- [211] W.A. Gibbons, J.A. Sogn, A. Stern, L.C. Craig, L.F. Johnson,  $^{13}\text{C}$  nuclear magnetic resonance spectrum of gramicidin S-A, a decapeptide antibiotic, *Nature*, 227 (1970) 840-842.
- [212] T. Kato, M. Waki, S. Matsuura, N. Izumiya, The Correlation between Conformation and Biological Activity of Gramicidin S Analogs, *J. Biochem.*, 68 (1970) 751-753.
- [213] J.A. Sogn, L.C. Craig, W.A. Gibbons, Complete Assignment of the  $^{13}\text{C}$  Nuclear Magnetic Resonance Spectrum of the Decapeptide Gramicidin S-A by Selective Biosynthetic Enrichment Studies, *J. Am. Chem. Soc.*, 96 (1974) 3306-3309.
- [214] R.A. Komoroski, I.R. Peat, G.C. Levy, High field carbon-13 NMR spectroscopy. Conformational mobility in gramicidin S and frequency dependence of  $^{13}\text{C}$  spin-lattice relaxation times, *Biochem. Biophys. Res. Commun.*, 65 (1975) 272-279.
- [215] I.D. Rae, E.R. Stimson, H.A. Scheraga, Nuclear overhauser effects and the conformation of gramicidin S, *Biochem. Biophys. Res. Commun.*, 77 (1977) 225-229.
- [216] S.E. Hull, R. Karlsson, P. Main, M.M. Woolfson, E.J. Dodson, The crystal structure of a hydrated gramicidin S-urea complex, *Nature*, 275 (1978) 206.
- [217] I.D. Rae, H.A. Scheraga, Shielding effects of the D-Phe aromatic ring in the  $^1\text{H}$  NMR spectrum of gramicidin S, *Biochem. Biophys. Res. Commun.*, 81 (1978) 481-485.
- [218] M. Kuo, C.R. Jones, T.H. Mahn, P.R. Miller, L.J. Nicholls, W.A. Gibbons, Simplification and spin-spin analysis of the side chain proton magnetic resonance spectrum of the decapeptide gramicidin S using difference scalar decoupling and biosynthesis of specifically deuterated analogs, *J. Biol. Chem.*, 254 (1979) 10301-10306.
- [219] C.R. Jones, M. Kuo, W.A. Gibbons, Multiple solution conformations and internal rotations of the decapeptide gramicidin S, *J. Biol. Chem.*, 254 (1979) 10307-10312.
- [220] E.M. Krauss, S.I. Chan, Intramolecular hydrogen bonding in gramicidin S. 2. Ornithine, *J. Am. Chem. Soc.*, 104 (1982) 6953-6961.
- [221] E.M. Krauss, S.I. Chan, Spectroscopic studies of intramolecular hydrogen bonding in gramicidin S, *J. Am. Chem. Soc.*, 104 (1982) 1824-1830.
- [222] N. Niccolai, G. Valensin, C. Rossi, W.A. Gibbons, The Stereochemistry and Dynamics of Natural Products and Biopolymers from Proton Relaxation Spectroscopy: Spin-Label Delineation of Inner and Outer Protons of Gramicidin S Including Hydrogen Bonds, *J. Am. Chem. Soc.*, 104 (1982) 1534-1537.
- [223] N. Niccolai, L. Pogliani, C. Rossi, P. Corti, W.A. Gibbons, Proton relaxation mechanisms and the measurements of  $r_{\phi}$ ,  $r_{\psi}$  and transannular interproton distances in gramicidin S, *Biophys. Chem.*, 20 (1984) 217-223.
- [224] N. Niccolai, C. Rossi, P. Mascagni, P. Neri, W.A. Gibbons,  $^1\text{H}$ - $^{13}\text{C}$  selective NOE studies of the decapeptide gramicidin S, *Biochem. Biophys. Res. Commun.*, 124 (1984) 739-744.
- [225] D.S. Wishart, L.H. Kondejewski, P.D. Semchuk, B.D. Sykes, R.S. Hodges, A method for the facile solid-phase synthesis of gramicidin S and its analogs, *Lett. Pept. Sci.*, 3 (1996) 53-60.
- [226] C. Solanas, B.G. De La Torre, M. Fernández-Reyes, C.M. Santiveri, M.A. Jiménez, L. Rivas, A.I. Jiménez, D. Andreu, C. Cativiela, Sequence inversion and phenylalanine surrogates at the  $\beta$ -Turn enhance the antibiotic activity of gramicidin S, *J. Med. Chem.*, 53 (2010) 4119-4129.

- [227] M. Dygert, N. Gö, H.A. Scheraga, Use of a Symmetry Condition to Compute the Conformation of Gramicidin S, *Macromolecules*, 8 (1975) 750-761.
- [228] D. Mihailescu, J.C. Smith, Molecular Dynamics Simulation of the Cyclic Decapeptide Antibiotic, Gramicidin S, in Dimethyl Sulfoxide Solution, *J. Phys. Chem. B*, 103 (1999) 1586-1594.
- [229] D. Mihailescu, J.C. Smith, Atomic detail peptide-membrane interactions: Molecular dynamics simulation of gramicidin S in a DMPC bilayer, *BIOPHYS. J.*, 79 (2000) 1718-1730.
- [230] P. Debye, Polar molecules. By P. Debye, Ph.D., Pp. 172. New York: Chemical Catalog Co., Inc., 1929. \$ 3.50, *J. Chem. Technol. Biotechnol.*, 48 (1929) 1036-1037.
- [231] C. Yu, S.W. Unger, G.N. La Mar, NOE experiments for resonance and structure assignments of paramagnetic heme derivatives, *J. Magn. Reson.* (1969), 67 (1986) 346-350.
- [232] G.N. La Mar, D.B. Viscio, K.M. Smith, W.S. Caughey, M.L. Smith, NMR studies of low-spin ferric complexes of natural porphyrin derivatives. 1. Effect of peripheral substituents on the  $\pi$  electronic asymmetry in bisicyano complexes, *J. Am. Chem. Soc.*, 100 (1978) 8085-8092.
- [233] G.N. La Mar, D.L. Budd, D.B. Viscio, K.M. Smith, K.C. Langry, Proton nuclear magnetic resonance characterization of heme disorder in hemoproteins, *Proc. Natl. Acad. Sci. USA*, 75 (1978) 5755-5759.
- [234] R. Freeman, K.G.R. Pachler, G.N.L. Mar, Quenching the Nuclear Overhauser Effect in NMR Spectra of Carbon-13, *J. Chem. Phys.*, 55 (1971) 4586-4593.
- [235] G.N. La Mar, M.J. Minch, J.S. Frye, NMR studies of low-spin ferric complexes of natural porphyrin derivatives. 4. Proton relaxation characterization of the dimer structure of dicyanohemin in aqueous solution, *J. Am. Chem. Soc.*, 103 (1981) 5383-5388.
- [236] M.J. Chatfield, G.N. La Mar, W.O. Parker, K.M. Smith, H.-K. Leung, I.K. Morris, Nuclear Magnetic Resonance Study of the Molecular and Electronic Structure of the Stable Green Sulfhemin Prosthetic Group Extracted from Sulfmyoglobin, *J. Am. Chem. Soc.*, 110 (1988) 6352 - 6358.
- [237] R. Burgus, N. Ling, M. Butcher, R. Guillemin, Primary structure of somatostatin, a hypothalamic peptide that inhibits the secretion of pituitary growth hormone, *Proc. Nat. Acad. Sci. U.S.A.*, 70 (1973) 684-688.
- [238] P. Brazeau, W. Vale, R. Burgus, N. Ling, M. Butcher, J. Rivier, R. Guillemin, Hypothalamic polypeptide that inhibits the secretion of immunoreactive pituitary growth hormone, *Science*, 179 (1973) 77-79.
- [239] W. Vale, C. Rivier, M. Brown, Regulatory peptides of the hypothalamus, *Annu. Rev. Physiol.*, 39 (1977) 473-527.
- [240] P. Verheyden, E. De Wolf, H. Jaspers, G. Van Binst, Comparing conformations at low temperature and at high viscosity: Conformational study of somatostatin and two of its analogues in methanol and in ethylene glycol, *Int. J. Pept. Protein Res.*, 44 (1994) 401-409.
- [241] E.M.M. van den Berg, A.W.H. Jans, G. van Binst, Conformational properties of somatostatin. VI. In a methanol solution, *Biopolymers*, 25 (1986) 1895-1908.
- [242] P. Verheyden, W. Franco, H. Pepermans, G. Van Binst, Conformational study of a somatostatin analogue in DMSO/water by 2D NMR, *Biopolymers*, 30 (1990) 855-860.
- [243] P.M.F. Verheyden, D.H. Coy, G. Van Binst, Conformational study of somatostatin analogues in methanol at low temperature, *Magn. Reson. Chem.*, 29 (1991) 607-612.
- [244] V. Erspamer, P. Melchiorri, G. Falconieri-Erspamer, L. Negri, R. Corsi, C. Severini, D. Barra, M. Simmaco, G. Kreil, Deltorphins: a family of naturally occurring peptides with high affinity and selectivity for  $\delta$  opioid binding sites, *Proc. Natl. Acad. Sci. USA*, 86 (1989) 5188-5192.
- [245] M. Dizechi, E. Marschall, Viscosity of some binary and ternary liquid mixtures, *J. Chem. Eng. Data*, 27 (1982) 358-363.
- [246] K. Fushimi, A.S. Verkman, Low viscosity in the aqueous domain of cell cytoplasm measured by picosecond polarization microfluorimetry, *J. Cell. Biol.*, 112 (1991) 719-725.
- [247] S. Bicknese, N. Periasamy, S.B. Shohet, A.S. Verkman, Cytoplasmic viscosity near the cell plasma membrane: measurement by evanescent field frequency-domain microfluorimetry, *BIOPHYS. J.*, 65 (1993) 1272-1282.
- [248] E.O. Puchkov, Intracellular viscosity: Methods of measurement and role in metabolism, *Biochem. (Mosc) Suppl. Ser. A Membr. Cell. Biol.*, 7 (2013) 270-279.
- [249] P.H. Barry, J.M. Diamond, Effects of unstirred layers on membrane phenomena, *Physiol. Rev.*, 64 (1984) 763-872.
- [250] M.R. Ruff, B.M. Martin, E.I. Ginns, W.L. Farrar, C.B. Pert, CD4 receptor binding peptides that block HIV infectivity cause human monocyte chemotaxis: Relationship to vasoactive intestinal polypeptide, *FEBS Lett.*, 211 (1987) 17-22.
- [251] M. Marastoni, S. Salvadori, G. Balboni, V. Scaranari, S. Spisani, E. Reali, S. Traniello, R. Tomatis, Structure-activity relationships of cyclic and linear peptide T analogues, *Int. J. Pept. Protein Res.*, 41 (1993) 447-454.
- [252] A.C. De Dios, D.N. Sears, R. Tycko, NMR studies of peptide T, an inhibitor of HIV infectivity, in an aqueous environment, *J. Pept. Science*, 10 (2004) 622-630.
- [253] B. Gysin, R. Schwyzer, Liposome-mediated labeling of adrenocorticotropin fragments parallels their biological activity, *FEBS Lett.*, 158 (1983) 12-16.
- [254] H.U. Gremlich, U.P. Fringeli, R. Schwyzer, Conformational Changes of Adrenocorticotropin Peptides upon Interaction with Lipid Membranes Revealed by Infrared Attenuated Total Reflection Spectroscopy, *Biochemistry*, 22 (1983) 4257-4264.
- [255] H.U. Gremlich, U.P. Fringeli, R. Schwyzer, Interaction of Adrenocorticotropin-(11-24)-tetradecapeptide with Neutral Lipid Membranes Revealed by Infrared Attenuated Total Reflection Spectroscopy, *Biochemistry*, 23 (1984) 1808-1810.
- [256] B. Gysin, R. Schwyzer, Hydrophobic and Electrostatic Interactions between Adrenocorticotropin-(1-24)-tetracosapeptide and Lipid Vesicles. Amphiphilic Primary Structures, *Biochemistry*, 23 (1984) 1811-1818.
- [257] R. Schwyzer, Molecular Mechanism of Opioid Receptor Selection, *Biochemistry*, 25 (1986) 6335-6342.
- [258] A. De Marco, L. Zetta, E. Menegatti, P.L. Luisi,  $^1\text{H-NMR}$  of reverse micelles. II: Conformational studies of peptides and proteins in the AOT/water/isooctane system, *J. Biochem. Biophys. Methods*, 12 (1986) 335-347.
- [259] M.A. Castiglione-morelli, T. Tancredi, E. Trivellone, F. Leij, A. Pastore, S. Salvadori, R. Tomatis, P.A. Temussi, A 500-MHz Proton Nuclear Magnetic Resonance Study of  $\mu$  Opioid Peptides in a Simulated Receptor Environment, *J. Med. Chem.*, 30 (1987) 2067-2073.
- [260] P.A. Temussi, T. Tancredi, A. Pastore, M.A. Castiglione-Morelli, Experimental attempt to simulate receptor site environment. A 500-MHz proton nuclear magnetic resonance study of enkephalin amides, *Biochemistry*, 26 (1987) 7856-7863.
- [261] W. Huang, D.G. Levitt, Theoretical calculation of the dielectric constant of a bilayer membrane, *BIOPHYS. J.*, 17 (1977) 111-128.

- [262] P. Balaram, A.A. Bothner-By, J. Dadok, Negative Nuclear Overhauser Effects as Probes of Macromolecular Structure, *J. Am. Chem. Soc.*, 94 (1972) 4015-4017.
- [263] L. Jannelli, A. Sacco, Thermodynamic and physical behavior of binary mixtures involving sulfolane II. Viscosity, dielectric constant, solid + liquid phase diagram of mixtures of benzene + sulfolane, *J. Chem. Thermodyn.*, 4 (1972) 715-722.
- [264] G. Kartha, K.K. Bhandary, K.D. Kopple, A. Go, P.P. Zhu, Synthesis and conformation studies by x-ray crystallography and nuclear magnetic resonance of cyclo(L-Phe-L-Pro-D-Ala)<sub>2</sub>, *J. Am. Chem. Soc.*, 106 (1984) 3844-3850.
- [265] L.M. Gierasch, A.L. Rockwell, K.F. Thompson, M.S. Briggs, Conformation-function relationships in hydrophobic peptides: Interior turns and signal sequences, *Biopolymers*, 24 (1985) 117-135.
- [266] B.M. Cwilong, Sublimation in a Wilson chamber, *Proc. R. Soc. A* 190 (1947) 137.
- [267] S.C. Mossop, The Freezing of Supercooled Water, *Proc. Phys. Soc. B*, 68 (1955) 193.
- [268] R.S. Chahal, R.D. Miller, Supercooling of water in glass capillaries, *Br. J. Appl. Phys.*, 16 (1965) 231.
- [269] C.A. Angell, Supercooled Water, in: F. Franks (Ed.) *Water and Aqueous Solutions at Subzero Temperatures*, Springer US, Boston, MA, 1982, pp. 1-81.
- [270] V. Gutmann, E. Scheiber, G. Resch, Supercooled water. Considerations about the system organization of liquid water, *Monatsh. Chem.*, 120 (1989) 671-690.
- [271] E.B. Moore, V. Molinero, Structural transformation in supercooled water controls the crystallization rate of ice, *Nature*, 479 (2011) 506.
- [272] J. Hallett, The Temperature Dependence of the Viscosity of Supercooled Water, *Proc. Phys. Soc.*, 82 (1963) 1046.
- [273] Y.A. Osipov, B.V. Zhelezny, N.F. Bondarenko, The Shear Viscosity of Water Supercooled to -35°C, *Russ. J. Phys. Chem.*, 51 (1977) 1264-1265.
- [274] A.F. Collings, N. Bajenov, A High Precision Capillary Viscometer and Further Relative Results for the Viscosity of Water, *Metrologia*, 19 (1983) 61.
- [275] A. Dehaoui, B. Issenmann, F. Caupin, Viscosity of deeply supercooled water and its coupling to molecular diffusion, *Proc. Nat. Acad. Sci. U.S.A.*, 112 (2015) 12020.
- [276] J.S. Thompson, H. Gehring, B.L. Vallee, Structure and function of carboxypeptidase A $\alpha$  in supercooled water, *Proc. Nat. Acad. Sci. U.S.A.*, 77 (1980) 132-136.
- [277] F. Franks, T. Wakabayashi, Heat Capacities of Undercooled Aqueous Solutions of Polyvinylpyrrolidone, *Z. Phys. Chem.*, 155 (1987) 171-180.
- [278] C.R. Babu, V.J. Hilser, A.J. Wand, Direct access to the cooperative substructure of proteins and the protein ensemble via cold denaturation, *Nat. Struct. Mol. Biol.*, 11 (2004) 352.
- [279] K. Modig, E. Liepinsh, G. Otting, B. Halle, Dynamics of Protein and Peptide Hydration, *J. Am. Chem. Soc.*, 126 (2004) 102-114.
- [280] A.K. Simorellis, W.D. Van Horn, P.F. Flynn, Dynamics of low temperature induced water shedding from AOT reverse micelles, *J. Am. Chem. Soc.*, 128 (2006) 5082-5090.
- [281] C. Mattea, J. Qvist, B. Halle, Dynamics at the protein-water interface from <sup>17</sup>O spin relaxation in deeply supercooled solutions, *BIOPHYS. J.*, 95 (2008) 2951-2963.
- [282] M. Davidovic, C. Mattea, J. Qvist, B. Halle, Protein Cold Denaturation as Seen From the Solvent, *J. Am. Chem. Soc.*, 131 (2009) 1025-1036.
- [283] T. Szyperski, J.L. Mills, NMR-based structural biology of proteins in supercooled water, *J. Struct. Funct. Genomics*, 12 (2011) 1-7.
- [284] L. Poppe, H.v. Halbeek, NMR spectroscopy of hydroxyl protons in supercooled carbohydrates, *Nat. Struct. Mol. Biol.*, 1 (1994) 215.
- [285] H. van Halbeek, S. Sheng, NMR studies of the structure and dynamics of carbohydrates in aqueous solution, in: S.B. Petersen, B. Svensson, S. Pedersen (Eds.) *Progress in Biotechnology*, Elsevier, 1995, pp. 15-28.
- [286] S.Q. Sheng, H. Vanhalbeek, Evidence for a Transient Interresidue Hydrogen Bond in Sucrose in Aqueous Solution Obtained by Rotating-Frame Exchange NMR Spectroscopy Under Supercooled Conditions, *Biochem. Biophys. Res. Commun.*, 215 (1995) 504-510.
- [287] J.J. Skalicky, D.K. Sukumaran, J.L. Mills, T. Szyperski, Toward structural biology in supercooled water, *J. Am. Chem. Soc.*, 122 (2000) 3230-3231.
- [288] J.J. Skalicky, J.L. Mills, S. Sharma, T. Szyperski, Aromatic ring-flipping in supercooled water: Implications for NMR-based structural biology of proteins, *J. Am. Chem. Soc.*, 123 (2001) 388-397.
- [289] J.L. Mills, T. Szyperski, Protein dynamics in supercooled water: The search for slow motional modes, *J. Biomol. NMR*, 23 (2002) 63-67.
- [290] V.V. Krishnan, W.H. Fink, R.E. Feeney, Y. Yeh, Translational dynamics of antifreeze glycoprotein in supercooled water, *Biophys. Chem.*, 110 (2004) 223-230.
- [291] K.T. Schroeder, J.J. Skalicky, N.L. Greenbaum, NMR spectroscopy of RNA duplexes containing pseudouridine in supercooled water, *RNA*, 11 (2005) 1012-1016.
- [292] T. Szyperski, J.L. Mills, D. Perl, J. Balbach, Combined NMR-observation of cold denaturation in supercooled water and heat denaturation enables accurate measurement of  $\Delta C_p$  of protein unfolding, *Eur. Biophys. J.*, 35 (2006) 363-366.
- [293] H.Y. Kim, M.K. Cho, D. Riedel, C.O. Fernandez, M. Zweckstetter, Dissociation of amyloid fibrils of  $\alpha$ -synuclein in supercooled water, *Angew. Chem. Int. Ed.*, 47 (2008) 5046-5048.
- [294] Y. Shen, T. Szyperski, Structure of the protein BPTI derived with NOESY in supercooled water: Validation and refinement of solution structures, *Angew. Chem. Int. Ed.*, 47 (2008) 324-326.
- [295] J.B. Jordan, L. Poppe, M. Haniu, T. Arvedson, R. Syed, V. Li, H. Kohno, H. Kim, P.D. Schnier, T.S. Harvey, L.P. Miranda, J. Cheetham, B.J. Sasu, Hepcidin revisited, disulfide connectivity, dynamics, and structure, *J. Biol. Chem.*, 284 (2009) 24155-24167.
- [296] H. Farooq, R. Soong, D. Courtier-Murias, C. Anklin, A. Simpson, Tailoring <sup>1</sup>H spin dynamics in small molecules via supercooled water: A promising approach for metabolite identification and validation, *Anal. Chem.*, 84 (2012) 6759-6766.
- [297] M.K. Cho, S. Xiang, H.Y. Kim, S. Becker, M. Zweckstetter, Cold-induced changes in the protein ubiquitin, *PLoS ONE*, 7 (2012).
- [298] F. Mallamace, C. Corsaro, D. Mallamace, S. Vasi, C. Vasi, H.E. Stanley, S.H. Chen, Some thermodynamical aspects of protein hydration water, *J. Chem. Phys.*, 142 (2015).
- [299] L. Pavone, O. Crescenzi, T. Tancredi, P.A. Temussi, NMR studies of flexible peptides in cavities mimicking the synaptic cleft, *FEBS Lett.*, 513 (2002) 273-276.
- [300] A. Pastore, S. Salvadori, P.A. Temussi, Peptides and proteins in a confined environment: NMR spectra at natural isotopic abundance, *J. Pept. Sci.*, 13 (2007) 342-347.
- [301] D. Sanfelice, T. Tancredi, A. Politou, A. Pastore, P.A. Temussi, Cold Denaturation and Aggregation: A Comparative NMR Study of Titin I28 in Bulk and in a Confined Environment, *J. Am. Chem. Soc.*, 131 (2009) 11662-11663.

- [302] A.M. Spring, M.W. Germann, Supercooled aqueous nuclear magnetic resonance using agarose gels, *ANAL. Biochem.*, 427 (2012) 79-81.
- [303] J. Jonas, T. DeFries, D.J. Wilbur, Molecular motions in compressed liquid water, *J. Chem. Phys.*, 65 (1976) 582-588.
- [304] C.A. Angell, E.D. Finch, P. Bach, Spin-echo diffusion coefficients of water to 2380 bar and  $-20^{\circ}\text{C}$ , *J. Chem. Phys.*, 65 (1976) 3063-3066.
- [305] T. DeFries, J. Jonas, Molecular motions in compressed liquid heavy water at low temperatures, *J. Chem. Phys.*, 66 (1977) 5393-5399.
- [306] T. DeFries, J. Jonas, Pressure dependence of NMR proton spin-lattice relaxation times and shear viscosity in liquid water in the temperature range  $-15$   $-10^{\circ}\text{C}$ , *J. Chem. Phys.*, 66 (1977) 896-901.
- [307] C.A. Angell, Supercooled Water, *Annu. Rev. Phys. Chem.*, 34 (1983) 593-630.
- [308] J. Zhang, X. Peng, A. Jonas, J. Jonas, NMR Study of the Cold, Heat, and Pressure Unfolding of Ribonuclease A, *Biochemistry*, 34 (1995) 8631-8641.
- [309] J. Jonas, High-resolution nuclear magnetic resonance studies of proteins, *Biochim. Biophys. Acta*, 1595 (2002) 145-159.
- [310] J. Jonas, High Pressure Studies Using NMR Spectroscopy, in: *Encyclopedia of Spectroscopy and Spectrometry*, Elsevier Ltd, 2010, pp. 854-864.
- [311] J. Roche, C.A. Royer, C. Roumestand, Monitoring protein folding through high pressure NMR spectroscopy, *Prog. Nucl. Magn. Reson. Spectrosc.*, 102-103 (2017) 15-31.
- [312] K. Akasaka, Protein studies by high-pressure NMR, in: *Experimental Approaches of NMR Spectroscopy: Methodology and Application to Life Science and Materials Science*, Springer Singapore, 2017, pp. 3-36.
- [313] D.J. Kerwood, M.J. Cavaluzzi, P.N. Borer, Structure of SL4 RNA from the HIV-1 Packaging Signal, *Biochemistry*, 40 (2001) 14518-14529.
- [314] M.K. Ahn, Electron spin relaxation of di-tertiary-butyl nitroxide in supercooled water, *J. Chem. Phys.*, 64 (1976) 134-138.
- [315] H.J. Sass, G. Musco, S. J. Stahl, P. T. Wingfield, S. Grzesiek, Solution NMR of proteins within polyacrylamide gels: Diffusional properties and residual alignment by mechanical stress or embedding of oriented purple membranes, *J. Biomol. NMR*, 18 (2000) 303-309.
- [316] E. Bismuto, G. Irace, The effect of molecular confinement on the conformational dynamics of the native and partly folded state of apomyoglobin, *FEBS Lett.*, 509 (2001) 476-480.
- [317] D. Bolis, A.S. Politou, G. Kelly, A. Pastore, P.A. Temussi, Protein stability in nanocages: a novel approach for influencing protein stability by molecular confinement, *J. Mol. Biol.*, 336 (2004) 203-212.
- [318] L.
- [319] M. Ikura, A. Bax, Isotope-filtered 2D NMR of a protein-peptide complex: study of a skeletal muscle myosin light chain kinase fragment bound to calmodulin, *J. Am. Chem. Soc.*, 114 (1992) 2433-2440.
- [320] V. Bernier, R. Stocco, M.J. Bogusky, J.G. Joyce, C. Parachoniak, K. Grenier, M. Arget, M.C. Mathieu, G.P. O'Neill, D. Slipetz, M.A. Crackower, C.M. Tan, A.G. Therien, Structure-function relationships in the neuropeptide S receptor: molecular consequences of the asthma-associated mutation N107I, *J. Biol. Chem.*, 281 (2006) 24704-24712.
- [321] A.L. Roth, E. Marzola, A. Rizzi, M. Arduin, C. Trapella, C. Corti, R. Vergura, P. Martinelli, S. Salvadori, D. Regoli, M. Corsi, P. Cavanni, G. Calo, R. Guerrini, Structure-activity studies on neuropeptide S: identification of the amino acid residues crucial for receptor activation, *J. Biol. Chem.*, 281 (2006) 20809-20816.
- [322] L.A. Munishkina, E.M. Cooper, V.N. Uversky, A.L. Fink, The effect of macromolecular crowding on protein aggregation and amyloid fibril formation, *J. Mol. Recognit.*, 17 (2004) 456-464.
- [323] A. Pastore, S.R. Martin, A. Politou, K.C. Kondapalli, T. Stemmler, P.A. Temussi, Unbiased Cold Denaturation: Low- and High-Temperature Unfolding of Yeast Frataxin under Physiological Conditions, *J. Am. Chem. Soc.*, 129 (2007) 5374-5375.
- [324] M. Ausubel, R. Brent, R.E. Kingston, D.D. Moore, J.G. Seidman, J.A. Smith, S. K., *Current protocols in molecular biology*, Mol. Reprod. Dev., 1 (1989) 146-146.
- [325] R. Kim, H. Yokota, S.H. Kim, Electrophoresis of proteins and protein-protein complexes in a native agarose gel, *Anal. Biochem.*, 282 (2000) 147-149.
- [326] C.N. Johnson, A.M. Spring, S. Desai, R.P. Cunningham, M.W. Germann, DNA sequence context conceals  $\alpha$ -anomeric lesions, *J. Mol. Biol.*, 416 (2012) 425-437.
- [327] G.G. Stokes, On the Theories of the Internal Friction of Fluids in Motion, and of the Equilibrium and Motion of Elastic Solids, in: G.G. Stokes (Ed.) *Mathematical and Physical Papers*, Cambridge University Press, Cambridge, 1845, pp. 75-129.
- [328] C. Barus, Note on the Dependence of Viscosity on Pressure and Temperature, *Proc. Am. Acad. Arts Sci.*, 27 (1891) 13-18.
- [329] P.W. Bridgman, The Viscosity of Liquids under Pressure, *Proc. Nat. Acad. Sci.*, 11 (1925) 603-606.
- [330] J. Jonas, S.T. Adamy, P.J. Grandinetti, Y. Masuda, S.J. Morris, D.M. Campbell, Y. Li, High-pressure NMR study of transport and relaxation in complex liquid of 2-ethylhexyl cyclohexanecarboxylate and 2-ethylhexyl benzoate, *J. Phys. Chem.*, 94 (1990) 1157-1164.
- [331] K.R. Rajagopal, On implicit constitutive theories for fluids, *J. Fluid Mech.*, 550 (2006) 243-249.
- [332] F.T. Akyildiz, D. Siginer, A note on the steady flow of Newtonian fluids with pressure dependent viscosity in a rectangular duct, *Int. J. Eng. Sci.*, 104 (2016) 1-4.
- [333] A. Daryasafar, K. Shahbazi, Prediction of dynamic viscosity of *n*-alkanes at high pressures using a rigorous approach, *Pet. Sci. Technol.*, 36 (2018) 333-337.
- [334] S. Feng, Z. Liu, Q. Bi, H. Pan, Viscosity Measurements of *n*-Dodecane at Temperatures between 303 K and 693 K and Pressures up to 10 MPa, *J. Chem. Eng. Data*, 63 (2018) 671-678.
- [335] V. Volpe, R. Pantani, Determination of the effect of pressure on viscosity at high shear rates by using an injection molding machine, *J. Appl. Polym. Sci.*, 135 (2018).
- [336] K. Akasaka, High pressure NMR spectroscopy, in: *Subcellular Biochemistry*, Springer New York, 2015, pp. 707-721.
- [337] R.C. Hardy, R.L. Cottington, Viscosity of deuterium oxide and water from  $5^{\circ}$  to  $125^{\circ}\text{C}$ , *J. Chem. Phys.*, 17 (1949) 509-510.
- [338] C.H. Cho, J. Urquidi, S. Singh, G.W. Robinson, Thermal Offset Viscosities of Liquid  $\text{H}_2\text{O}$ ,  $\text{D}_2\text{O}$ , and  $\text{T}_2\text{O}$ , *J. Phys. Chem. B*, 103 (1999) 1991-1994.
- [339] J. Jonas, R. Winter, P.J. Grandinetti, D. Driscoll, High-pressure 2D NOESY experiments on phospholipid vesicles, *J. Magn. Reson.* (1969), 87 (1990) 536-547.
- [340] J. Jonas, C.L. Xie, A. Jonas, P.J. Grandinetti, D. Campbell, D. Driscoll, High-resolution  $^{13}\text{C}$  NMR study of pressure effects on the main phase transition in L- $\alpha$ -dipalmitoyl phosphatidylcholine vesicles, *Proc. Nat. Acad. Sci. U.S.A.*, 85 (1988) 4115-4117.

- [341] C. Mayer, K. Müller, K. Weisz, G. Kothe, Deuteron N.M.R. relaxation studies of phospholipid membranes, *Liq. Cryst.*, 3 (1988) 797-806.
- [342] Y. Kuroda, K. Kitamura, Intra-and Intermolecular  $^1\text{H}$ - $^1\text{H}$  Nuclear Overhauser Effect Studies on the Interactions of Chlorpromazine with Lecithin Vesicles, *J. Am. Chem. Soc.*, 106 (1984) 1-6.
- [343] Z.C. Xu, D.S. Cafiso, Phospholipid packing and conformation in small vesicles revealed by two-dimensional  $^1\text{H}$  nuclear magnetic resonance cross-relaxation spectroscopy, *Biophys. J.*, 49 (1986) 779-783.
- [344] N.E. Gabriel, M.F. Roberts, Short-chain lecithin long-chain phospholipid unilamellar vesicles: asymmetry, dynamics, and enzymatic hydrolysis of the short-chain component, *Biochemistry*, 26 (1987) 2432-2440.
- [345] N.A. Walker, D.M. Lamb, S.T. Adamy, J. Jonas, M.P. Dare-Edwards, Self-diffusion in the compressed, highly viscous liquid 2-ethylhexyl benzoate, *J. Phys. Chem.*, 92 (1988) 3675-3679.
- [346] S.T. Adamy, S.T. Kerrick, J. Jonas, High-Pressure 2D NOESY Study of Liquid 2-Ethylhexyl Benzoate, *Z. Phys. Chem.*, 184 (1994) 185.
- [347] P.A. Mirau, F.A. Bovey, Two-dimensional NMR analysis of the conformational and dynamic properties of  $\alpha$ -helical poly( $\gamma$ -benzyl L-glutamate), *J. Am. Chem. Soc.*, 108 (1986) 5130-5134.
- [348] H. Andersen Niels, L. Eaton Hugh, X. Lai, Quantitative small molecule NOESY. A practical guide for derivation of cross-relaxation rates and internuclear distances, *Magn. Reson. Chem.*, 27 (1989) 515-528.
- [349] J.D. Baleja, J. Moul, B.D. Sykes, Distance measurement and structure refinement with NOE data, *J. Magn. Reson.* (1969), 87 (1990) 375-384.
- [350] N. Bloembergen, E.M. Purcell, R.V. Pound, Relaxation Effects in Nuclear Magnetic Resonance Absorption, *Phys. Rev.*, 73 (1948) 679-712.
- [351] R.E.D. McClung, D. Kivelson, ESR Linewidths in Solution. V. Studies of Spin-Rotational Effects Not Described by Rotational Diffusion Theory, *J. Chem. Phys.*, 49 (1968) 3380-3391.
- [352] H.C. Torrey, Nuclear Spin Relaxation by Translational Diffusion, *Phys. Rev.*, 92 (1953) 962-969.
- [353] N.L. Allinger, Conformational analysis. 130. MM2. A hydrocarbon force field utilizing  $V_1$  and  $V_2$  torsional terms, *J. Am. Chem. Soc.*, 99 (1977) 8127-8134.
- [354] M. Spraul, A.S. Freund, R.E. Nast, R.S. Withers, W.E. Maas, O. Corcoran, Advancing NMR Sensitivity for LC-NMR-MS Using a Cryoflow Probe: Application to the Analysis of Acetaminophen Metabolites in Urine, *Anal. Chem.*, 75 (2003) 1546-1551.
- [355] O. Corcoran, M. Spraul, LC-NMR-MS in drug discovery, *Drug Discov. Today*, 8 (2003) 624-631.
- [356] M. Godejohann, L.-H. Tseng, U. Braumann, J. Fuchser, M. Spraul, Characterization of a paracetamol metabolite using on-line LC-SPE-NMR-MS and a cryogenic NMR probe, *J. Chrom. A*, 1058 (2004) 191-196.
- [357] J.-L. Wolfender, J.-M. Nuzillard, J.J.J. van der Hooft, J.-H. Renault, S. Bertrand, Accelerating Metabolite Identification in Natural Product Research: Toward an Ideal Combination of Liquid Chromatography-High-Resolution Tandem Mass Spectrometry and NMR Profiling, in *Silico Databases, and Chemometrics*, *Anal. Chem.*, 91 (2019) 704-742.
- [358] K.F. Morris, C.S. Johnson, Diffusion-ordered two-dimensional nuclear magnetic resonance spectroscopy, *J. Am. Chem. Soc.*, 114 (1992) 3139-3141.
- [359] K.F. Morris, C.S. Johnson, Resolution of discrete and continuous molecular size distributions by means of diffusion-ordered 2D NMR spectroscopy, *J. Am. Chem. Soc.*, 115 (1993) 4291-4299.
- [360] K.F. Morris, P. Stilbs, C.S. Johnson, Analysis of mixtures based on molecular size and hydrophobicity by means of diffusion-ordered 2D NMR, *Anal. Chem.*, 66 (1994) 211-215.
- [361] A.A. Colbourne, G.A. Morris, M. Nilsson, Local Covariance Order Diffusion-Ordered Spectroscopy: A Powerful Tool for Mixture Analysis, *J. Am. Chem. Soc.*, 133 (2011) 7640-7643.
- [362] S. Viel, F. Ziarelli, S. Caldarelli, Enhanced diffusion-edited NMR spectroscopy of mixtures using chromatographic stationary phases, *Proc. Natl. Acad. Sci. USA*, 100 (2003) 9696-9698.
- [363] G. Pages, C. Delaurent, S. Caldarelli, Simplified Analysis of Mixtures of Small Molecules by Chromatographic NMR Spectroscopy, *Angew. Chem. Int. Ed.*, 45 (2006) 5950-5953.
- [364] G. Pages, C. Delaurent, S. Caldarelli, Investigation of the Chromatographic Process via Pulsed-Gradient Spin-Echo Nuclear Magnetic Resonance. Role of the Solvent Composition in Partitioning Chromatography, *Anal. Chem.*, 78 (2006) 561-566.
- [365] S. Caldarelli, Chromatographic NMR: a tool for the analysis of mixtures of small molecules, *Magn. Reson. Chem.*, 45 (2007) S48-S55.
- [366] C. Carrara, S. Viel, F. Ziarelli, G. Excoffier, C. Delaurent, S. Caldarelli, Chromatographic NMR in NMR solvents, *J. Magn. Reson.*, 194 (2008) 303-306.
- [367] R. Evans, S. Haiber, M. Nilsson, G.A. Morris, Isomer resolution by micelle-assisted diffusion-ordered spectroscopy, *Anal. Chem.*, 81 (2009) 4548-4550.
- [368] M.E. Zielinski, K.F. Morris, Using perdeuterated surfactant micelles to resolve mixture components in diffusion-ordered NMR spectroscopy, *Magn. Reson. Chem.*, 47 (2009) 53-56.
- [369] J.S. Kavakka, V. Parviainen, K. Wähälä, I. Kilpeläinen, S. Heikkinen, Enhanced chromatographic NMR with polyethyleneglycol. A novel resolving agent for diffusion ordered spectroscopy, *Magn. Reson. Chem.*, 48 (2010) 777-781.
- [370] A.K. Rogerson, J.A. Aguilar, M. Nilsson, G.A. Morris, Simultaneous enhancement of chemical shift dispersion and diffusion resolution in mixture analysis by diffusion-ordered NMR spectroscopy, *Chem. Commun.*, 47 (2011) 7063-7064.
- [371] C. Pemberton, R. Hoffman, A. Aserin, N. Garti, New insights into silica-based NMR "chromatography", *J. Magn. Reson.*, 208 (2011) 262-269.
- [372] A. Tal, L. Frydman, Single-scan multidimensional magnetic resonance, *Prog. Nucl. Magn. Reson. Spectrosc.*, 57 (2010) 241-292.
- [373] N.H. Meyer, K. Zangger, Simplifying proton NMR spectra by instant homonuclear broadband decoupling, *Angew. Chem. Int. Ed.*, 52 (2013) 7143-7146.
- [374] K. Kazimierczuk, V. Orekhov, Non-uniform sampling: Post-Fourier era of NMR data collection and processing, *Magn. Reson. Chem.*, 53 (2015) 921-926.
- [375] K. Zangger, Pure shift NMR, *Prog. Nucl. Magn. Reson. Spectrosc.*, 86-87 (2015) 1-20.
- [376] G. Dal Poggetto, L. Castanar, R.W. Adams, G.A. Morris, M. Nilsson, Dissect and Divide: Putting NMR Spectra of Mixtures under the Knife, *J. Am. Chem. Soc.*, 141 (2019) 5766-5771.
- [377] A.J. Simpson, G. Woods, O. Mehrzad, Spectral Editing of Organic Mixtures into Pure Components Using NMR Spectroscopy and Ultraviscous Solvents, *Anal. Chem.*, 80 (2008) 186-194.
- [378] P. Lameiras, L. Boudesocque, Z. Mouloungui, J.H. Renault, J.M. Wieruszkeski, G. Lippens, J.M. Nuzillard,

- Glycerol and glycerol carbonate as ultraviscous solvents for mixture analysis by NMR, *J. Magn. Reson.*, 212 (2011) 161-168.
- [379] P. Lameiras, J.-M. Nuzillard, Highly Viscous Binary Solvents: DMSO-*d*<sub>6</sub>/Glycerol and DMSO-*d*<sub>6</sub>/Glycerol-*d*<sub>8</sub> for Polar and Apolar Mixture Analysis by NMR, *Anal. Chem.*, 88 (2016) 4508-4515.
- [380] P. Lameiras, S. Patis, J. Jakhilal, S. Castex, P. Clivio, J.M. Nuzillard, Small Molecule Mixture Analysis by Heteronuclear NMR under Spin Diffusion Conditions in Viscous DMSO–Water Solvent, *Chem. Eur. J.*, 23 (2017) 4923-4928.
- [381] P. Lameiras, S. Mougeolle, F. Pedinielli, J.-M. Nuzillard, Polar mixture analysis by NMR under spin diffusion conditions in viscous sucrose solution and agarose gel, *Faraday Discuss.*, 218 (2019) 233-246.
- [382] E. Adair, C. Afonso, N.G.A. Bell, A.N. Davies, M.A. Delsuc, R. Godfrey, R. Goodacre, J.A. Hawkes, N. Hertkorn, D. Jones, P. Lameiras, A. Le Guennec, A. Lubben, M. Nilsson, L. Paša-Tolić, J. Richards, R.P. Rodgers, C.P. Rüger, P. Schmitt-Kopplin, P.J. Schoenmakers, P. Sidebottom, D. Staerk, S. Summerfield, D. Uhrin, P. van Delft, J.J.J. van der Hoof, F.H.M. van Zelst, A. Zherebker, High resolution techniques: General discussion, *Faraday Discuss.*, 218 (2019) 247-267.
- [383] F. Pedinielli, J.-M. Nuzillard, P. Lameiras, Mixture Analysis in Viscous Solvents by NMR Spin Diffusion Spectroscopy: ViscY. Application to High- and Low-Polarity Organic Compounds Dissolved in Sulfolane/Water and Sulfolane/DMSO-*d*<sub>6</sub> Blends, *Analytical Chemistry*, 92 (2020) 5191-5199.
- [384] J.I. Garcia, H. Garcia-Marin, E. Pires, Glycerol based solvents: synthesis, properties and applications, *Green Chem.*, 16 (2014) 1007-1033.
- [385] J.R. Ochoa-Gómez, O. Gómez-Jiménez-Aberasturi, C. Ramírez-López, M. Belsué, A Brief Review on Industrial Alternatives for the Manufacturing of Glycerol Carbonate, a Green Chemical, *Org. Process Res. Dev.*, 16 (2012) 389-399.
- [386] Y. Chernyak, Dielectric Constant, Dipole Moment, and Solubility Parameters of Some Cyclic Acid Esters, *J. Chem. Eng. Data*, 51 (2006) 416-418.
- [387] K. Stott, J. Keeler, T.L. Hwang, A.J. Shaka, J. Stonehouse, Excitation Sculpting in High-Resolution Nuclear Magnetic Resonance Spectroscopy: Application to Selective NOE Experiments, *J. Am. Chem. Soc.*, 117 (1995) 4199-4200.
- [388] K. Stott, J. Keeler, Q.N. Van, A.J. Shaka, One-Dimensional NOE Experiments Using Pulsed Field Gradients, *J. Magn. Reson.*, 125 (1997) 302-324.
- [389] R. Brüschweiler, C. Griesinger, O.W. Sørensen, R.R. Ernst, Combined use of hard and soft pulses for  $\omega_1$  decoupling in two-dimensional NMR spectroscopy, *J. Magn. Reson.*, 78 (1988) 178-185.
- [390] B. Plainchont, A. Martinez, S. Tisse, J.P. Bouillon, J.M. Wieruszkeski, G. Lippens, D. Jeannerat, J.M. Nuzillard, An alternative scheme for the multiplexed acquisition of 1D and 2D NMR spectra, *J. Magn. Reson.*, 206 (2010) 68-73.
- [391] Y.H. Lee, D.T. Wong, Saliva: an emerging biofluid for early detection of diseases, *Am. J. Dent.*, 22 (2009) 241-248.
- [392] G.A.N. Gowda, F. Tayyari, T. Ye, Y. Suryani, S. Wei, N. Shanaiah, D. Raftery, Quantitative Analysis of Blood Plasma Metabolites Using Isotope Enhanced NMR Methods, *Anal. Chem.*, 82 (2010) 8983-8990.
- [393] P. Sandusky, E. Appiah-Amponsah, D. Raftery, Use of optimized 1D TOCSY NMR for improved quantitation and metabolomic analysis of biofluids, *J. Biomol. NMR*, 49 (2011) 281-290.
- [394] T.W. Fan, A.N. Lane, Applications of NMR spectroscopy to systems biochemistry, *Prog. Nucl. Magn. Reson. Spectrosc.*, 92-93 (2016) 18-53.
- [395] H. Koskela, Chapter 1 Quantitative 2D NMR Studies, in: *Annual Reports on NMR Spectroscopy*, Academic Press, 2009, pp. 1-31.
- [396] P. Sandusky, D. Raftery, Use of selective TOCSY NMR experiments for quantifying minor components in complex mixtures: Application to the metabolomics of amino acids in honey, *Anal. Chem.*, 77 (2005) 2455-2463.
- [397] P. Sandusky, D. Raftery, Use of Semiselective TOCSY and the Pearson Correlation for the Metabonomic Analysis of Biofluid Mixtures: Application to Urine, *Anal. Chem.*, 77 (2005) 7717-7723.
- [398] M. Lin, M.J. Shapiro, Mixture Analysis by NMR Spectroscopy, *Anal. Chem.*, 69 (1997) 4731-4733.
- [399] R. Bruschiweiler, F. Zhang, Covariance nuclear magnetic resonance spectroscopy, *J. Chem. Phys.*, 120 (2004) 5253-5260.
- [400] W.M. Haynes, D.R. Lide, B.T. J., *CRC Handbook of Chemistry and Physics - 97<sup>th</sup> Edition*, 2016.
- [401] T.L. Hwang, A.J. Shaka, Water Suppression That Works. Excitation Sculpting Using Arbitrary Wave-Forms and Pulsed-Field Gradients, *J. Magn. Reson. Ser. A*, 112 (1995) 275-279.
- [402] C. Dalvit, A. Vulpetti, Technical and practical aspects of <sup>19</sup>F NMR-based screening: Toward sensitive high-throughput screening with rapid deconvolution, *Magn. Reson. Chem.*, 50 (2012) 592-597.
- [403] A. Vulpetti, C. Dalvit, Design and generation of highly diverse fluorinated fragment libraries and their efficient screening with improved <sup>19</sup>F NMR methodology, *ChemMedChem*, 8 (2013) 2057-2069.
- [404] V.R.N. Telis, J. Telis-Romero, H.B. Mazzotti, A.L. Gabas, Viscosity of Aqueous Carbohydrate Solutions at Different Temperatures and Concentrations, *Int. J. Food Prop.*, 10 (2007) 185-195.
- [405] M.P. Longinotti, H.R. Corti, Viscosity of concentrated sucrose and trehalose aqueous solutions including the supercooled regime, *J. Phys. Chem. Ref. Data*, 37 (2008) 1503-1515.
- [406] L. Jannelli, M. Pansini, R. Jalenti, Partial molar volumes of C2-C5 normal and branched nitriles in sulfolane solutions at 30°C, *J. Chem. Eng. Data*, 29 (1984) 263-266.
- [407] J.A. Riddick, W.B. Bunger, T.K. Sakano, *Organic Solvents: Physical Properties and Methods of Purification*, 4<sup>th</sup> Edition, Wiley-Interscience, New York, 1986.
- [408] A. Sacco, G. Petrella, M. Castagnolo, A. Dell'atti, Excess volumes and viscosity of water-sulfolane mixtures at 30, 40 and 50°C, *Thermochim. Acta*, 44 (1981) 59-66.
- [409] L. Janelli, A.K. Rakshit, A. Sacco, Viscosity of Binary Liquid Mixtures Involving Sulfolane and Alcohols, *Z. Naturforsch. Sect. A J. Phys. Sci.*, 29 (1974) 355-358.
- [410] K. Stott, J. Stonehouse, J. Keeler, T.-L. Hwang, A.J. Shaka, Excitation Sculpting in High-Resolution Nuclear Magnetic Resonance Spectroscopy: Application to Selective NOE Experiments, *J. Am. Chem. Soc.*, 117 (1995) 4199-4200.
- [411] D.G. Gorenstein, B.A. Luxon, <sup>31</sup>P NMR, in: *Encyclopedia of Spectroscopy and Spectrometry*, Elsevier Ltd, 1999, pp. 2204-2212.
- [412] O. Kühn, *Phosphorus-31 NMR Spectroscopy: A Concise Introduction for the Synthetic Organic and Organometallic Chemist*, Springer, 2009.
- [413] T.R. Tritton, I.M. Armitage, Phosphorus-31 NMR studies of *E. coli* ribosomes, *Nucleic Acids Res.*, 5 (1978) 3855-3869.

## Glossary

1D: one-dimensional  
2D: two-dimensional  
AY: Ala-Tyr  
CAMELSPIN: cross-relaxation appropriate for minimolecules emulated by locked spins  
CAR: conformation-activity relationship  
CPA conformer population analysis  
CTFEP: chlorotrifluoroethylene polymer  
D<sub>2</sub>O: deuterium oxide  
DNA: deoxyribonucleic acid  
DMF: dimethylformamide  
DMF-*d*<sub>7</sub>: dimethylformamide-*d*<sub>7</sub>  
DMSO: dimethylsulfoxide  
DMSO-*d*<sub>6</sub>: dimethylsulfoxide-*d*<sub>6</sub>  
DPFGSE: double pulse field gradient spin echo  
EG: ethylene glycol  
EG-*d*<sub>6</sub>: ethylene glycol-*d*<sub>6</sub>  
EM: energy minimization  
FT-NMR: fourier transform nuclear magnetic resonance  
GL: glycerol  
GL-*d*<sub>8</sub>: glycerol-*d*<sub>8</sub>  
GC: glycerol carbonate  
GS: gramicidin S  
GY: Gly-Tyr  
HOE: heteronuclear Overhauser effect  
HOESY: heteronuclear Overhauser effect spectroscopy  
HMBC: heteronuclear multiple bond correlation  
HSQC: heteronuclear single quantum correlation  
LC: liquid chromatography  
LE: Leu-enkephalin  
LEA: Leu-enkephalinamide  
LV: Leu-Val  
LY: Leu-Tyr  
MM: molecular mechanics  
MS: mass spectrometry  
MW: molecular weight  
NMR nuclear magnetic resonance  
NOE: nuclear Overhauser effect  
NOESY: nuclear Overhauser effect spectroscopy  
ROESY: rotating frame Overhauser effect spectroscopy  
SPE: solid phase extraction  
TOCSY: total correlation spectroscopy  
VISCY: viscous solvents NMR spin diffusion spectroscopy  
VWD: von Willebrand disease